AEDC-TR-72-81
AFATL-TR-72-101

cy.2

AERODYNAMIC LOADS DATA ON THE M-117 BOMB IN THE FLOW FIELD OF THE TRIPLE EJECTION RACK AT MACH NUMBERS FROM 0.5 TO 1.3

Willard E. Summers

ARO, Inc.

June 1972

PROPULSION WIND TUNNEL FACILITY
ARNOLD ENGINEERING DEVELOPMENT CENTER
AIR FORCE SYSTEMS COMMAND
ARNOLD AIR FORCE STATION, TENNESSEE

NOTICES

When U. S. Government drawings specifications, or other data are used for any purpose other than a definitely related Government procurement operation, the Government thereby incurs no responsibility nor any obligation whatsoever, and the fact that the Government may have formulated, furnished, or in any way supplied the said drawings, specifications, or other data, is not to be regarded by implication or otherwise, or in any manner licensing the holder or any other person or corporation, or conveying any rights or permission to manufacture, use, or sell any patented invention that may in any way be related thereto.

Qualified users may obtain copies of this report from the Defense Documentation Center.

References to named commercial products in this report are not to be considered in any sense as an endorsement of the product by the United States Air Force or the Government.

AERODYNAMIC LOADS DATA ON THE M-117 BOMB IN THE FLOW FIELD OF THE TRIPLE EJECTION RACK AT MACH NUMBERS FROM 0.5 TO 1.3

Willard E. Summers
ARO, Inc.

FOREWORD

The work reported herein was sponsored by the Air Force Armament Laboratory (AFATL/DLGC/Maj W. A. Miller), Air Force Systems Command (AFSC), under Program Element 62602F, Project 2567.

The test results presented were obtained by ARO, Inc. (a subsidiary of Sverdrup & Parcel and Associates, Inc.), contract operator of the Arnold Engineering Development Center (AEDC), AFSC, Arnold Air Force Station, Tennessee, under Contract F40600-72-C-0003. The test was conducted from January 27 through February 7, 1972, under ARO Project No. PC0220. The manuscript was submitted for publication on May 3, 1972.

This technical report has been reviewed and is approved.

GEORGE F. GAREY
Lt Colonel, USAF
Chief Air Force Test Director, PWT
Directorate of Test

FRANK J. PASSARELLO
Colonel, USAF
Acting Director of Test

ABSTRACT

Experimental data were obtained to check the validity of store forces and moments acquired from theoretical calculations which employed mathematical models to simulate the M-117 bombs and the Triple Ejection Rack (TER). Data were obtained using 0.10-scale models of the physical geometry of the M-117 and TER, and using mathematically simulated geometries representing the M-117 and TER. Store force and moment data were obtained for each store geometry at various locations and orientations relative to the corresponding TER configuration. In addition, free-stream stability data and some separation trajectories were obtained for the M-117 model which represented the physical store geometry. Data were obtained at Mach numbers from 0.5 to 1.3 for the force and moment data, and from 0.5 to 0.8 for the separation trajectory data. During the early part of the test, it was found that the test results for the two models did not correlate well. Consequently, the major portion of the test consisted of obtaining data on the actual M-117 bomb geometry and TER. Results of the test with the M-117 model showed that the changes in forces and moments with store pitch angle were nonlinear, and the curve slopes varied significantly with store position relative to the rack. Store forces and moments were a strong function of Mach number, especially for the store at the number one TER position.

CONTENTS

APPENDIXES

Figure | Page

Page

II. TABLES

NOMENCLATURE

b	Store reference dimension, ft, full scale
C_A	Store axial-force coefficient, axial force/$q_\infty S$
C_ℓ	Store rolling-moment coefficient, rolling moment/$q_\infty Sb$
C_{ℓ_p}	Store roll-damping derivative, $dC_\ell/d(pb/2V_\infty)$
C_m	Store pitching-moment coefficient, referenced to the store cg, pitching moment/$q_\infty Sb$
$C_{m_{\Delta\theta}}$	Slope of the C_m versus $\Delta\theta$ curve evaluated at $\Delta\theta = 0$, per degree
C_{m_q}	Store pitch-damping derivative, $dC_m/d(qb/2V_\infty)$
C_N	Store normal-force coefficient, normal force/$q_\infty S$
$C_{N_{\Delta\theta}}$	Slope of the C_N versus $\Delta\theta$ curve evaluated at $\Delta\theta = 0$, per degree
C_n	Slope yawing-moment coefficient, referenced to the store cg, yawing moment/$q_\infty Sb$
C_{n_r}	Store yaw-damping derivative, $dC_n/d(rb/2V_\infty)$
C_Y	Store side-force coefficient, side force/$q_\infty S$
cg	Center of gravity
D	Full-scale store diameter, ft
F_Z	TER ejector force, lb
H	Pressure altitude, ft
I_x	Full-scale moment of inertia about the store X_B axis, slug-ft^2
I_y	Full-scale moment of inertia about the store Y_B axis, slug-ft^2

I_z	Full-scale moment of inertia about the store Z_B axis, slug-ft^2
M_∞	Free-stream Mach number
$\overline{m}$	Full-scale store mass, slugs
p	Store angular velocity about the X_B axis, radians/sec
p_∞	Free-stream static pressure, psfa
q	Store angular velocity about the Y_B axis, radians/sec
q_∞	Free-stream dynamic pressure, psf
r	Store angular velocity about the Z_B axis, radians/sec
S	Store reference area, ft^2
t	Real trajectory time from initiation of trajectory, sec
V_∞	Free-stream velocity, ft/sec
X	Travel of the store cg in the pylon-axis system X_P direction, ft, full scale measured from the prelaunch position on the TER
X_{cg}	Full-scale cg location, ft from nose of store
X_L	Ejector piston location relative to the store cg, positive forward of store cg, ft full scale
Y	Travel of the store cg in the pylon-axis system Y_P direction, ft, full scale measured from the prelaunch position on the TER
Z	Travel of the store cg in the pylon-axis system Z_P direction, ft, full scale measured from the prelaunch position on the TER
Z_E	Ejector stroke length, ft, full scale
α	TER-model angle of attack relative to the free-stream velocity vector, deg
$\Delta\theta$	Angle between the store longitudinal axis and its projection in the X_P-Y_P plane. Positive when the store nose is raised toward the negative Z_P axis, deg
ΔPHI	Angle between the projection of the store lateral axis in the Y_P-Z_P plane and the Y_P axis. Positive for clockwise rotation when looking along the positive X_P axis

ΔPSI Angle between the projection of the store longitudinal axis in the X_P-Y_P plane and the X_P axis. Positive when the store nose is to the right when looking along the positive X_P axis, deg

FLIGHT-AXIS SYSTEM COORDINATES

Directions

X_F Parallel to the free-stream wind vector; positive direction is forward as seen by the pilot

Y_F Perpendicular to the X_F and Z_F directions; positive direction is to the right as seen by the pilot

Z_F In the aircraft plane of symmetry, perpendicular to the free-stream wind vector; positive direction is downward

The flight-axis system origin is coincident with the aircraft cg and remains fixed with respect to the parent aircraft during store separation. The X_F, Y_F, and Z_F coordinate axes do not rotate with respect to the initial flight direction and attitude.

STORE BODY-AXIS SYSTEM COORDINATES

Directions

X_B Parallel to the store longitudinal axis; positive direction is upstream in the prelaunch position

Y_B Perpendicular to the store longitudinal axis and parallel to the flight-axis system X_F-Y_F plane when the store is at zero roll angle; positive direction is to the right looking upstream when the store is at zero yaw and roll angles

Z_B Perpendicular to both the X_B and Y_B axes; positive direction is downward as seen by the pilot when the store is at zero pitch and roll angles.

The store body-axis system origin is coincident with the store cg and moves with the store during separation from the parent airplane. The X_B, Y_B, and Z_B coordinate axes rotate with the store in pitch, yaw, and roll so that mass moments of inertia about the three axes are not time-varying quantities.

PYLON-AXIS SYSTEM COORDINATES

Directions

X_P Parallel to the store longitudinal axis in the prelaunch carriage position; positive direction is forward as seen by the pilot

Y_P Perpendicular to the X_P axis and parallel to the flight-axis system X_F-Y_F plane; positive direction is to the right as seen by the pilot

Z_P Perpendicular to both the X_P and Y_P axes; positive direction is downward

The pylon-axis system origin is coincident with the store cg in the prelaunch carriage position. The axes are rotated with respect to the flight-axis system by the prelaunch yaw and pitch angles of the store. Both the origin and the direction of the coordinate axes remain fixed with respect to the flight-axis system throughout the trajectory.

SECTION I
INTRODUCTION

This investigation was conducted in the Aerodynamic Wind Tunnel (4T) to obtain data for the purpose of checking the validity of store forces and moments acquired from theoretical calculations which employed mathematical models to simulate the M-117 bombs and the Triple Ejection Rack (TER). Data were obtained on 0.10-scale models which represented the true physical geometries of the M-117 and TER, and for models which represented mathematically simulated geometries of the M-117 and TER.

Store force and moment data were obtained for each store geometry at various locations and orientations relative to the corresponding TER configuration. Data were obtained at Mach numbers from 0.5 to 1.3 for TER angles of attack of 0 and 5 deg. At each Mach number, data were obtained at translational displacements from the carriage position of X/D = 0 to -1, Y/D = 0 to 0.714, and Z/D = 0 to 3. The store was pitched through the allowable angle-of-attack range at each position (limited by physical interference between store and TER), to a maximum of ±20 deg. Data were obtained at a yaw angle of 0 deg for all cases and at 5 deg for selected cases, with a store roll to give $\Delta\phi = 0$ at all $\Delta\psi$-$\Delta\theta$ combinations.

Free-stream stability data were obtained for the true M-117 geometry at Mach numbers from 0.5 to 1.3.

Store separation trajectory data were obtained for the M-117 bomb from the TER. The models representing the true geometry of the M-117 and TER were used during these tests. Trajectories were obtained at Mach numbers from 0.5 to 0.8 at a simulated altitude of 5000 ft.

During all tests, the TER model was supported from the main tunnel support system, and the instrumented store model was supported by the balance which was attached to the Captive Trajectory Support (CTS) system.

SECTION II
APPARATUS

2.1 TEST FACILITY

Tunnel 4T is a closed-loop, continuous flow, variable density tunnel in which the Mach number can be varied from 0.1 to 1.3. At all Mach numbers, the stagnation pressure can be varied from 300 to 3700 psfa. The test section is 4 ft square and 12.5 ft long with perforated, variable porosity (0.5- to 10-percent open) walls. It is completely enclosed in a plenum chamber from which the air can be evacuated, allowing part of the tunnel airflow to be removed through the perforated walls of the test section.

For store separation and aerodynamic loads survey testing, two separate and independent support systems are used to support the models. The parent model (TER for the present test) is inverted in the test section and supported by an offset sting attached

to the main pitch sector. The store model is supported by the CTS which extends down from the tunnel top wall and provides store movement (six degrees of freedom) independent of the parent model. An isometric drawing of a typical store separation installation is shown in Fig. 1, Appendix I.

Also shown in Fig. 1 is a block diagram of the computer control loop used during captive trajectory testing. The analog system and the digital computer work as an integrated unit and, utilizing required input information, control the store movement during a trajectory. Store positioning is accomplished by use of six individual d-c electric motors. Maximum translational travel of the CTS is ±15 in. from the tunnel centerline in the lateral and vertical directions and 36 in. in the axial direction. Maximum angular displacements are ±45 deg in pitch and yaw and ±360 deg in roll. A more complete description of the test facility can be found in the Test Facilities Handbook.[1] A schematic showing the test section details and the location of the models in the tunnel is given in Fig. 2.

2.2 TEST ARTICLES

Models used during the test were 0.10-scale models of the M-117 bomb and TER. Two separate geometric configurations were used for both the M-117 and the TER. One configuration consisted of M-117 bombs and a TER which represented the true physical geometry of the full-scale bomb and TER. The other configuration consisted of bombs and a TER which represented mathematically simulated geometries of the respective models.

Each configuration consisted of a bomb that could be installed on an internal strain-gage balance, two dummy bomb models, and the TER model. Each TER had provisions for mounting the dummy bomb models on the shoulder stations. Details and dimensions of the store models are shown in Fig. 3, and a photograph of the models is shown in Fig. 4. The TER details and dimensions are presented in Fig. 5, and a photograph of the TER models is shown in Fig. 6. The relative location of the store models when in the carriage position on the TER was the same for both configurations, as shown in Fig. 7.

The test store and balance were supported by the CTS, and the TER models were supported by the main support system. Basic details of the support structure near the models are shown in Fig. 8, and a photograph of a typical test configuration installed in the tunnel is shown in Fig. 9.

2.3 INSTRUMENTATION

A six-component internal strain-gage balance was used to obtain the force and moment data on the store models. Translational and angular positions of the store model were obtained from the CTS analog outputs. A digital readout from the main pitch sector was

[1]Test Facilities Handbook (Ninth Edition). "Propulsion Wind Tunnel Facility, Vol. 4." Arnold Engineering Development Center, July 1971.

used to monitor the TER angle of attack which was remotely controlled. The TER configurations were instrumented with spring-loaded plungers (touch wires) to provide an indication when the store was in its carriage position on the TER. This system was electrically wired to give a visual indication on the control console when contact between the store and touch wire was made. An additional electrical circuit was used to automatically stop the CTS movement if the store model or sting support contacted the TER or its support structure.

SECTION III
TEST DESCRIPTION

3.1 TEST CONDITIONS

Store free-stream stability data and force and moment survey data were obtained at Mach numbers of 0.5, 0.8, 0.9, 1.1, and 1.3 at a Reynolds number of 3 million per foot. Separation trajectory data were obtained at Mach numbers of 0.5, 0.7, and 0.8 at a Reynolds number of 3 million per foot.

For a given test run, tunnel conditions were held constant at the desired Mach number and Reynolds number while the test data were obtained.

3.2 DATA ACQUISITION

Store force and moment survey data were obtained in the following manner. After tunnel conditions were established, the store was manually positioned to the carriage position on the TER. Operational control of the CTS was then switched to the digital computer, which controlled the store movement through commands to the CTS (see block diagram, Fig. 1). Preselected positions and orientations of the store model were programmed in the computer which allowed automatic data acquisition. The reference axis system for the data is shown in Fig. 10, identification of test configurations is given in Fig. 11, and store positions and orientations at which data were obtained are listed in Table I, Appendix II.

To obtain a separation trajectory, test conditions were established in the tunnel and the TER model was positioned at the desired angle of attack. The store model was then oriented to a position corresponding to the store carriage location. After the store was set at the desired initial position, operational control of the CTS was switched to the digital computer which controlled the store movement during the trajectory through commands to the CTS analog system (see block diagram, Fig. 1). Data from the wind tunnel, consisting of measured model forces and moments, wind tunnel operating conditions, and CTS rig positions, were input to the digital computer for use in the full-scale trajectory calculations.

The digital computer was programmed to solve the six-degrees-of-freedom equations to calculate the angular and linear displacements of the store relative to the TER. In general, the program involves using the last two successive measured values of each static aerodynamic coefficient to predict the magnitude of the coefficients over the next time

interval of the trajectory. These predicted values are used to calculate the new position and attitude of the store at the end of the time interval. The CTS is then commanded to move the store model to this new position and the aerodynamic loads are measured. If these new measurements agree with the predicted values, the process is continued over another time interval of the same magnitude. If the measured and predicted values do not agree within the desired precision, the calculation is repeated over a time interval half the previous value. This process is repeated until a complete trajectory has been obtained.

In applying the wind tunnel data to the calculations of the full-scale store trajectories, the measured forces and moments are reduced to coefficient form and then applied with proper full-scale store dimensions and flight dynamic pressure. Dynamic pressure was calculated using a flight velocity equal to the free-stream velocity component plus the components of store velocity relative to the aircraft and a density corresponding to the simulated altitude.

The initial portion of each launch trajectory incorporated simulated ejector forces in addition to the measured aerodynamic forces acting on the store. The ejector force used was a constant 1200-lb force, which was terminated at an ejector stroke length of 0.2552 ft. The ejector force was considered to act perpendicular to the rack mounting surface. The location of the applied ejector force and other full-scale store parameters used in the trajectory calculations are listed in Table II.

3.3 CORRECTIONS

Balance, sting, and support deflections caused by the aerodynamic loads on the store models were accounted for in the data reduction program to calculate the true store-model angles. Corrections were also made for model weight tares to calculate the net aerodynamic forces on the store model.

3.4 PRECISION OF DATA

Estimated uncertainties in model positioning resulting from the ability of the CTS to set on a specified value were as follow:

X/D	Y/D	Z/D	$\Delta\theta$,deg	$\Delta\psi$,deg	$\Delta\phi$,deg
±0.003	±0.003	±0.003	±0.10	±0.10	±1.0

Uncertainties in the force and moment data obtained on the store models were calculated taking into consideration the probable inaccuracies in the balance measurements and tunnel conditions. The uncertainties in the coefficients are based on a 95-percent confidence level and are as follow:

M_∞	ΔC_N	ΔC_Y	ΔC_A	ΔC_ℓ	ΔC_m	ΔC_n
0.5	±0.01	±0.02	±0.02	±0.005	±0.07	±0.07
1.3	±0.007	±0.01	±0.009	±0.003	±0.04	±0.04

The uncertainties in the full-scale trajectory data resulting from balance inaccuracies based on a 95-percent confidence level are as follow:

M_∞	t	ΔX	ΔY	ΔZ	$\Delta\theta$	$\Delta\psi$
0.7	0.5	±0.04	±0.04	±0.03	±0.1	±0.1

Estimated uncertainty in setting Mach number was ±0.003, and the uncertainty in the TER angle of attack was estimated to be ±0.1 deg.

SECTION IV
RESULTS AND DISCUSSION

The simulated M-117 model was tested to obtain store force and moment data only in the presence of the simulated TER. Three types of data were obtained for the M-117 model which represented the true physical store geometry. These data consisted of (1) free-stream stability data, (2) store force and moment data in the presence of the TER, and (3) separation trajectory data from the TER.

Force and moment data obtained for the simulated configuration did not correlate well with the data for the true configuration. Consequently, most data were obtained on the true configuration. A limited amount of data is presented for the simulated configuration, and sufficient data are included for the true M-117 configuration to obtain estimates of store loads for all test positions.

During all testing to obtain force and moment data, the store roll was adjusted to produce $\Delta\phi = 0$ for all $\Delta\psi$-$\Delta\theta$ combinations so that the measured loads were always rotated to calculate the coefficients in the vertical and horizontal planes.

4.1 FREE-STREAM DATA

Free-stream data for the M-117 store model are presented in Fig. 12. Data are presented to show the effect of combination pitch and yaw angles on the aerodynamic coefficients at Mach numbers from 0.5 to 1.3. The data show a nonlinear variation of C_N and C_m with $\Delta\theta$, and the store is statically stable at all Mach numbers, with a stability margin equal to, or greater than, one caliber at most conditions.

4.2 FORCE AND MOMENT SURVEY DATA

The store force and moment data are presented to show the changes in coefficients with variations in store position and orientation relative to the rack and adjacent stores. Linear and angular displacements were measured relative to the store body axes at the carriage position, so that as angle of attack changed the reference axis orientation changed. The reference axis origin also changed with changes in TER carriage position (see Fig. 7). At the start of each survey, the store was positioned parallel to the rack and as close to Z/D = 0 as possible without the test store contacting the TER or adjacent stores. Data were obtained through the maximum pitch range possible (up to ±20 deg) at each

store cg test position. Side-force and yawing-moment coefficient data are included only for the cases when these coefficients varied significantly from values near zero.

Data for the simulated M-117 are shown in Figs. 13 and 14, and data for the M-117 are presented in Figs. 15 through 34. A comparison of the data for the simulated M-117 (Fig. 13) and the M-117 (Fig. 15) shows that the normal-force coefficient is significantly lower for the simulated model, and the pitching-moment characteristics are quite different. At the low pitch angles, the simulated model exhibits marginally stable to unstable static stability. An increase in axial-force coefficient is also indicated for the simulated model.

Data for the M-117 store at positions and orientations relative to the number 1 TER position (configuration 2) are shown in Figs. 15 through 28. These data (Fig. 15, for example) show a nonlinear variation of the coefficients with $\Delta\theta$, similar to that indicated for the free-stream data presented in Fig. 12. Although data were obtained for TER angles of attack of both 0 and 5 deg, most of the data are presented for $\alpha = 0$ deg. Selected data are presented for $\alpha = 5$ deg. When comparing the data at the two angles, it should be remembered that $\Delta\theta$ is measured with respect to the store axis orientation at the carriage position on the rack. Data presented in Fig. 16 show a comparison of the coefficients at $\alpha = 0$ and 5 deg. By shifting the $\alpha = 5$-deg curves 5 deg on the $\Delta\theta$ scale, the data for Z/D = 3.0 agree very well, although differences are indicated at Z/D = 0.2. A review of the data indicates that the change in flow field resulting from the TER angle of attack is small for store locations at Z/D > 1.5.

Data presented in Fig. 21 show that the C_N and C_m curve slopes ($C_{N_{\Delta\theta}}$ and $C_{m_{\Delta\theta}}$) at $\Delta\theta = 0$ are not constant with changes in store Z/D position. At $M_\infty = 0.5$, the slopes approach constant values for Z/D > 1.0. However, at $M_\infty \geq 0.9$ the slopes are very erratic, especially with respect to $C_{m_{\Delta\theta}}$. This is apparently a result of changes in the flow field resulting from local shock wave formation. Data shown in Fig. 15 (C_m versus $\Delta\theta$) are a good example of the increasingly erratic behavior of C_m at the higher Mach numbers. Changes in the coefficients with Mach number can also be seen in Fig. 22 which shows the variation of the store aerodynamic coefficients with Mach number at Z/D = 0. Note the large changes in C_N and C_m, especially in the $M_\infty = 0.65$ to 0.90 range.

Data presented in Figs. 23 through 26 showing the variations in the aerodynamic coefficients with Z/D ($\Delta\theta = 0$) indicate a significant decrease in C_N for Z/D < 0.5 at $M_\infty \geq 0.8$, whereas C_N continues to increase for Z/D < 0.5 at $M_\infty = 0.5$ and 0.65. This behavior is probably a result of local shock wave formation as discussed earlier. The nature of the C_m curves indicates that these local shocks have degenerated for Z/D > 0.5 at $M_\infty \leq 0.9$, although the effects are still evident for all Z/D positions at $M_\infty = 1.1$ and 1.3.

In general, the store axial-force coefficient increased somewhat as the store approached the rack. This increase in axial-force coefficient was more pronounced as Mach number increased. The only exception to this behavior was for the store at positions aft of the carriage position, as discussed in the following paragraph.

Changes in the store forces and moments with changes in axial and lateral store position (relative to the carriage position) are shown in Figs. 27 and 28. The most significant effects are indicated for the Z/D = 0 position. Moving the store aft produced a decrease in the store nose-down pitching-moment coefficient and a decrease in the store axial-force coefficient. At M_∞ = 0.5, the axial-force coefficient is negative for X/D < -0.33. This is apparently a result of the altered flow field on the tapered afterbody of the store caused by the adjacent store fins. The store axial-force coefficient decreased as the store moved into the Z/D = 0 position for the negative X/D positions. This is the reverse of the trend indicated for the surveys at X/D = 0. Lateral store movement produced small changes in the coefficients at M_∞ = 0.5. At M_∞ = 0.9 and 1.1, the presence of the shoulder-station store produced a fairly significant yawing moment at small Z/D values as the store moved out past the shoulder-station store.

Data obtained on the M-117 store at positions and orientations relative to the number 2 TER position (configuration 3) are shown in Figs. 29 through 33. In general, the Mach number effect is much less predominant for this configuration than for configuration 2. The yawing-moment coefficient shows the largest changes with both Mach number and store axial position. Variations of axial-force coefficient show the same trends as discussed for configuration 2, although negative values were never obtained.

4.3 SEPARATION TRAJECTORY DATA

Separation trajectory data were obtained for the M-117 from the TER number 1 and 2 positions (configurations 2 and 3) at simulated flight conditions of M_∞ = 0.5, 0.7, and 0.8 for level flight at 5000-ft altitude. A simulated ejector force of 1200 lb (constant) acting over an ejector stroke length of 0.255 ft was used for all trajectories. Other full-scale store parameters used in the trajectory calculations are shown in Table II. The trajectory data are presented in Fig. 34. The motions are similar, but the angular excursions are more pronounced for configuration 2. This effect increased with increasing Mach number.

SECTION V
CONCLUSIONS

As a result of this investigation of aerodynamic loads on the M-117 bomb in the flow field of the TER, the following conclusions have been reached:

1. Force and moment data for the simulated M-117 model in the presence of the simulated TER did not correlate well with data for the true M-117 geometry model in the presence of the TER.

For the M-117 representing the true physical store geometry:

2. The normal-force and pitching-moment curves were nonlinear with changes in $\Delta\theta$ for both the free-stream data and data for the store in the presence of the TER.

3. Store normal-force and pitching-moment curve slopes were essentially constant at the low Mach numbers for $Z/D > 1.0$. The curve slopes were erratic at $M_\infty \geq 0.9$ for all Z/D values.

4. Store normal-force coefficient showed a significant decrease when approaching the TER for $0 \leq Z/D < 0.5$ at $M_\infty \geq 0.8$, whereas the normal-force coefficient continued to increase in this Z/D range at M_∞ = 0.5 and 0.65. The corresponding pitching-moment data indicate possible local shock interference at $M_\infty = 0.9$ for $0 \leq Z/D \leq 0.6$, and at M_∞ = 1.1 and 1.3 for all Z/D values.

5. Store nose-down pitching-moment coefficient and axial-force coefficient decreased as the store moved downstream for small Z/D values. Store axial-force coefficient reached negative values for $X/D < -0.33$ from the TER number one position at $M_\infty = 0.5$.

6. Fairly significant yawing-moment coefficients were measured as the store moved laterally (past the shoulder station store) for $M_\infty \geq 0.9$ at small Z/D values.

7. Mach number effect was less for store positions relative to the TER number two (shoulder) position than for store positions near the TER number one (center) position.

APPENDIXES
I. ILLUSTRATIONS
II. TABLES

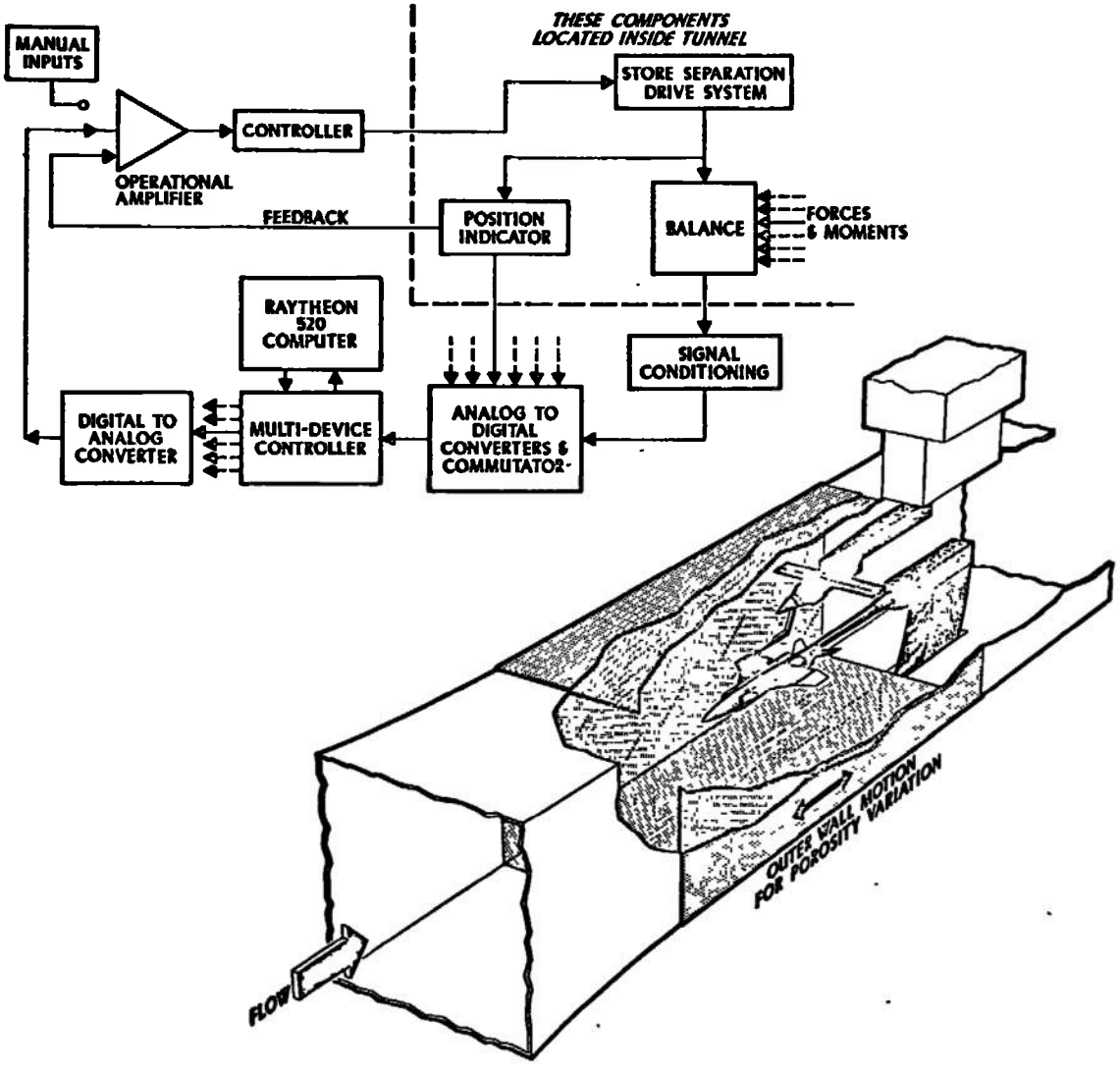

Fig. 1 Isometric Drawing of a Typical Store Separation Installation and a Block Diagram of the Computer Control Loop

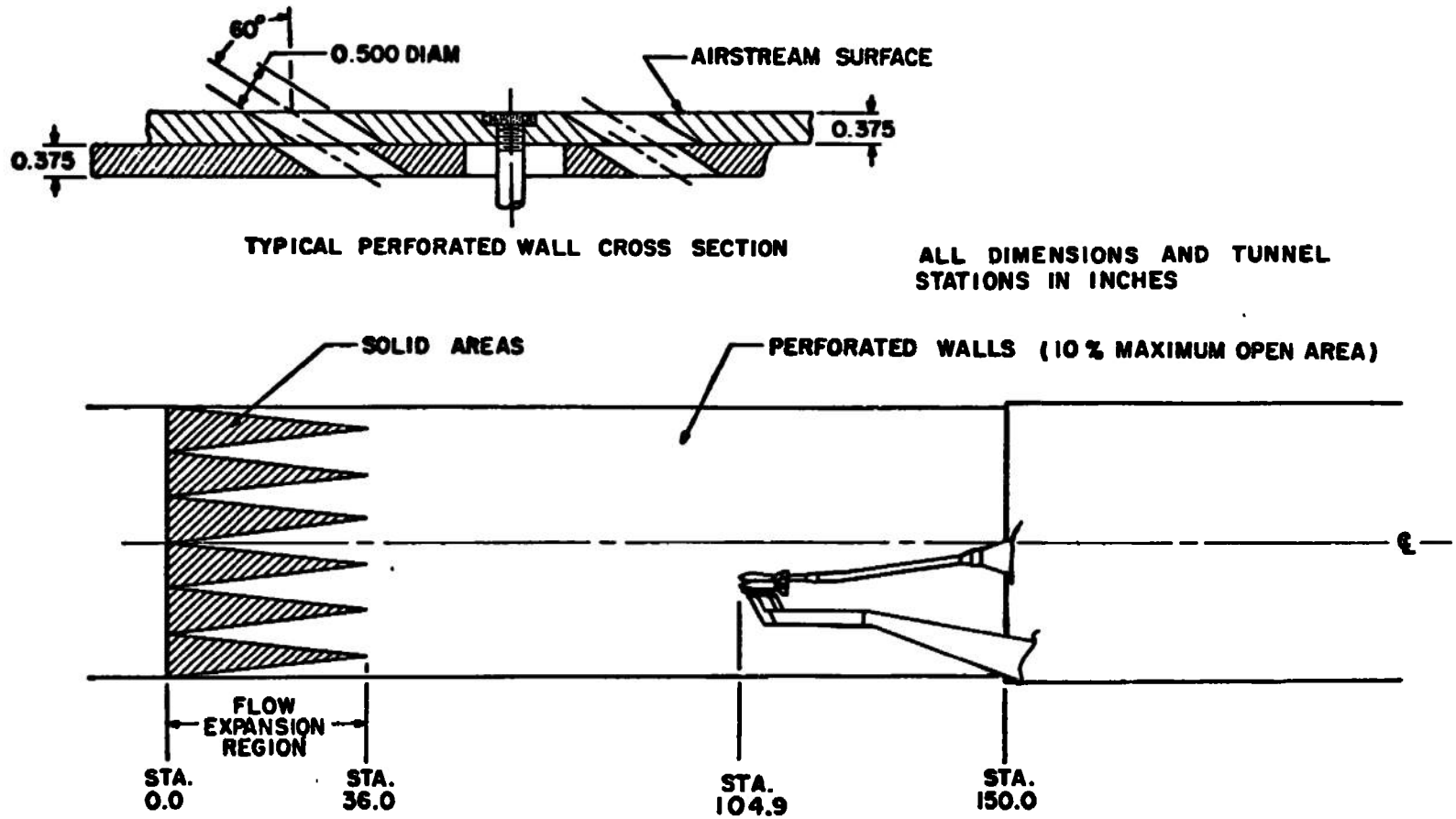

Fig. 2 Schematic of the Tunnel Test Section Showing Model Location

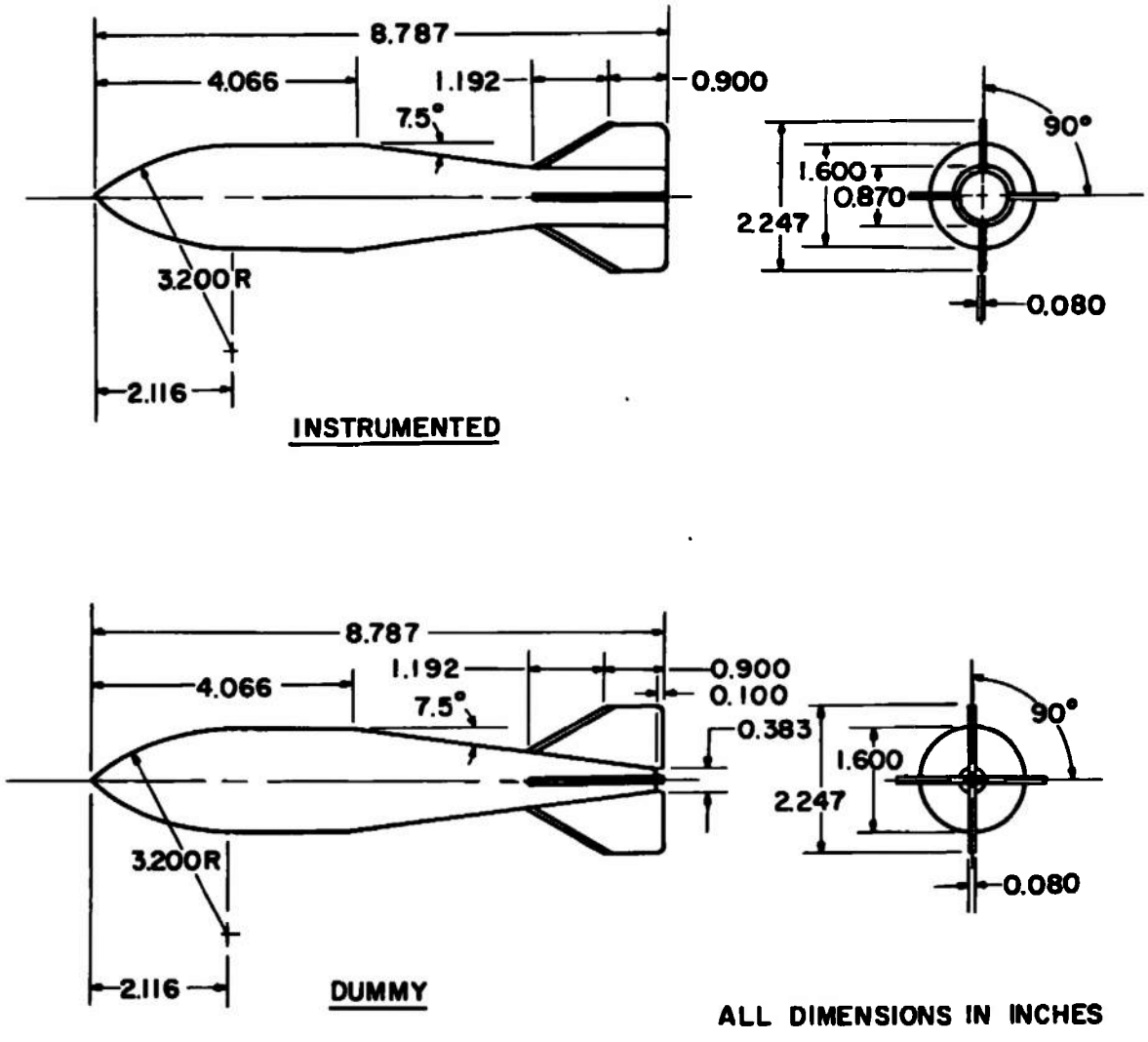

a. Geometrically Scaled Model

Fig. 3 Details and Dimensions of the M-117 Store Models

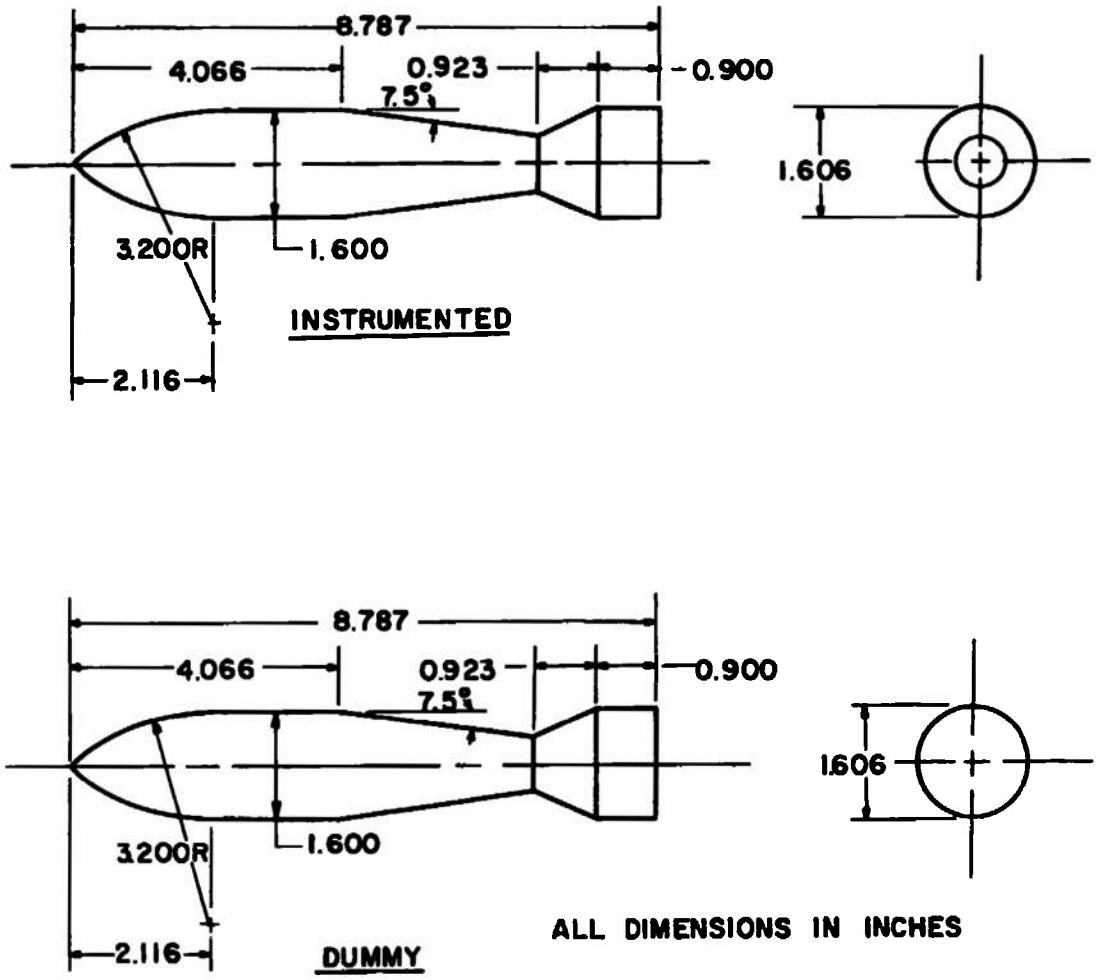

b. Mathematically Simulated Model
Fig. 3 Concluded

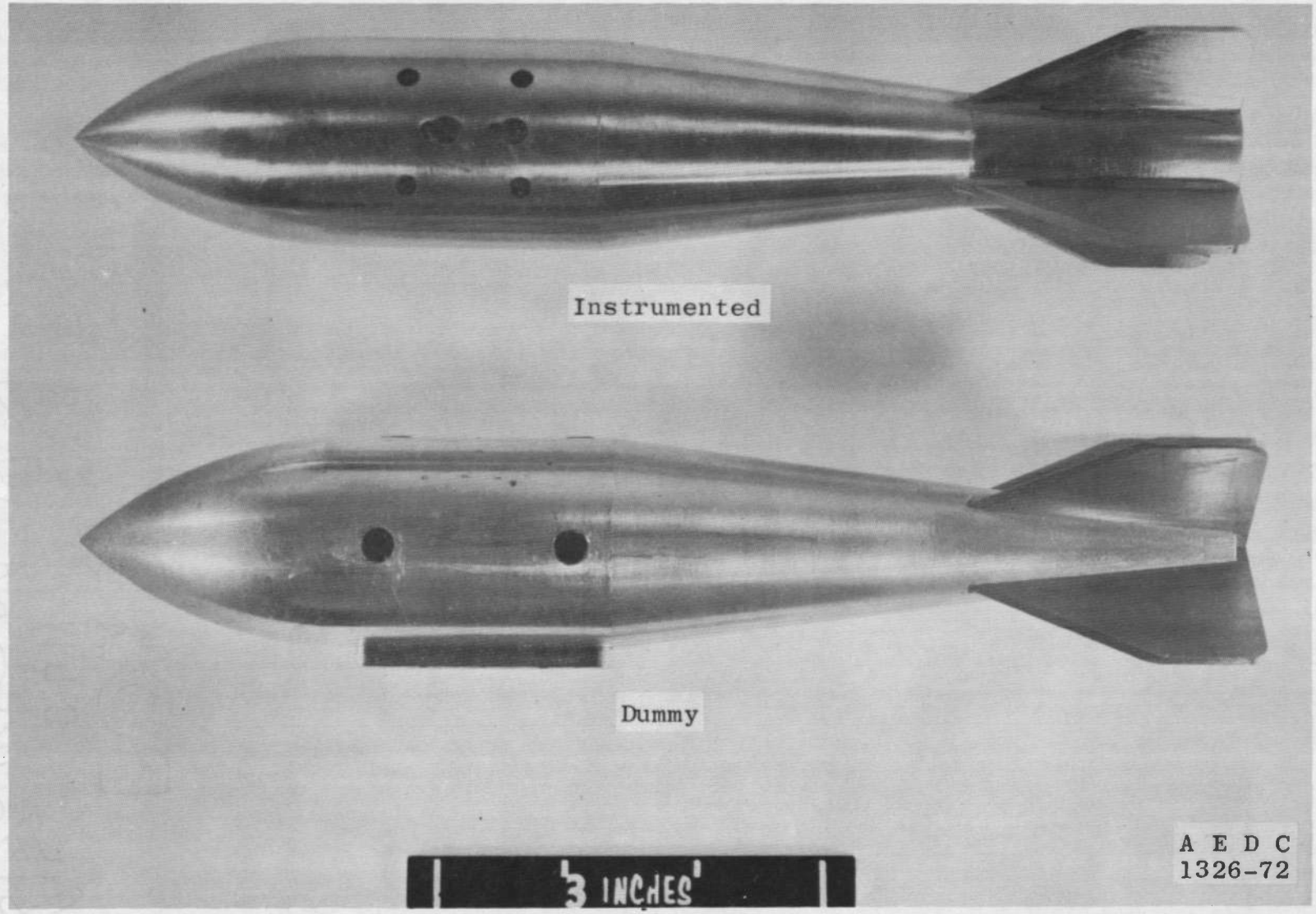

a. Geometrically Scaled Model

Fig. 4 Photographs of the M-117 Store Models

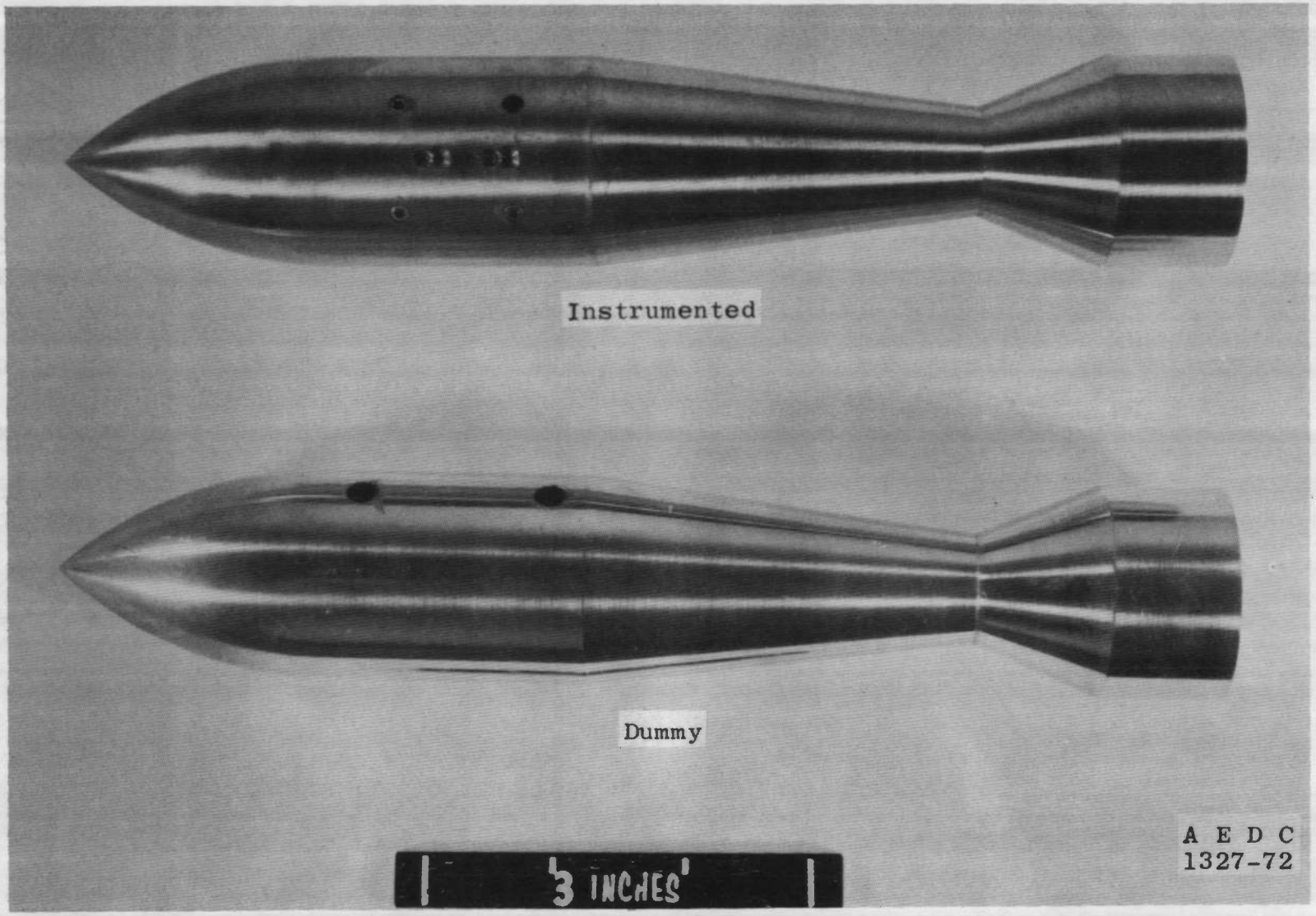

b. Mathematically Simulated Model
Fig. 4 Concluded

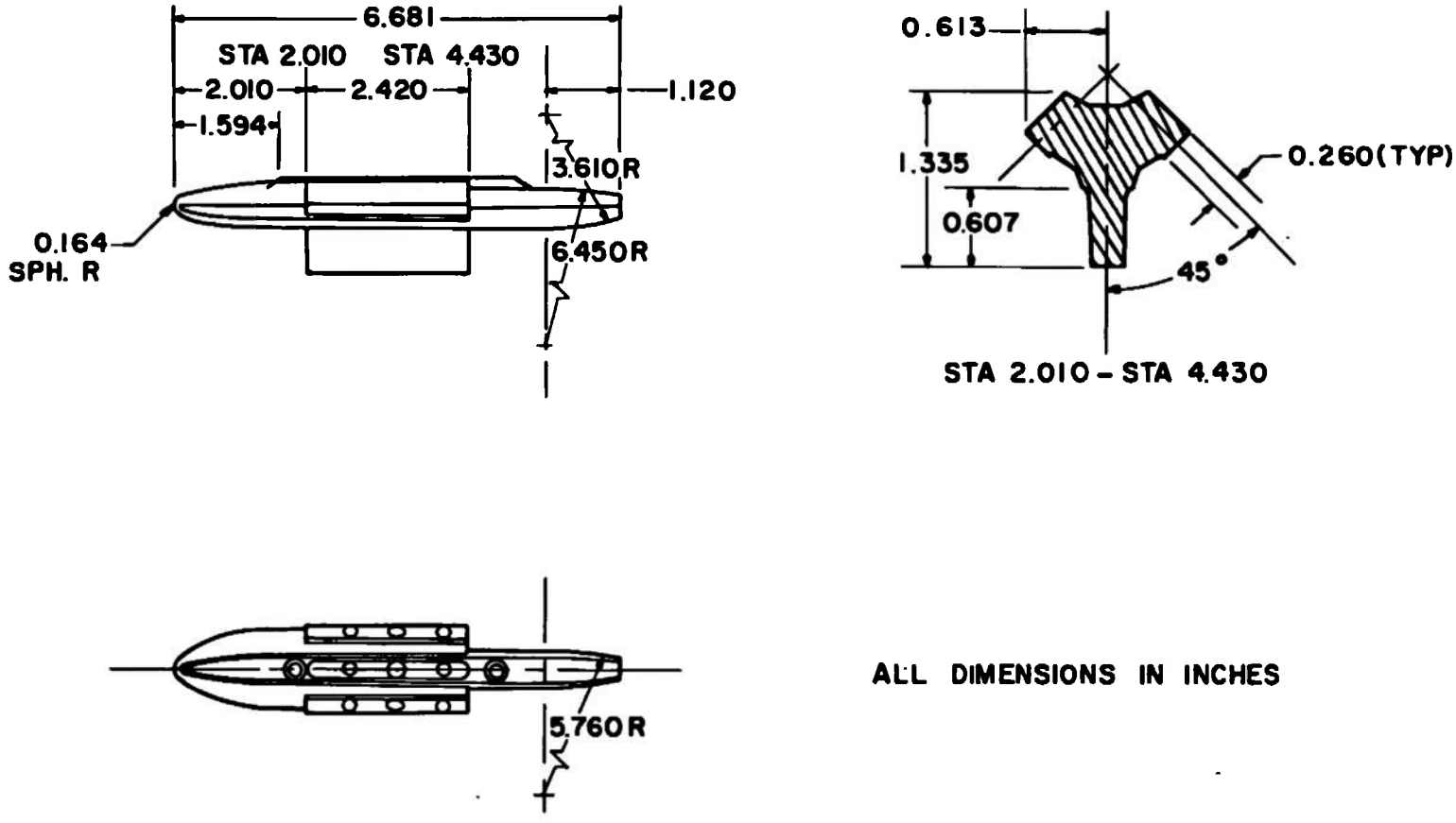

a. Geometrically Scaled Model

Fig. 5 Details and Dimensions of the Triple Ejection Rack Models

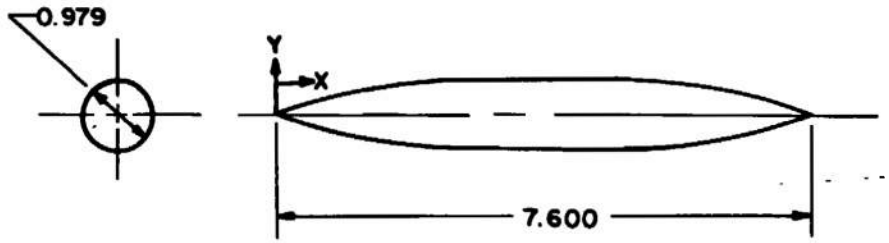

ALL DIMENSIONS IN INCHES

COORDINATES

X	Y	X	Y
0.0000	0.0000	4.8800	0.4882
0.0800	0.0292	4.9600	0.4870
0.1600	0.0576	5.0400	0.4850
0.2400	0.0850	5.1200	0.4822
0.3200	0.1115	5.2000	0.4786
0.4000	0.1372	5.2800	0.4742
0.4800	0.1619	5.3600	0.4691
0.5600	0.1857	5.4400	0.4631
0.6400	0.2087	5.5200	0.4563
0.7200	0.2307	5.6000	0.4487
0.8000	0.2518	5.6800	0.4403
0.8800	0.2721	5.7600	0.4312
0.9600	0.2914	5.8400	0.4212
1.0400	0.3098	5.9200	0.4104
1.1200	0.3080	6.0000	0.3992
1.2000	0.3232	6.0800	0.3865
1.2800	0.3598	6.1600	0.3733
1.3600	0.3746	6.2400	0.3594
1.4400	0.3885	6.3200	0.3446
1.5200	0.4016	6.4000	0.3291
1.6000	0.4137	6.4800	0.3127
1.6800	0.4250	6.5600	0.2956
1.7600	0.4353	6.6400	0.2776
1.8400	0.4448	6.7200	0.2589
1.9200	0.4533	6.8000	0.2393
2.0000	0.4609	6.8800	0.2190
2.0800	0.4677	6.9600	0.1978
2.1600	0.4735	7.0400	0.1759
2.2400	0.4785	7.1200	0.1532
2.3200	0.4825	7.2000	0.1296
2.4000	0.4857	7.2800	0.1053
2.4800	0.4879	7.3600	0.0802
2.5600	0.4893	7.4400	0.0542
2.6400	0.4896	7.5200	0.0223
4.8000	0.4896	7.6000	0.0000

b. Mathematically Simulated Model
Fig. 5 Concluded

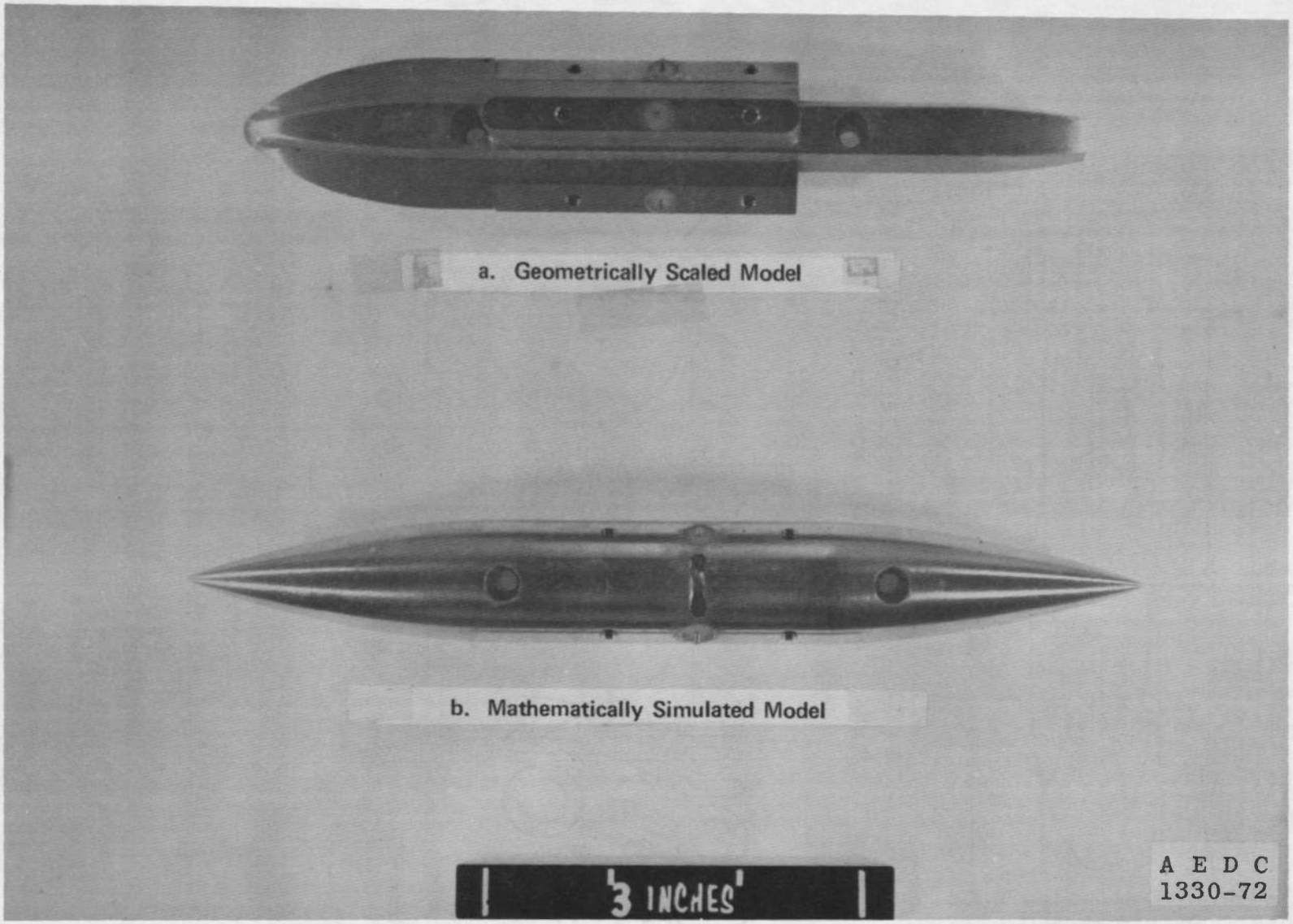

Fig. 6 Photographs of the Triple Ejection Rack Models

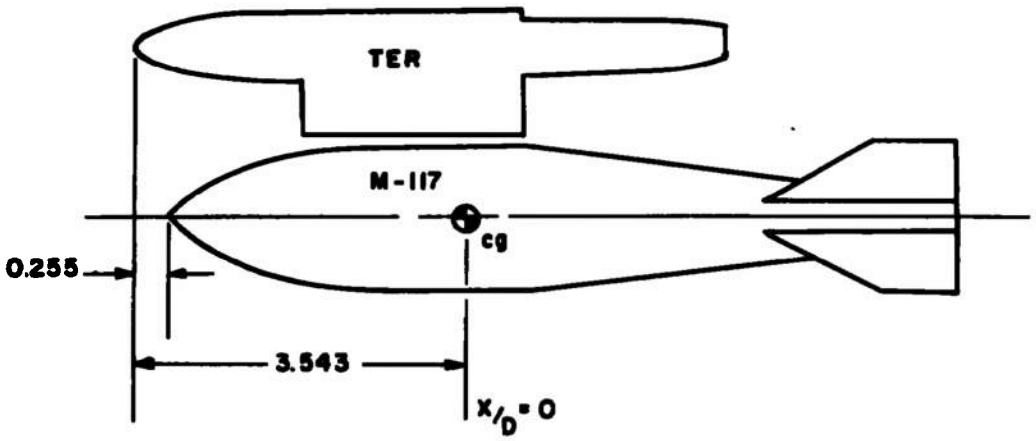

AXIAL LOCATION - TYPICAL ALL TER POSITIONS

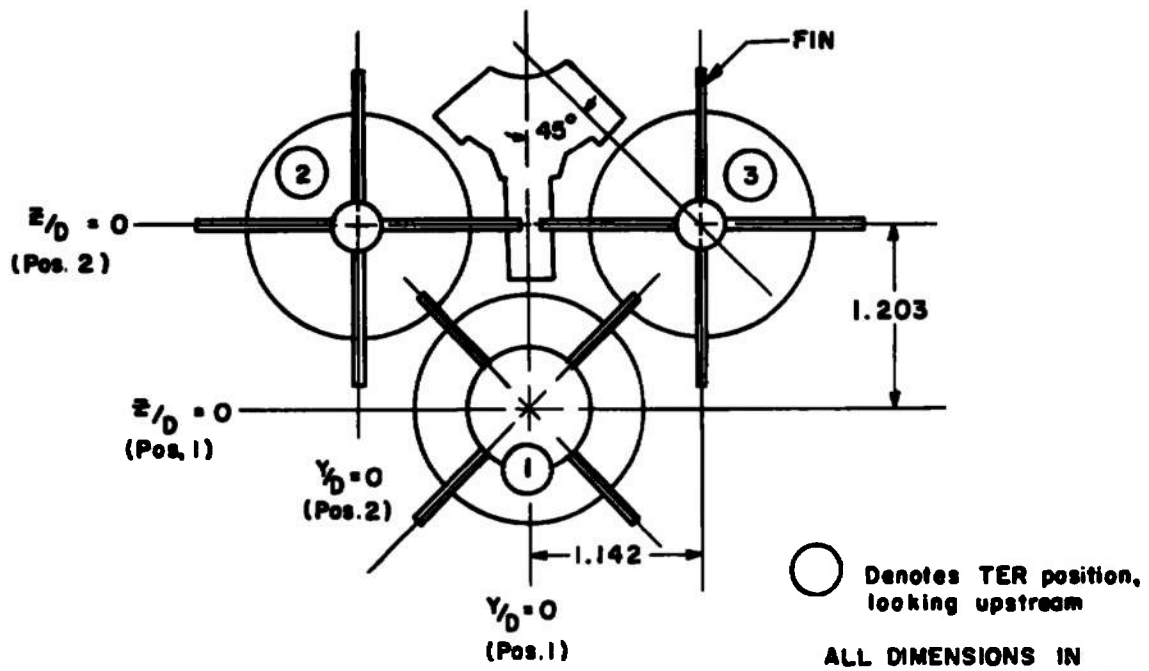

LATERAL AND VERTICAL LOCATIONS

a. Geometrically Scaled Model

Fig. 7 Relative Location of the Store Models when in the Carriage Position on the Triple Ejection Rack

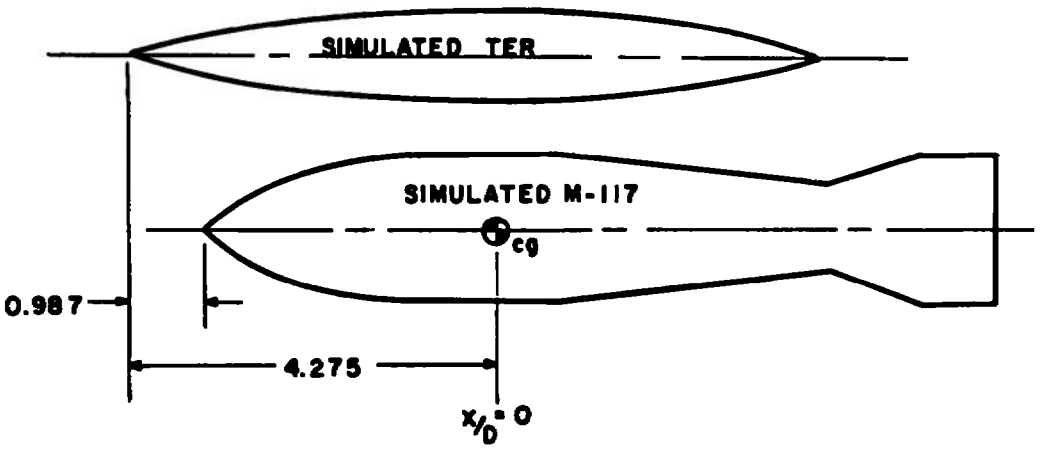

AXIAL LOCATION – TYPICAL ALL TER POSITIONS

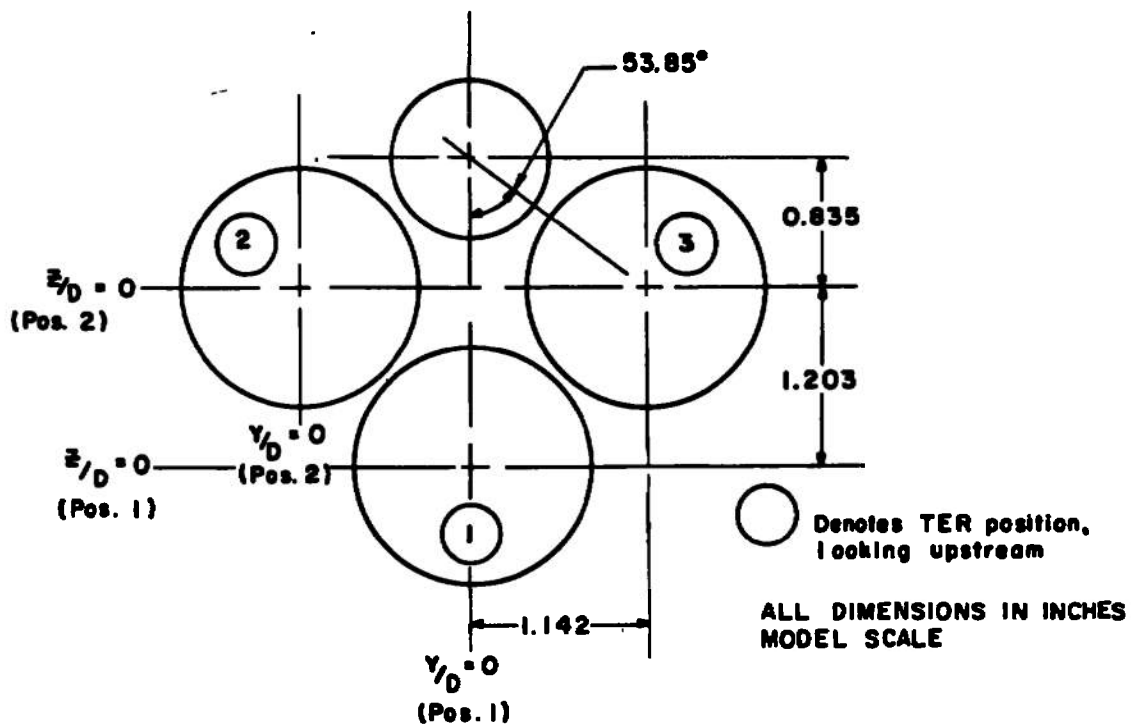

LATERAL AND VERTICAL LOCATIONS

b. Mathematically Simulated Model
Fig. 7 Concluded

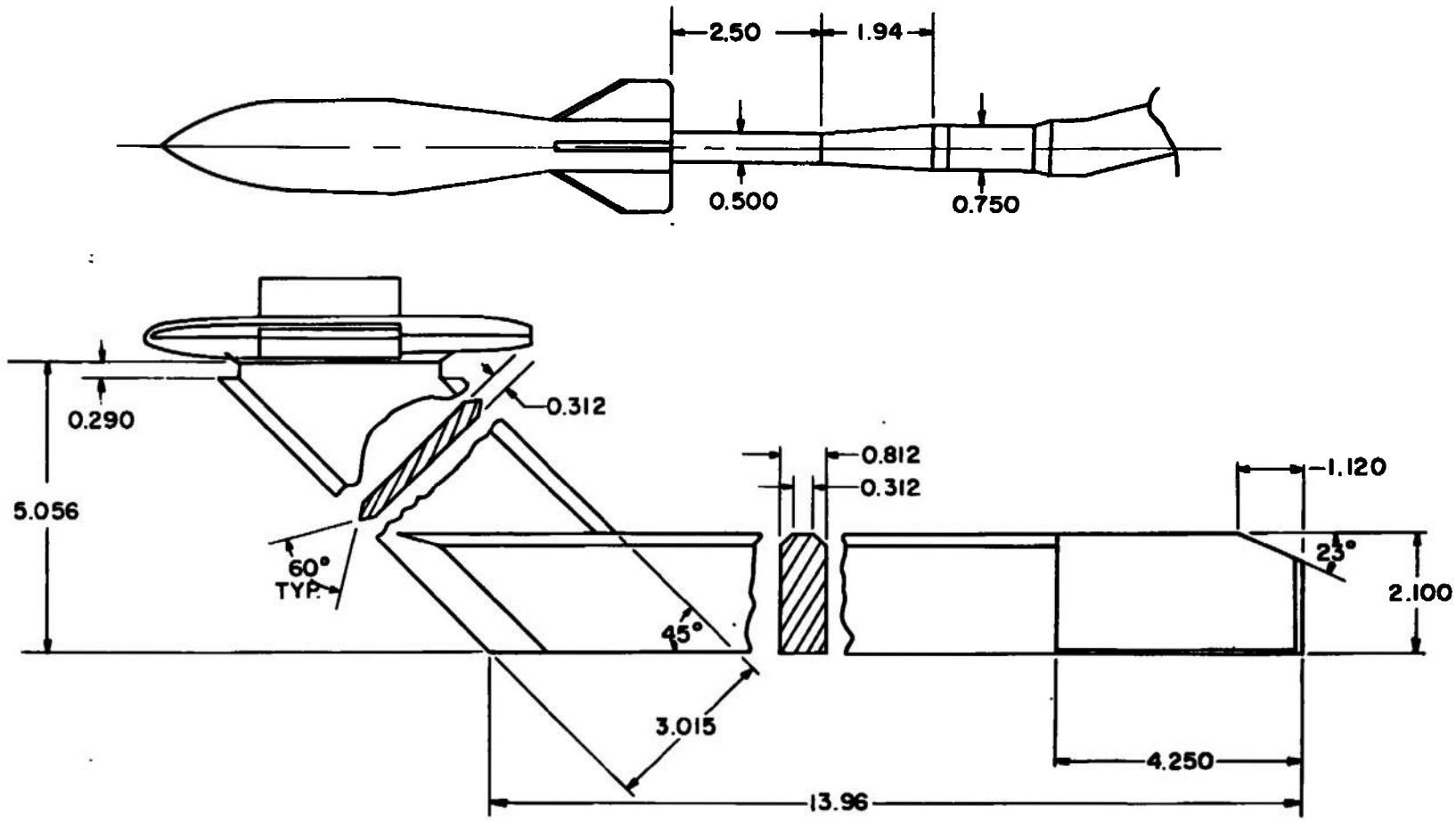

Fig. 8 Basic Details of the Model Support Structure near the Models

Fig. 9 Photograph of a Typical Test Configuration Installed in the Wind Tunnel

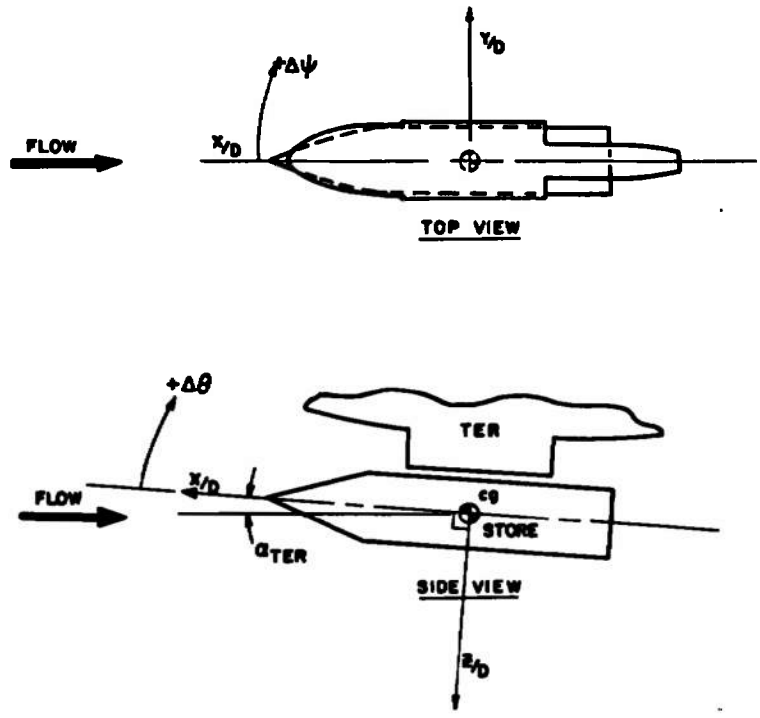

Δφ is positive for clockwise rotation when looking in positive $X_{/D}$ direction

Fig. 10 Reference Axis System for Store Force and Moment Survey Data

IDENTIFICATION	CONFIGURATION	MODELS
1	DUMMY, DUMMY, TEST	SIMULATED M-117. & SIMULATED TER WITH SIMULATED DUMMIES
2	DUMMY, DUMMY, TEST	M-117 & TER WITH M-117 DUMMIES
3	TEST, DUMMY	M-117 & TER WITH M-117 DUMMIES

ALL CONFIGURATIONS – LOOKING UPSTREAM

Fig. 11 Identification of Test Configurations

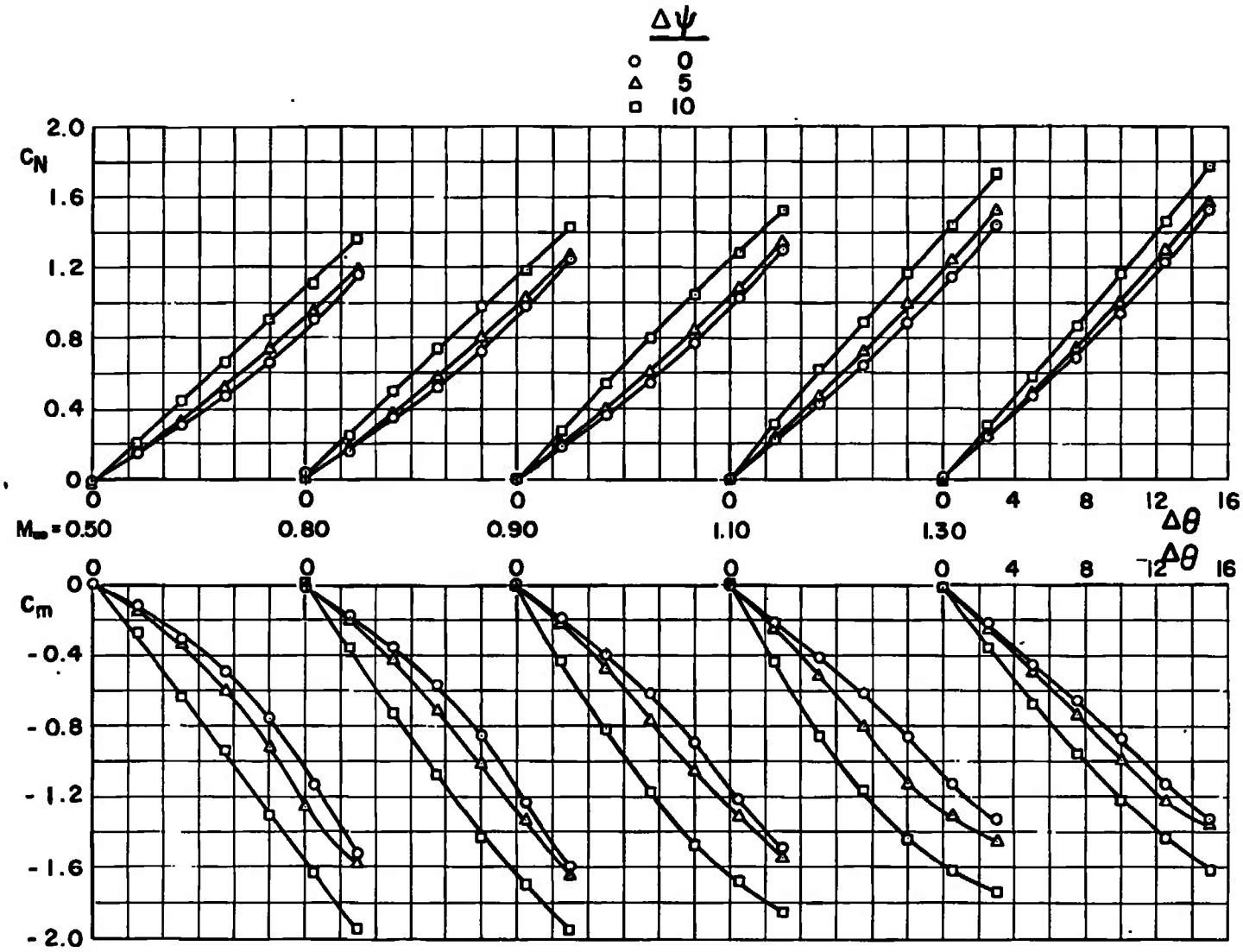

Fig. 12 Free-Stream Stability Data for the M-117 Store Model

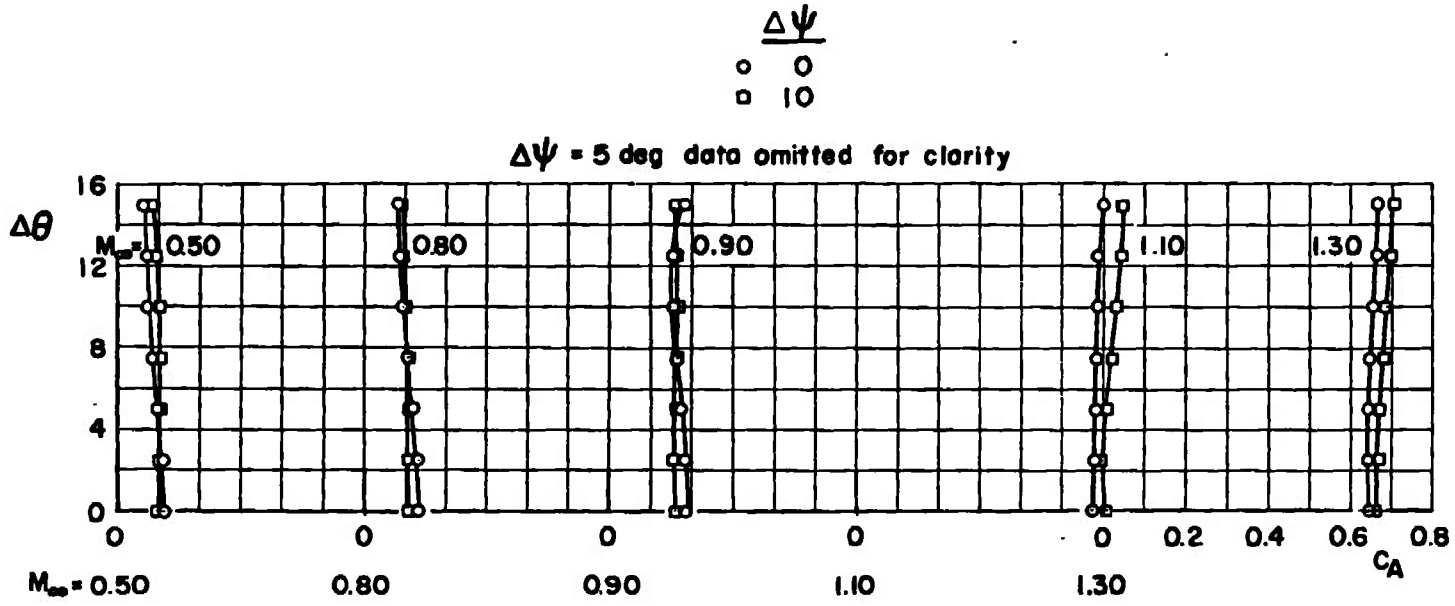

Fig. 12 Concluded

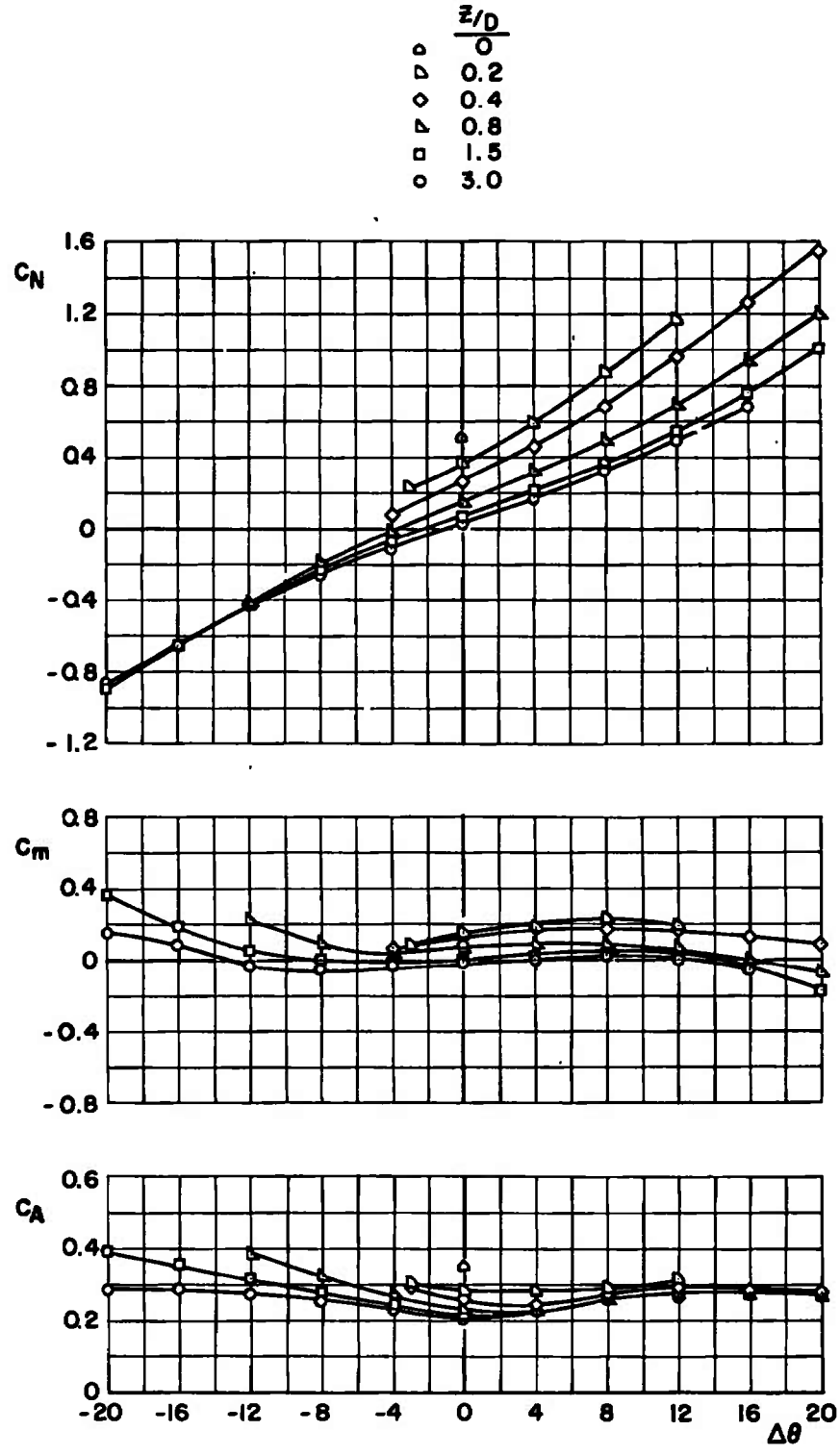

Fig. 13 Force and Moment Data for the Simulated M-117 Showing the Effect of Variations in $\Delta\theta$ at M_∞ = 0.5, Configuration 1; X/D = Y/D = 0, $\Delta\psi = \alpha = 0$

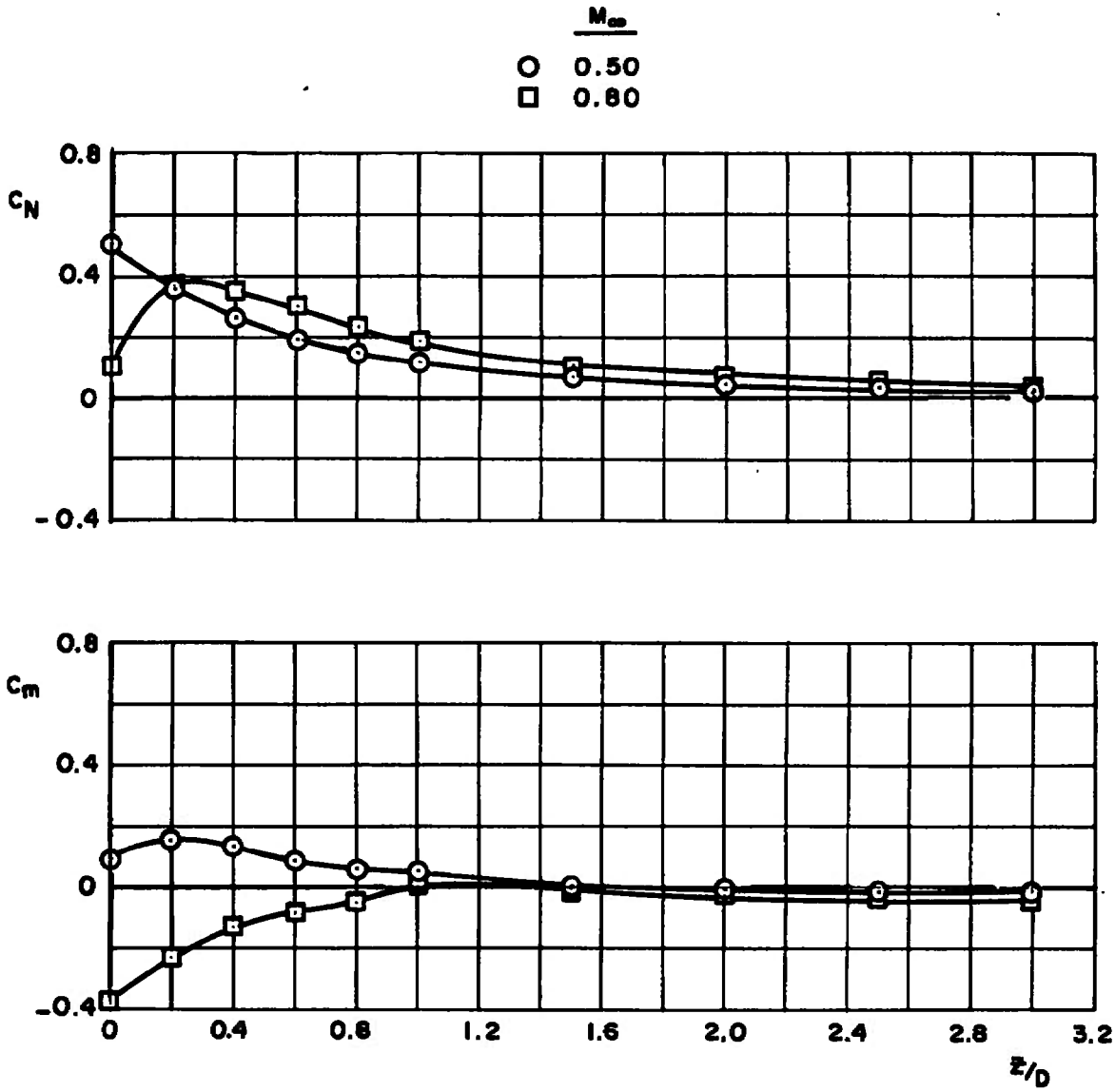

Fig. 14 Effect of Z/D Location on the Force and Moment Coefficients for the Simulated M-117, Configuration 1; X/D = Y/D = 0, $\Delta\psi = \Delta\theta = \alpha = 0$

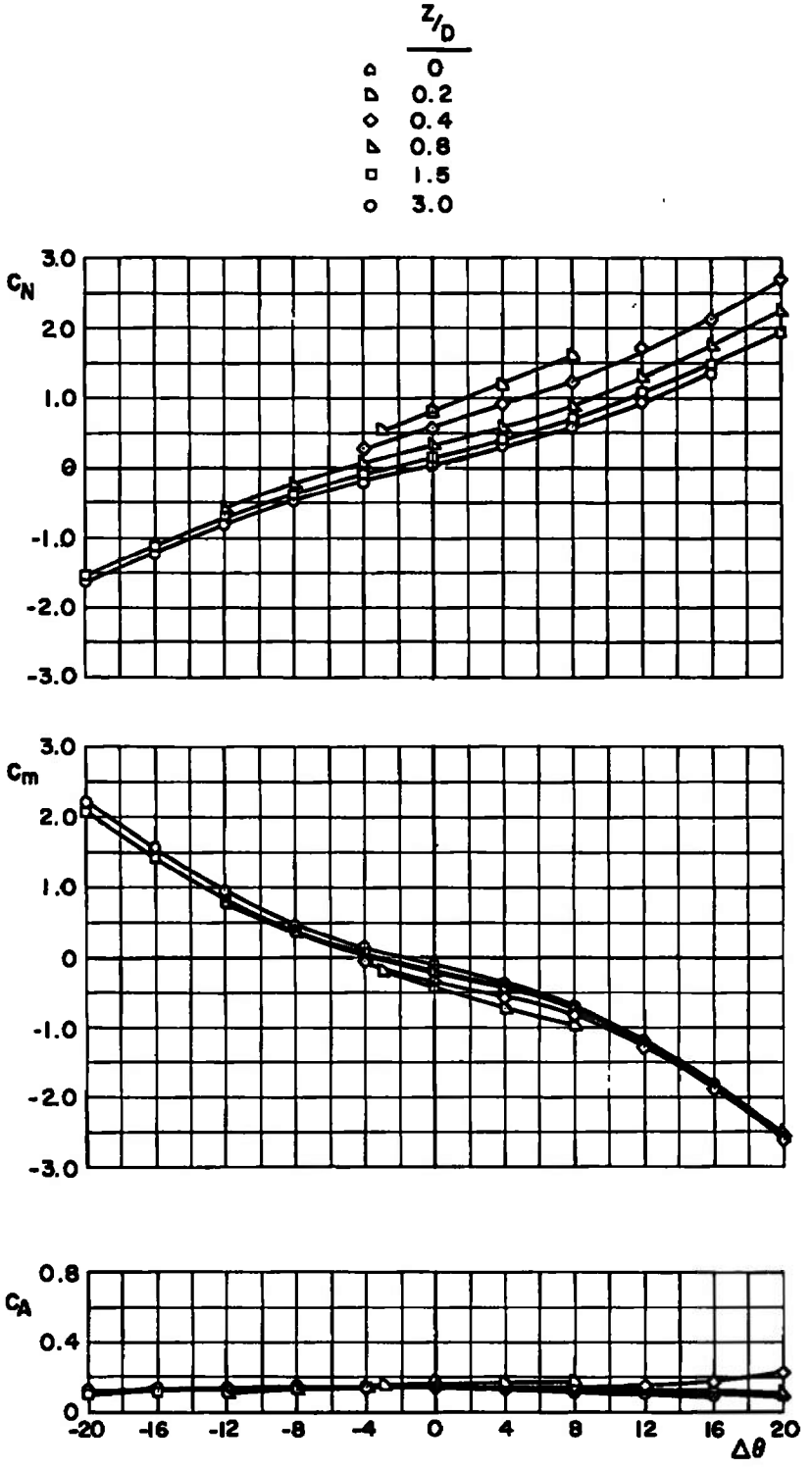

a. $M_\infty = 0.5$

Fig. 15 Force and Moment Data for the M-117 Showing the Effect of Variations in $\Delta\theta$, Configuration 2; X/D = Y/D = 0, $\Delta\psi = \alpha = 0$

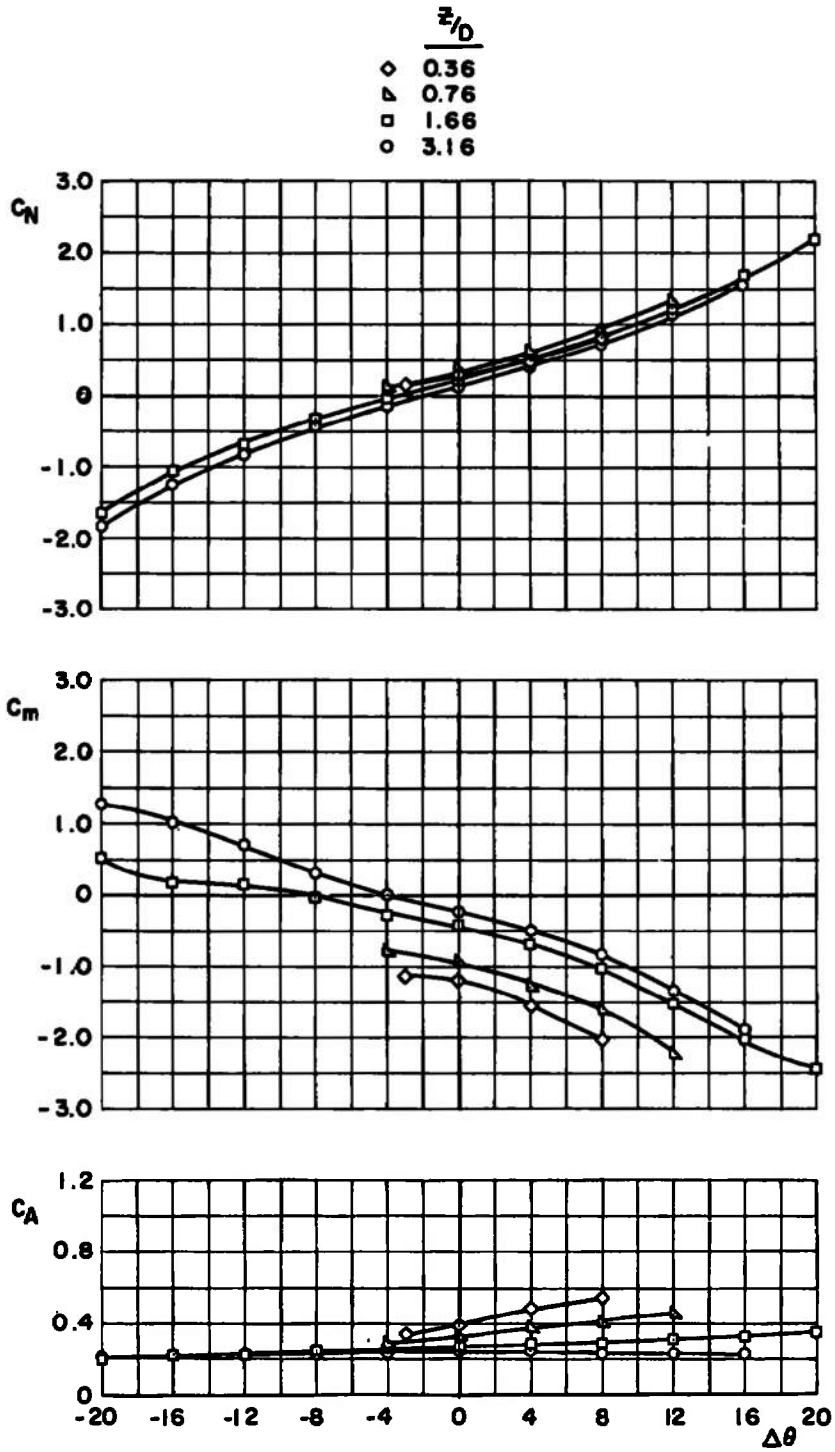

b. $M_\infty = 0.9$

Fig. 15 Continued

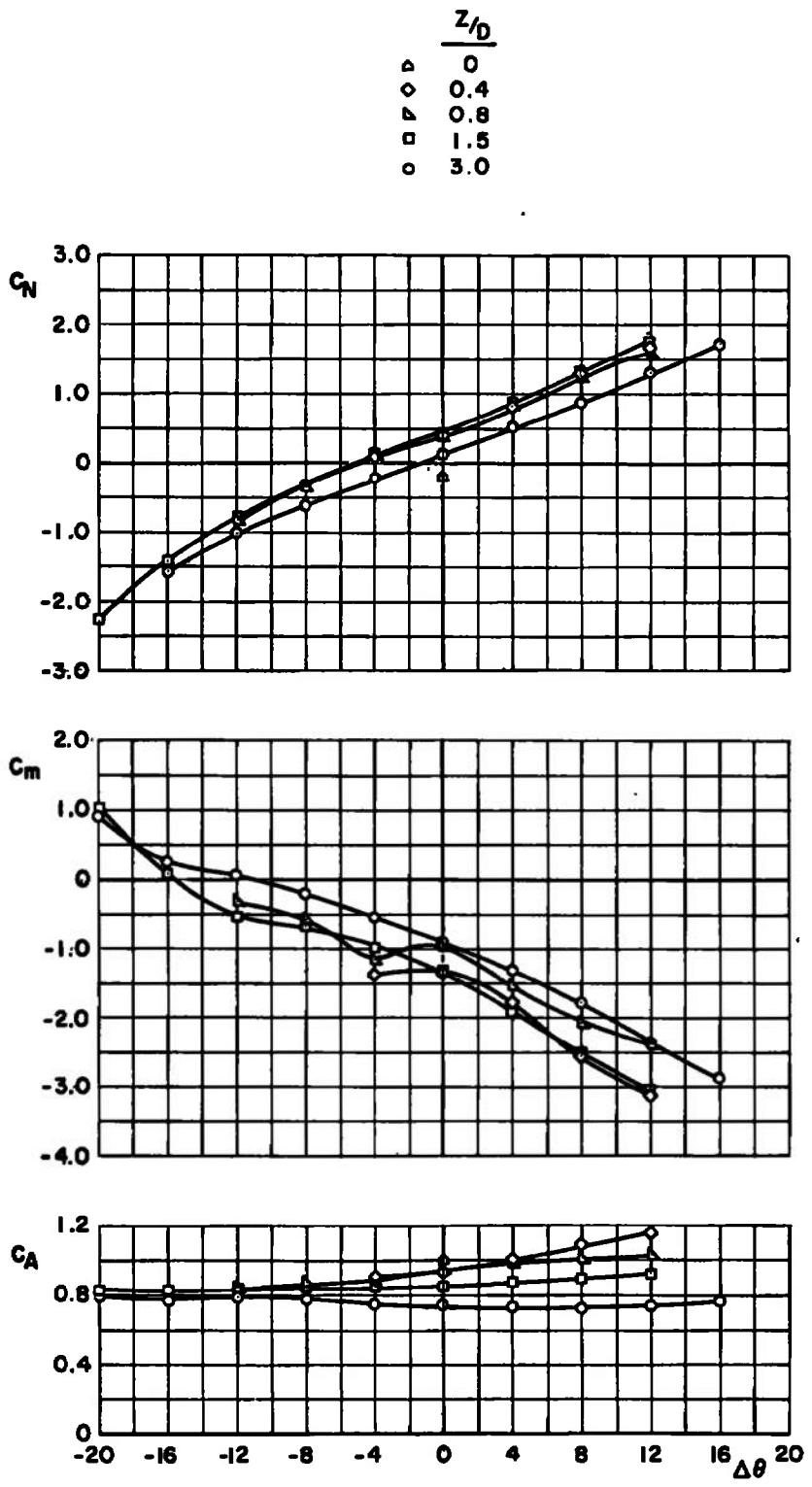

c. $M_\infty = 1.3$

Fig. 15 Concluded

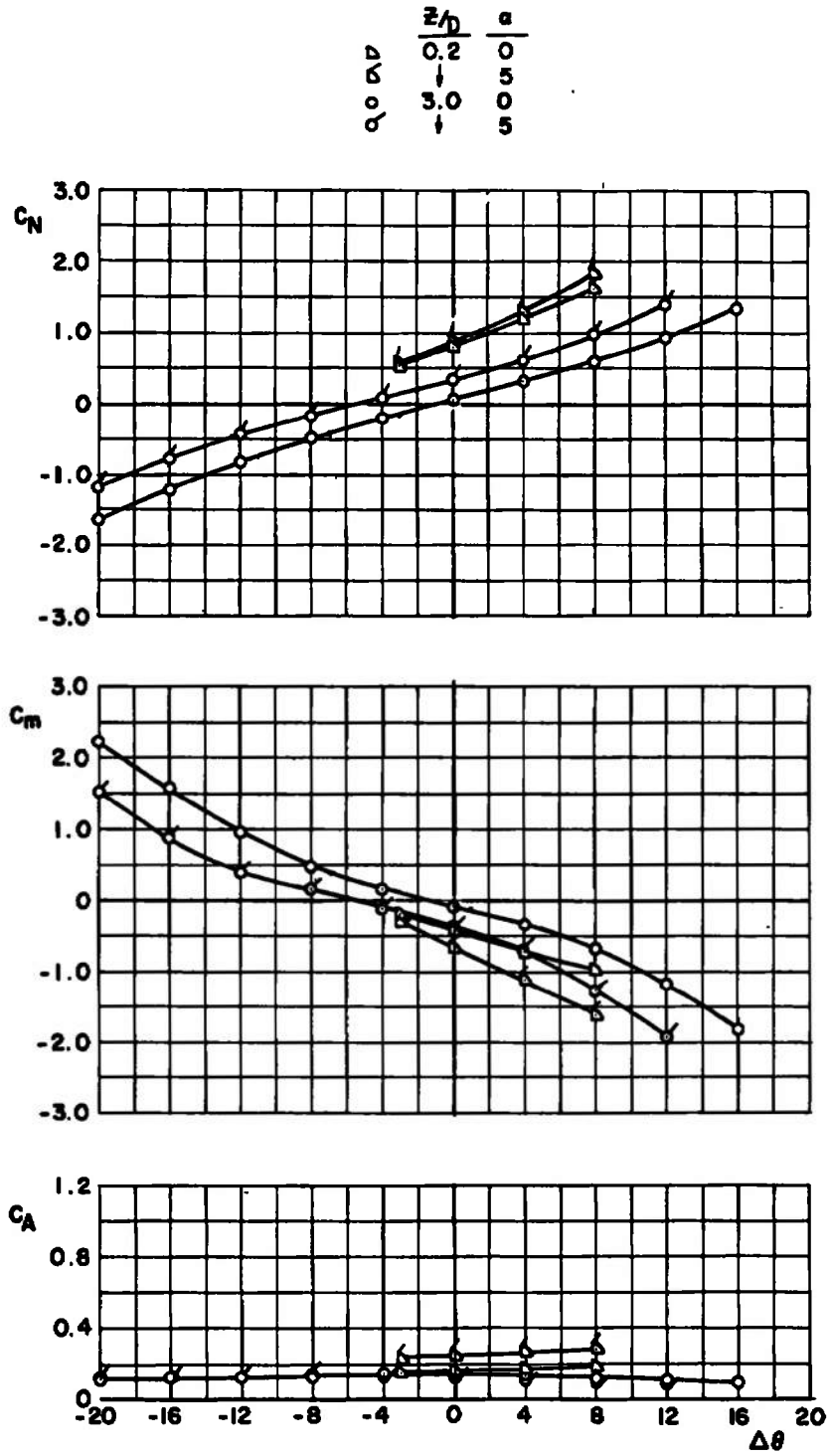

Fig. 16 Comparison of Force and Moment Data for the M-117 at α = 0 and 5 deg, M_∞ = 0.5, Configuration 2; X/D = Y/D = 0, $\Delta\psi$ = 0

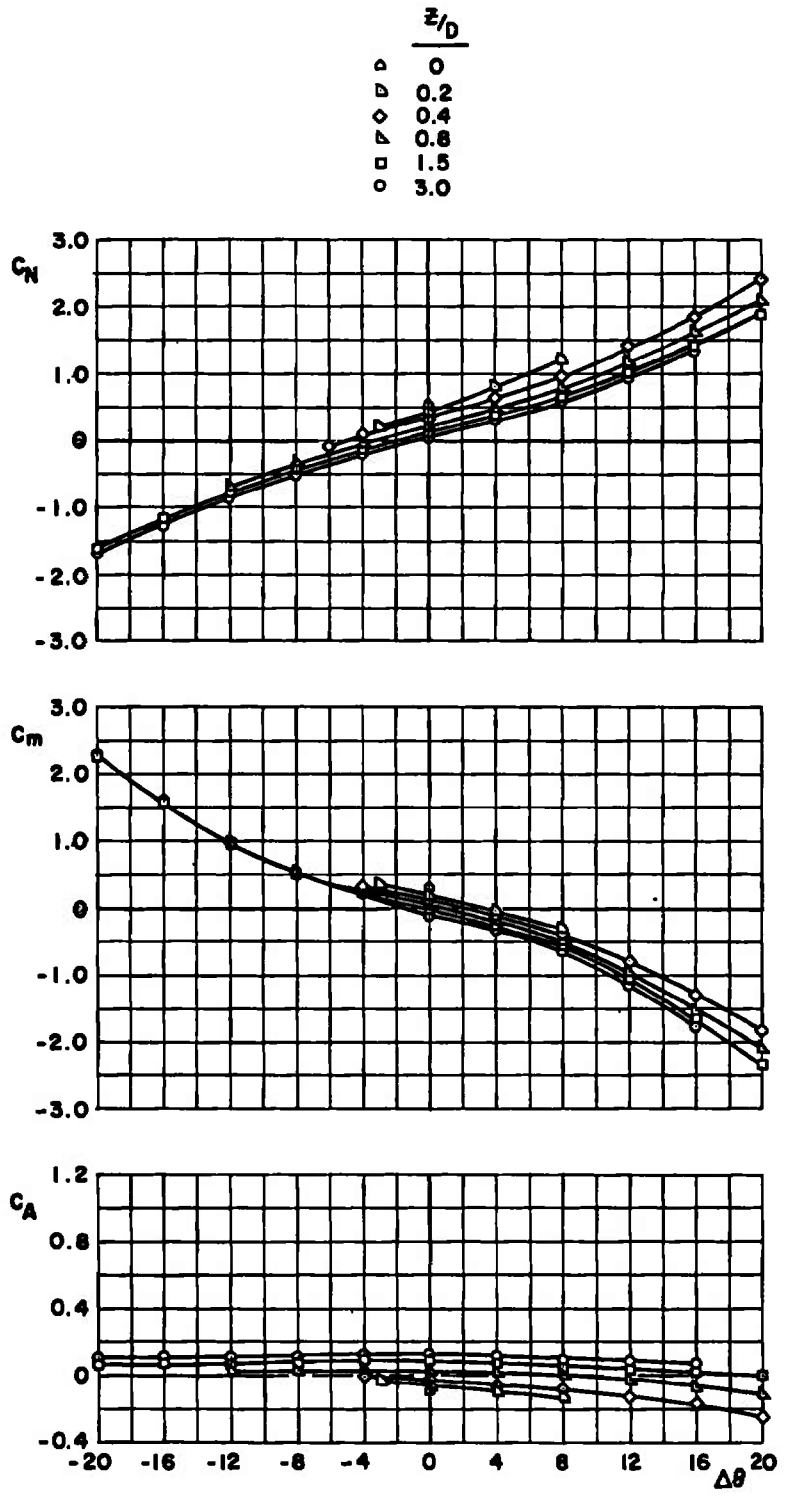

a. $M_\infty = 0.5$

Fig. 17 Force and Moment Data for the M-117 Showing the Effect of Variations in $\Delta\theta$, Configuration 2; X/D = -1, Y/D = 0, $\Delta\psi = \alpha = 0$

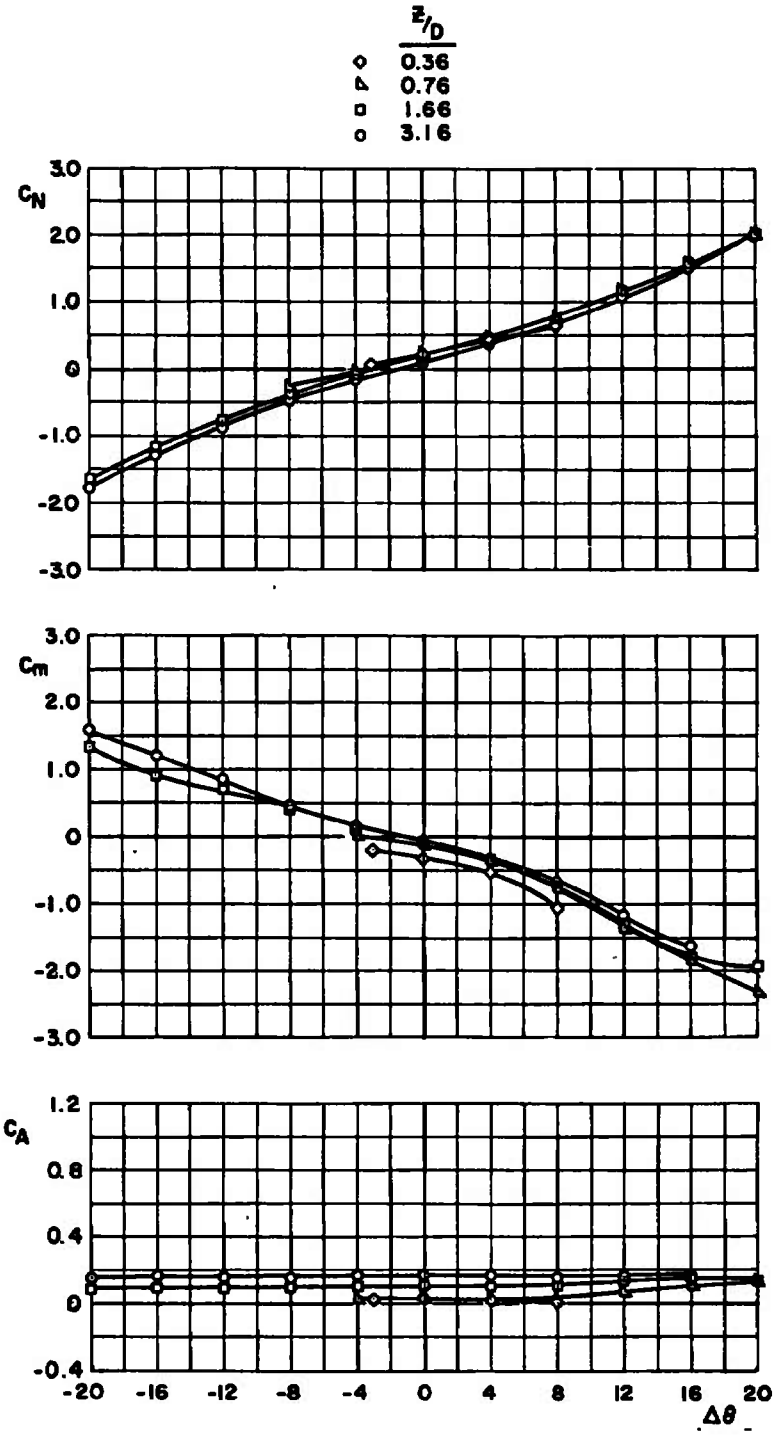

b. $M_\infty = 0.9$

Fig. 17 Continued

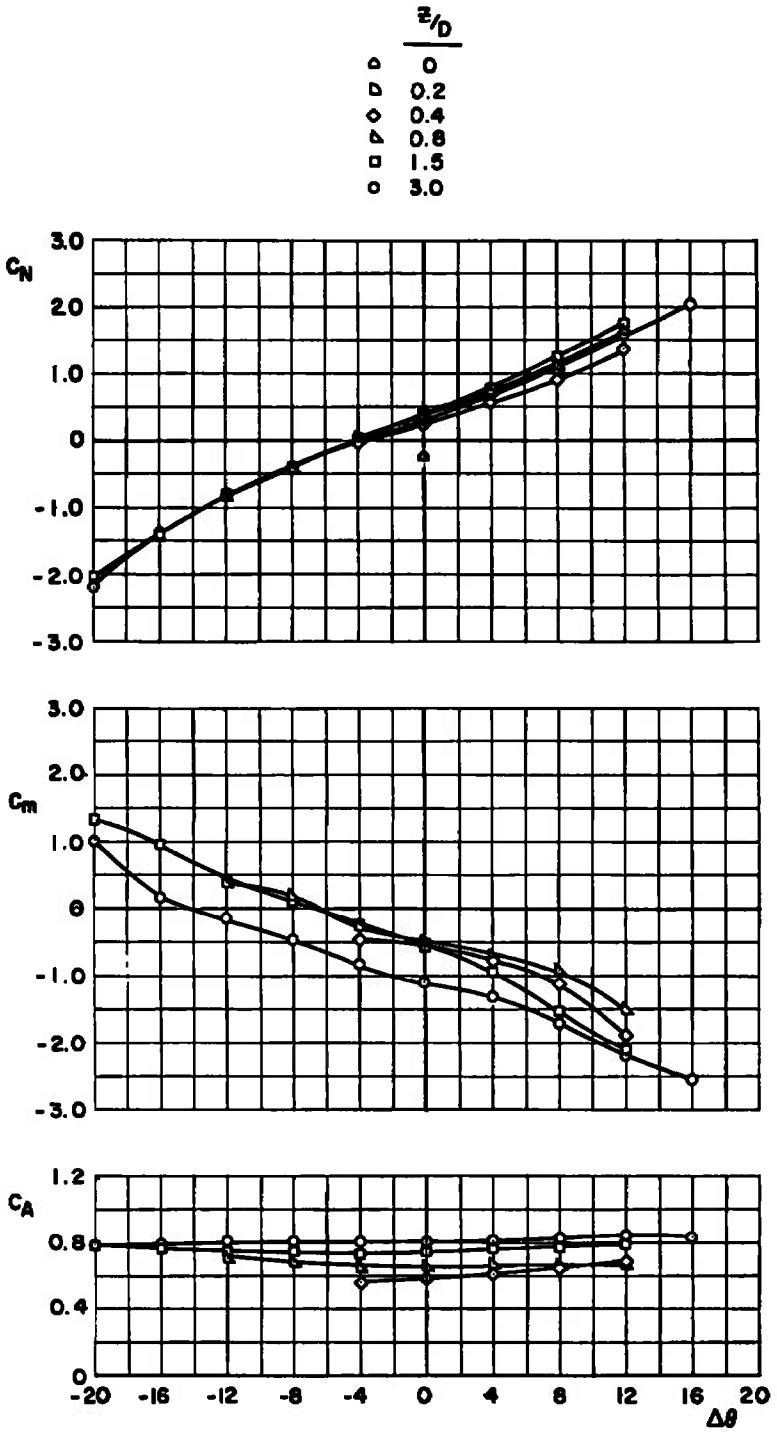

c. $M_\infty = 1.30$

Fig. 17 Concluded

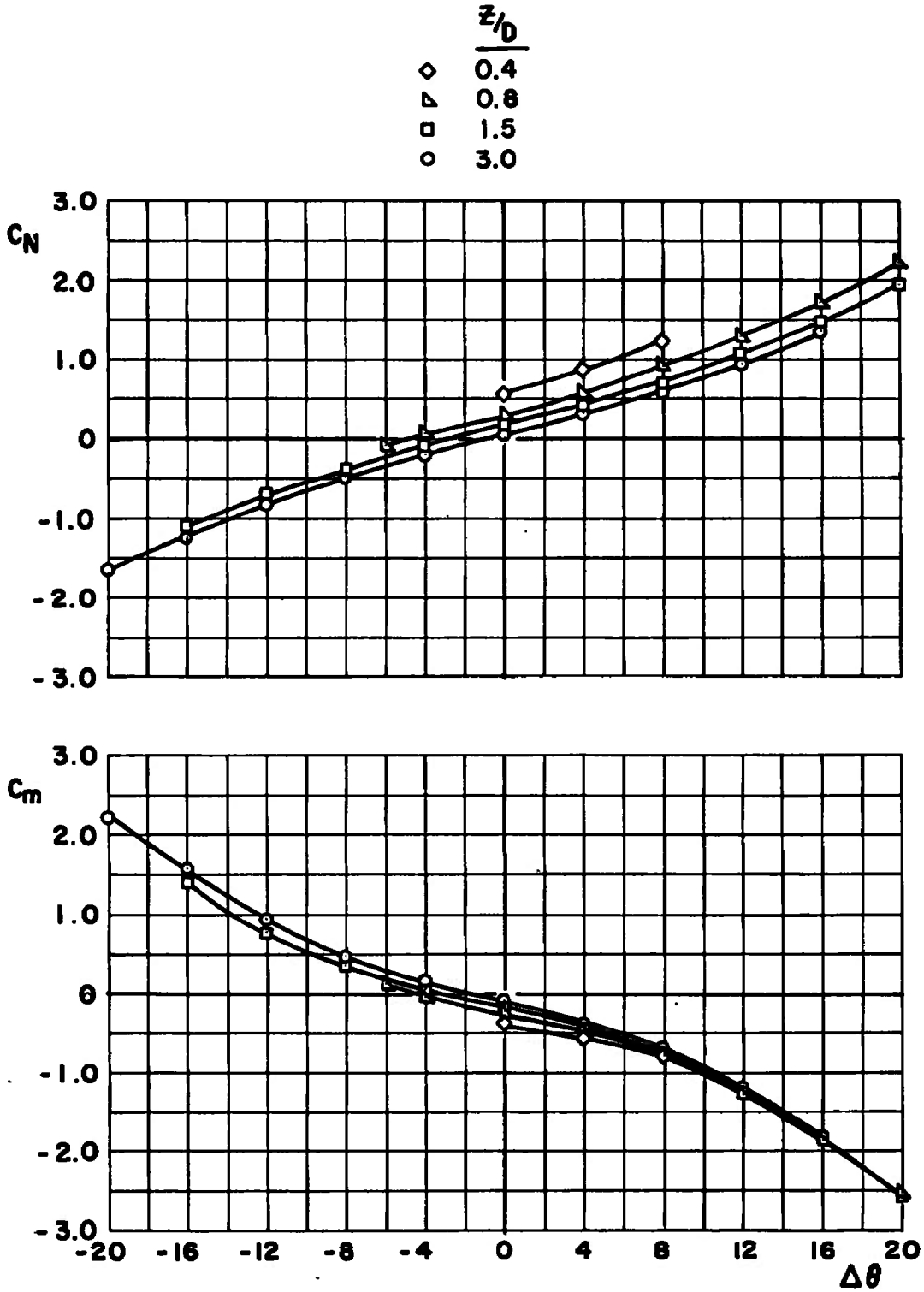

a. $M_\infty = 0.5$

Fig. 18 Force and Moment Data for the M-117 Showing the Effect of Variations in $\Delta\theta$, Configuration 2, Y/D = 0.357, X/D = 0, $\Delta\psi = \alpha = 0$

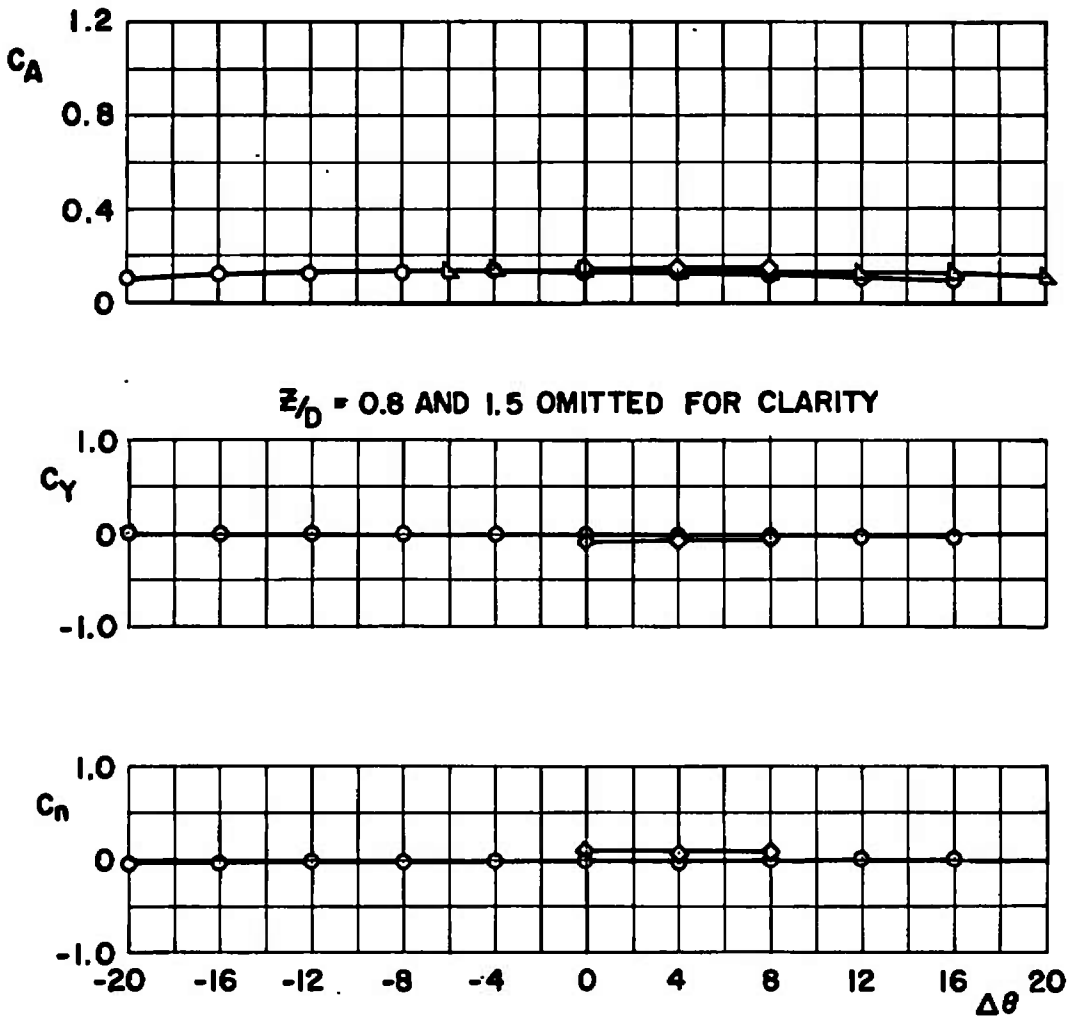

a. Concluded
Fig. 18 Continued

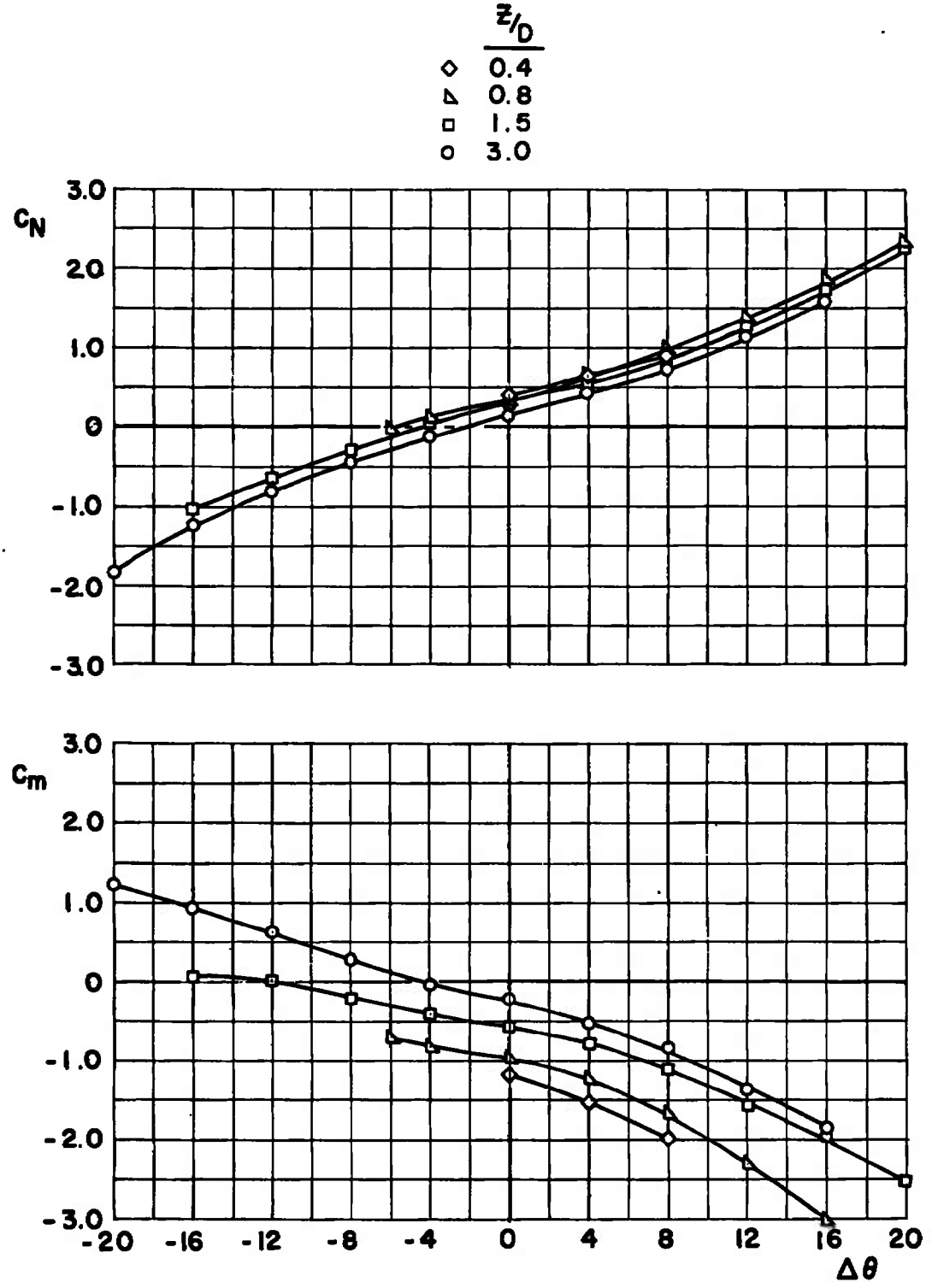

b. $M_\infty = 0.9$

Fig. 18 Continued

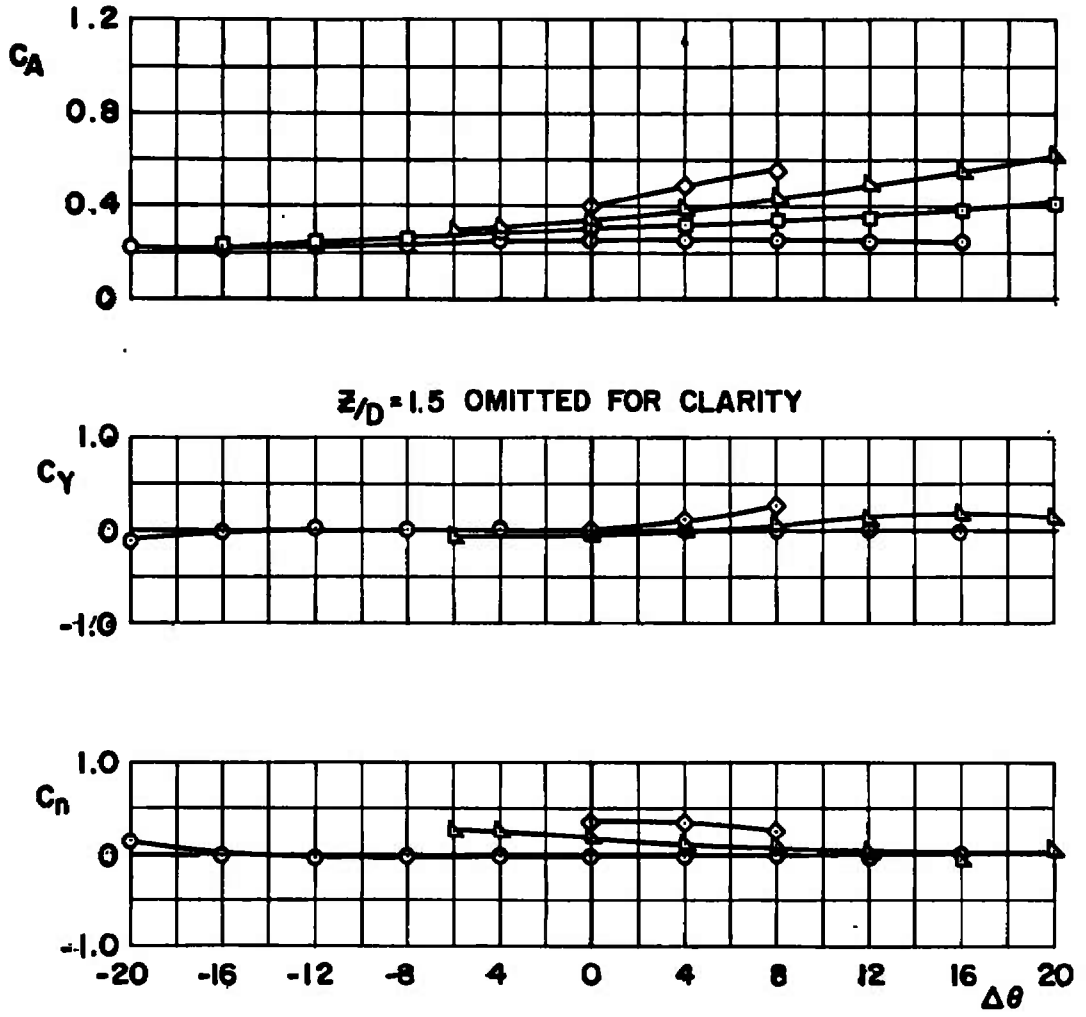

b. Concluded
Fig. 18 Continued

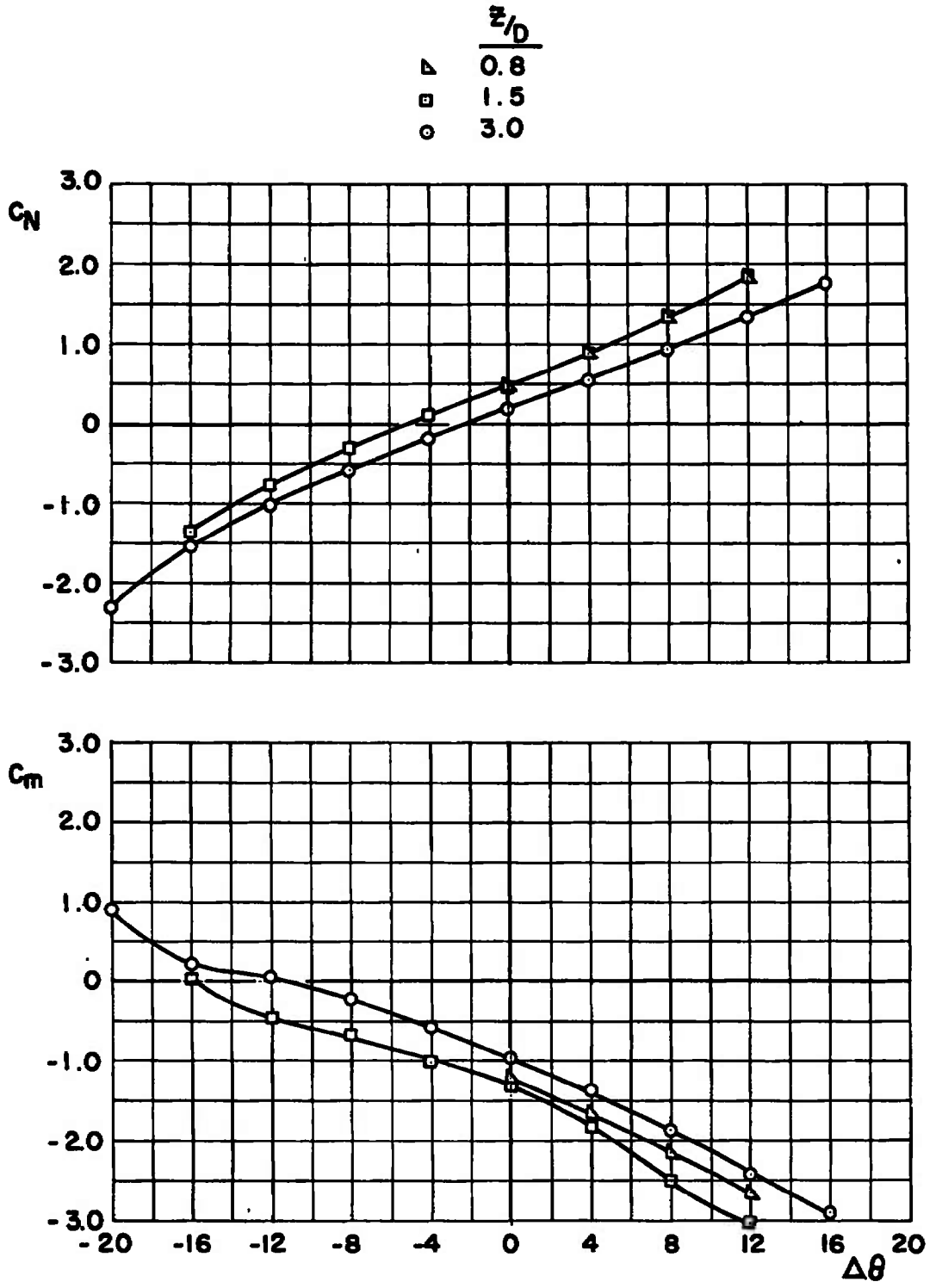

c. $M_\infty = 1.3$

Fig. 18 Continued

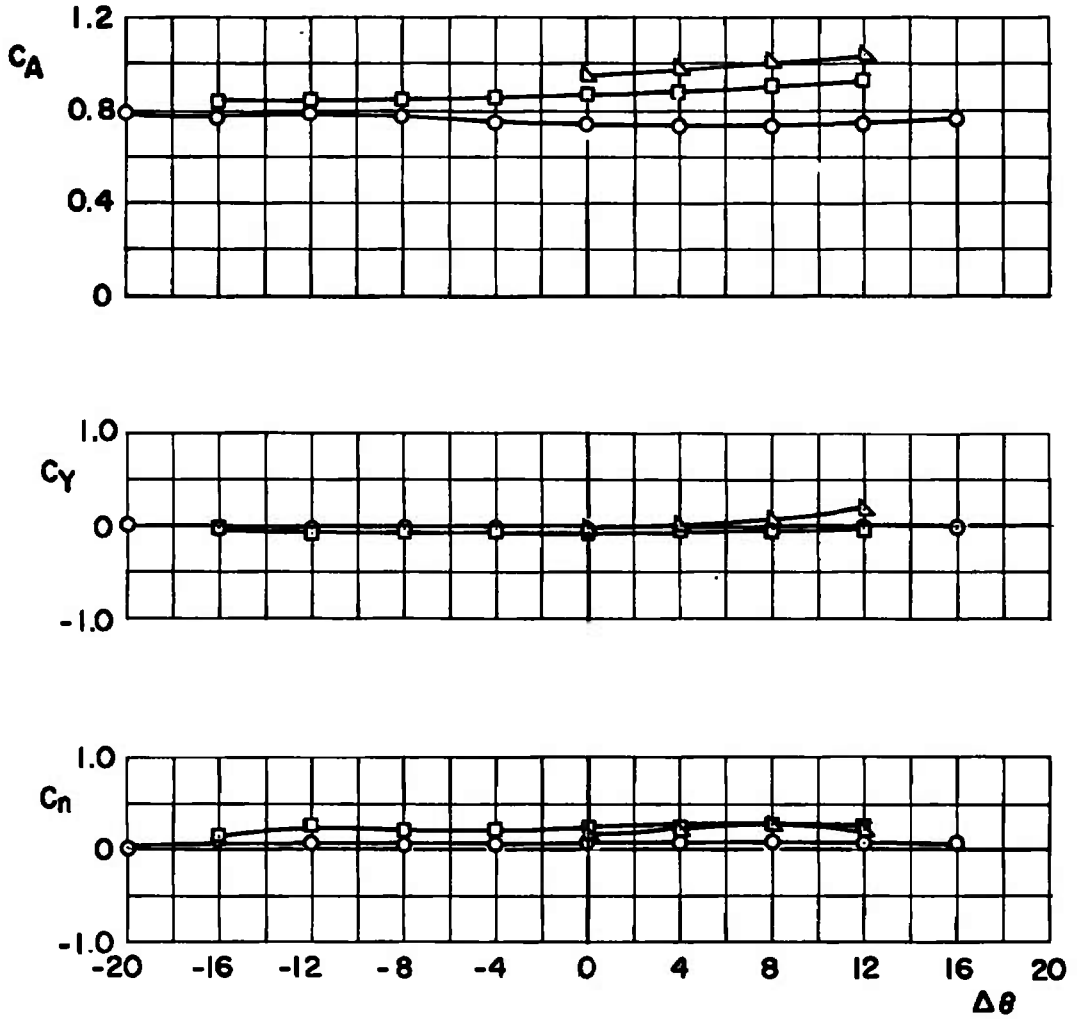

c. Concluded
Fig. 18 Concluded

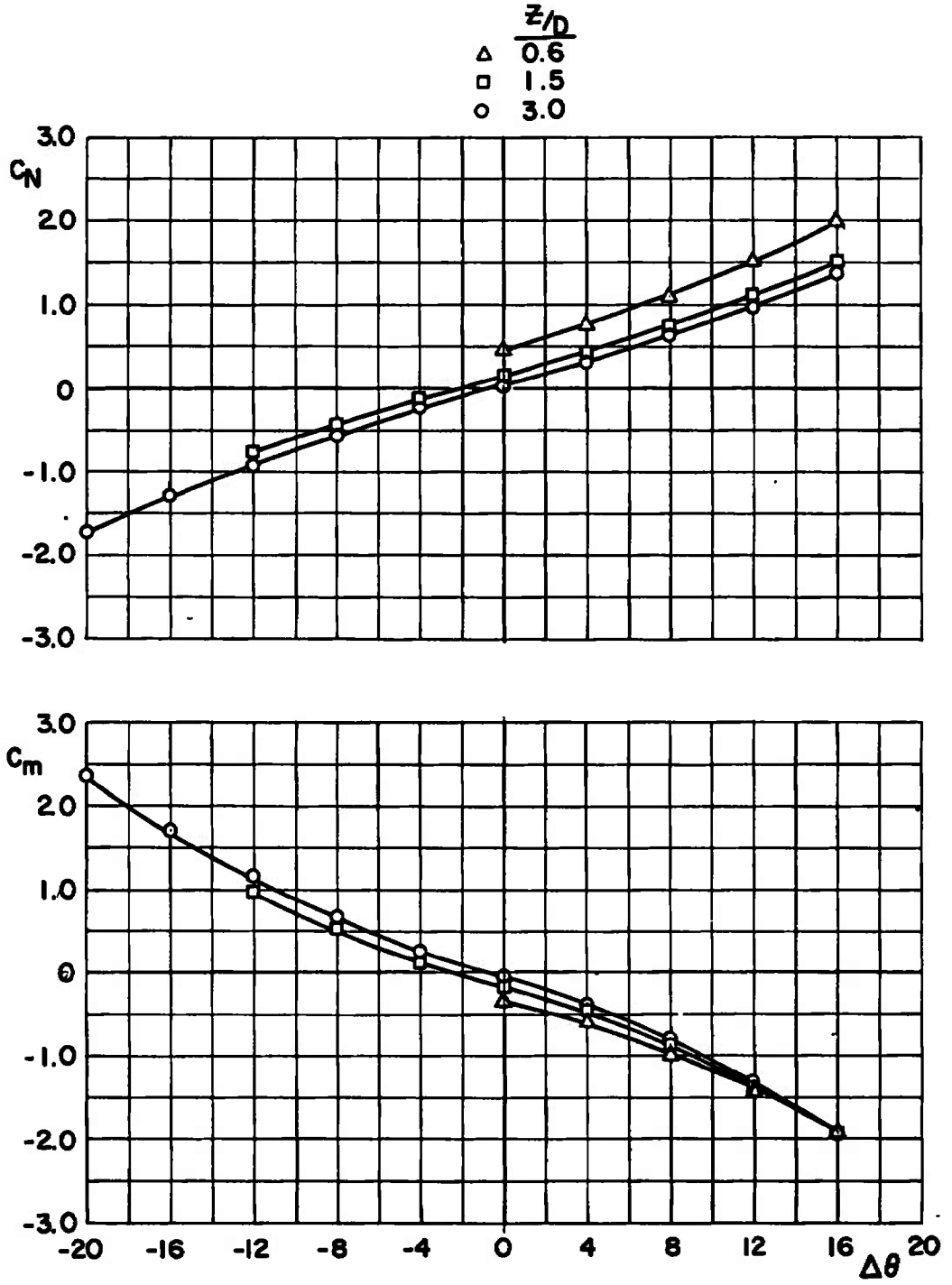

a. $M_\infty = 0.5$

Fig. 19 Force and Moment Data for the M-117 Showing the Effect of Variation in $\Delta\theta$, Configuration 2; $\Delta\psi$ = 5 deg, X/D = Y/D = 0, α = 0

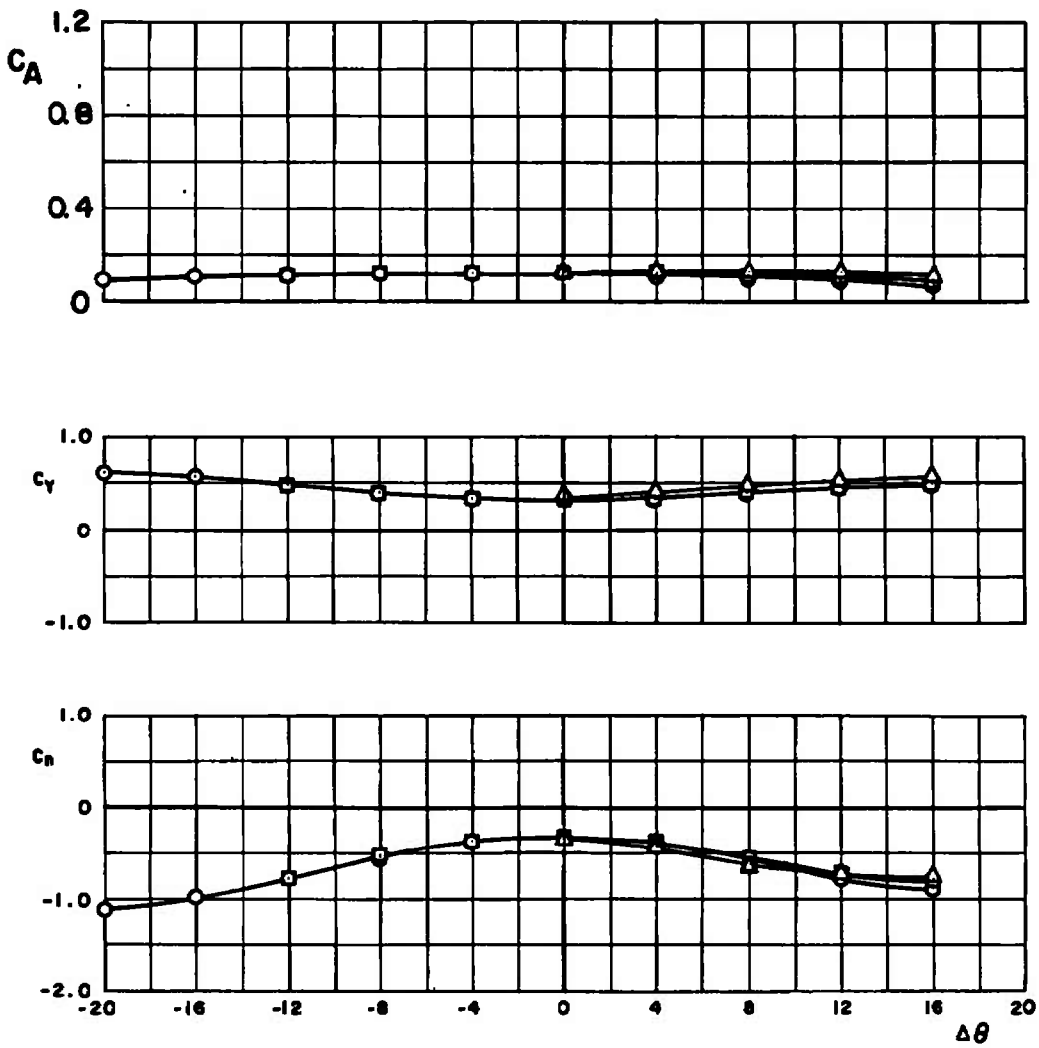

a. Concluded
Fig. 19 Continued

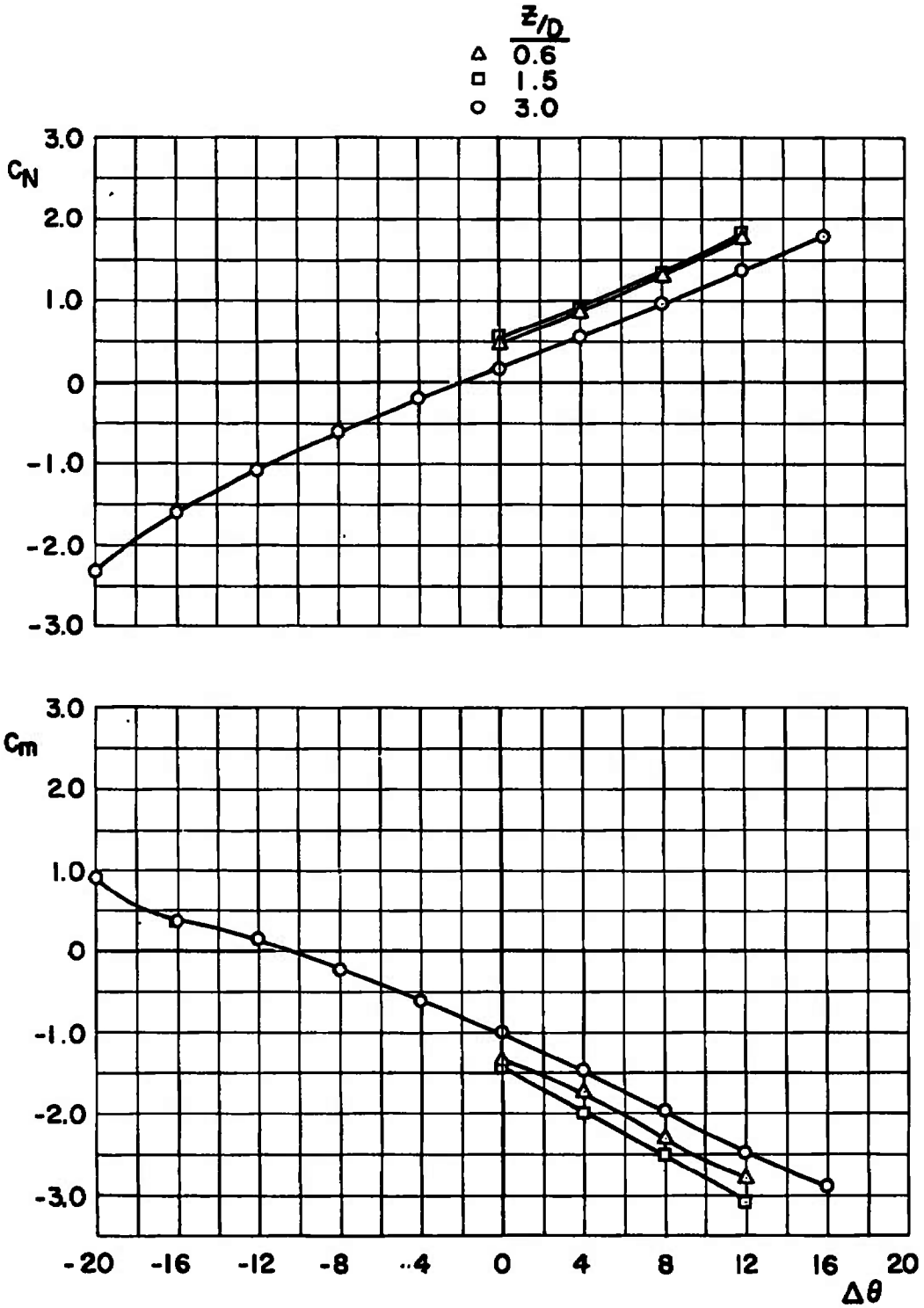

b. $M_\infty = 1.3$

Fig. 19 Continued

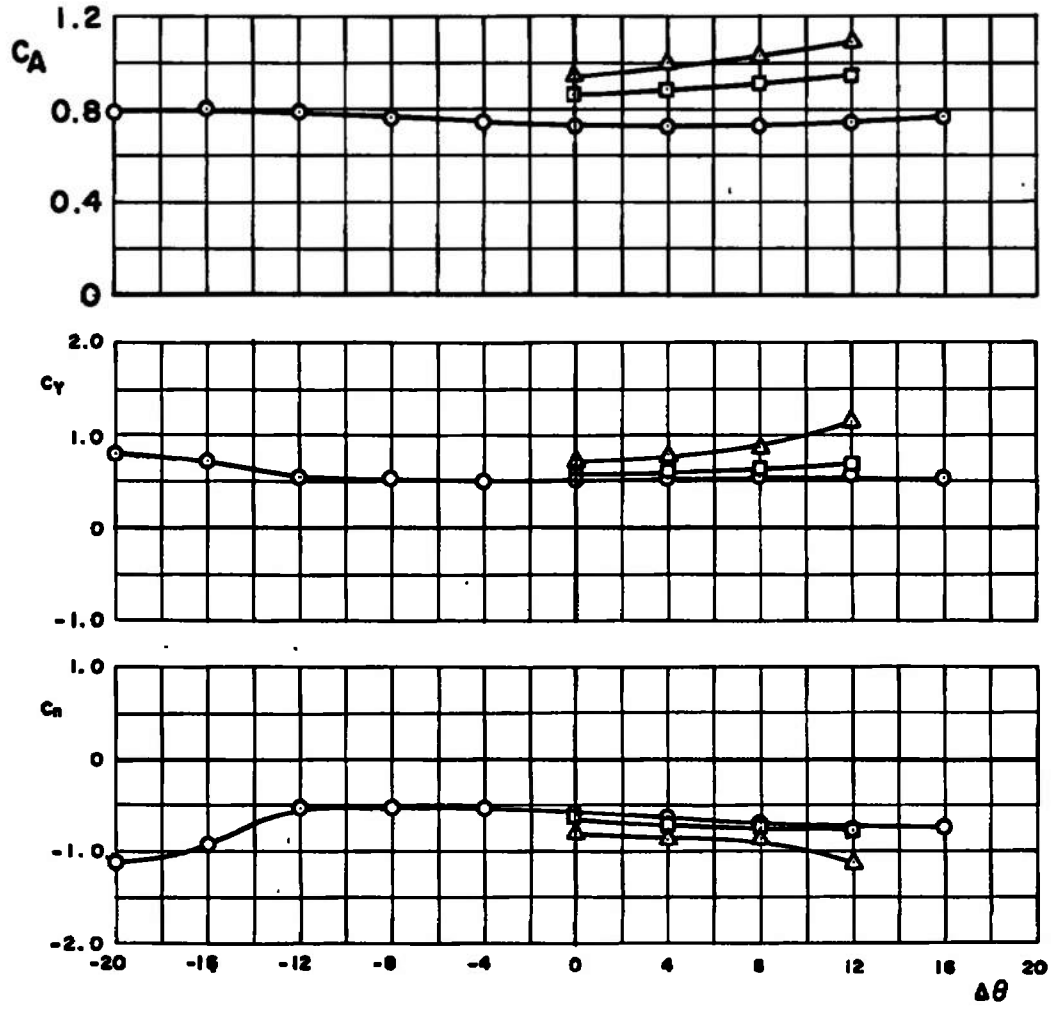

b. Concluded
Fig. 19 Concluded

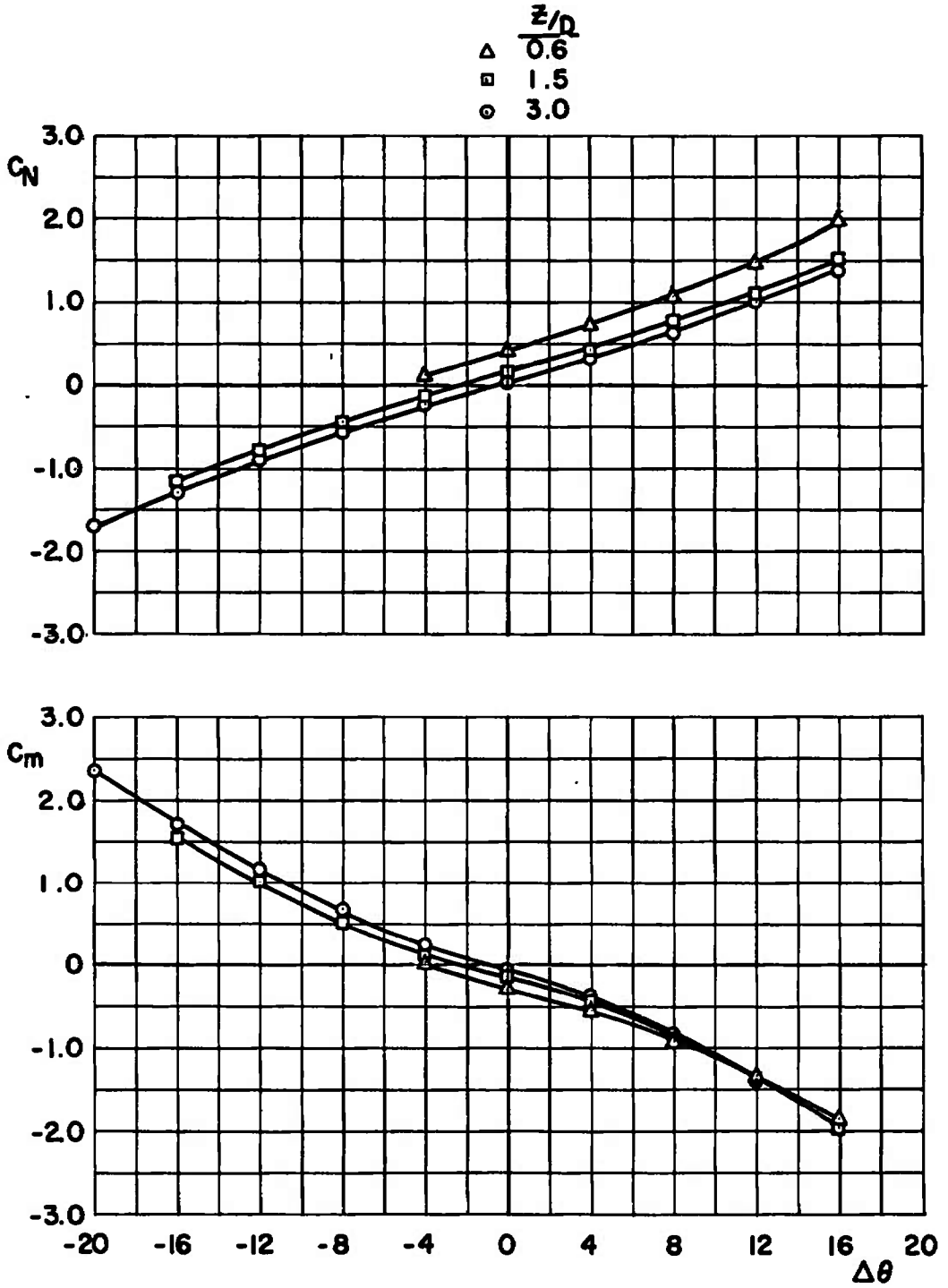

a. $M_\infty = 0.5$

Fig. 20 Force and Moment Data for the M-117 Showing the Effect of Variations in $\Delta\theta$, Configuration 2; Y/D = 0.357, $\Delta\psi$ = 5 deg, X/D = 0, α = 0

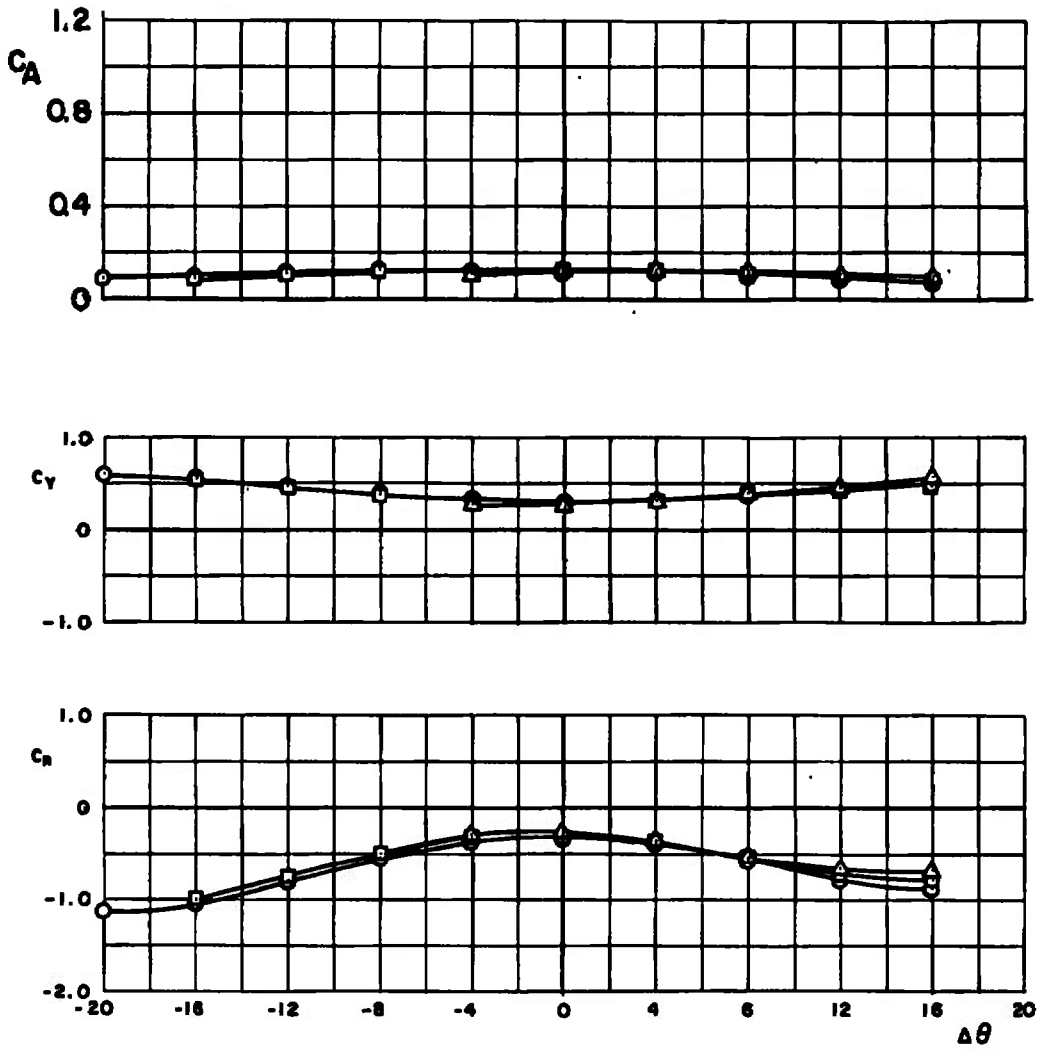

a. Concluded
Fig. 20 Continued

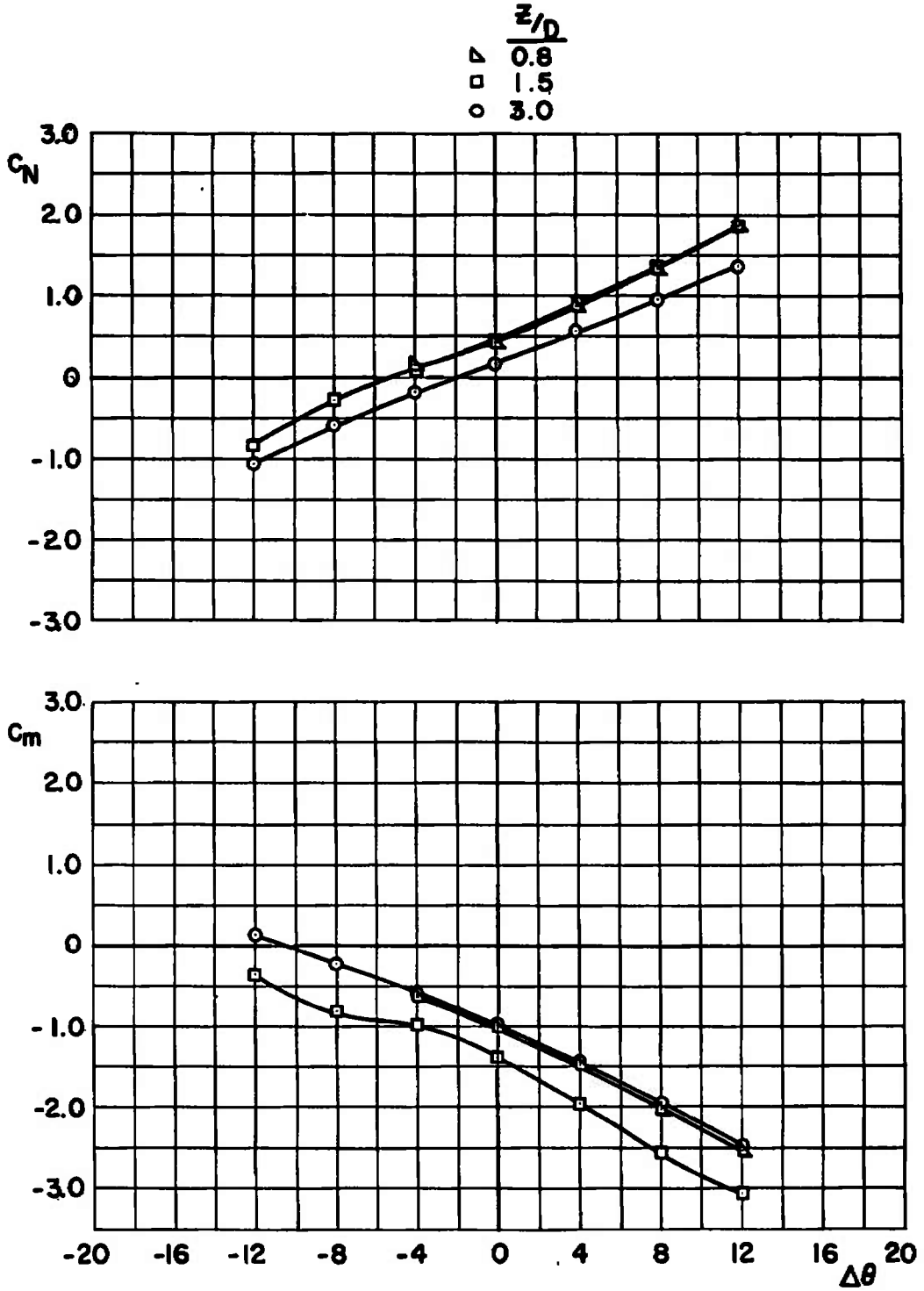

b. $M_\infty = 1.3$
Fig. 20 Continued

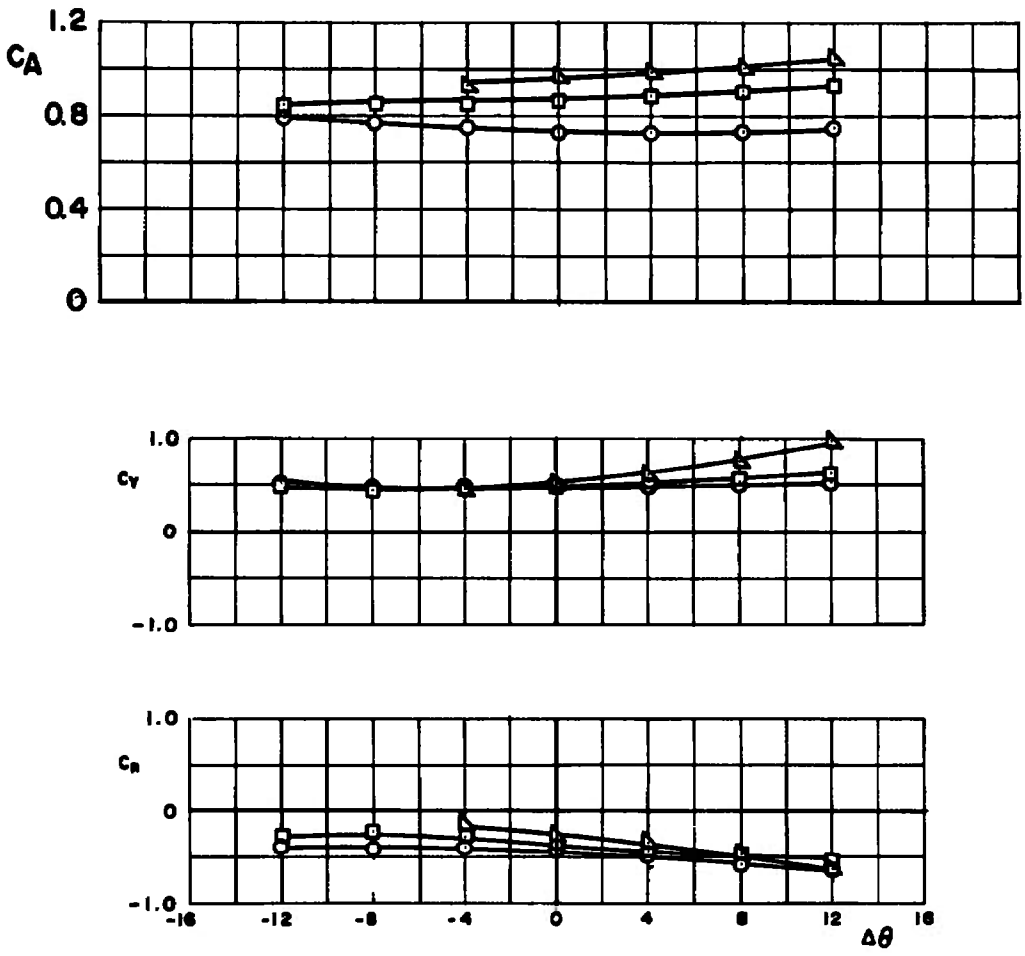

b. Concluded

Fig. 20 Concluded

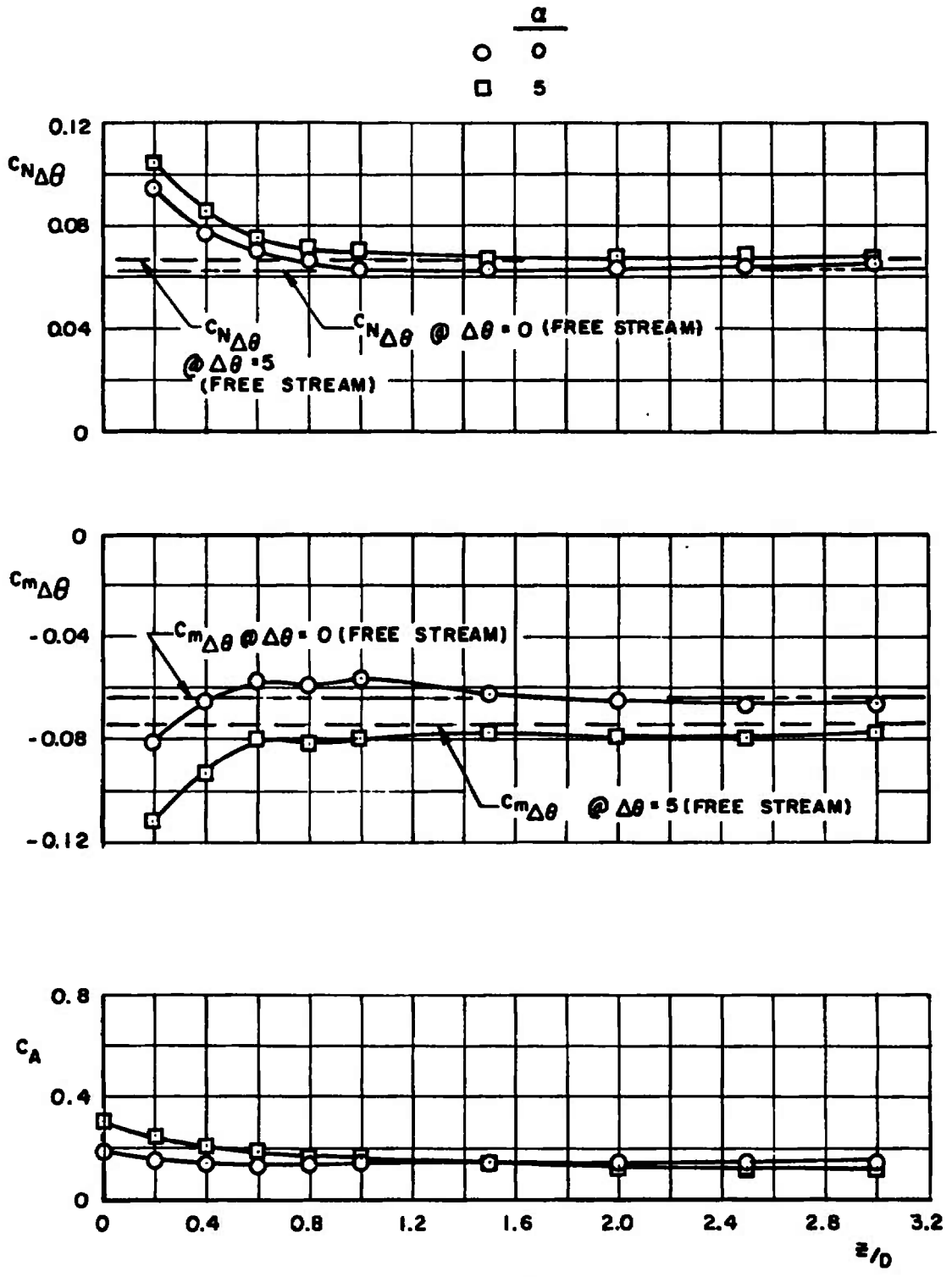

a. $M_\infty = 0.5$

Fig. 21 Effect of Z/D Location on the Normal-Force and Pitching-Moment Curve Slopes and Axial-Force Coefficient for the M-117, Configuration 2; X/D = Y/D = 0, $\Delta\psi = 0$

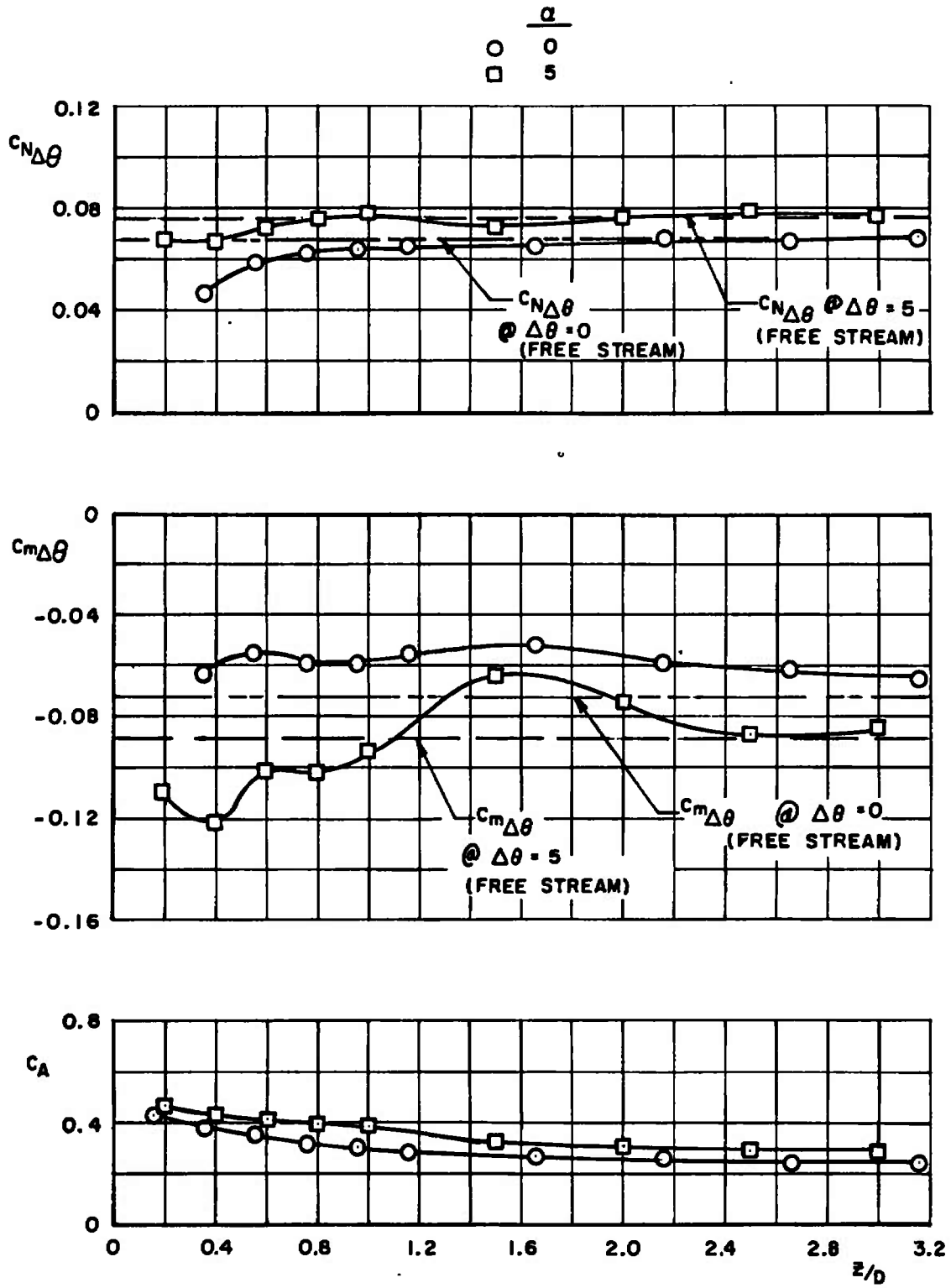

b. $M_\infty = 0.9$

Fig. 21 Concluded

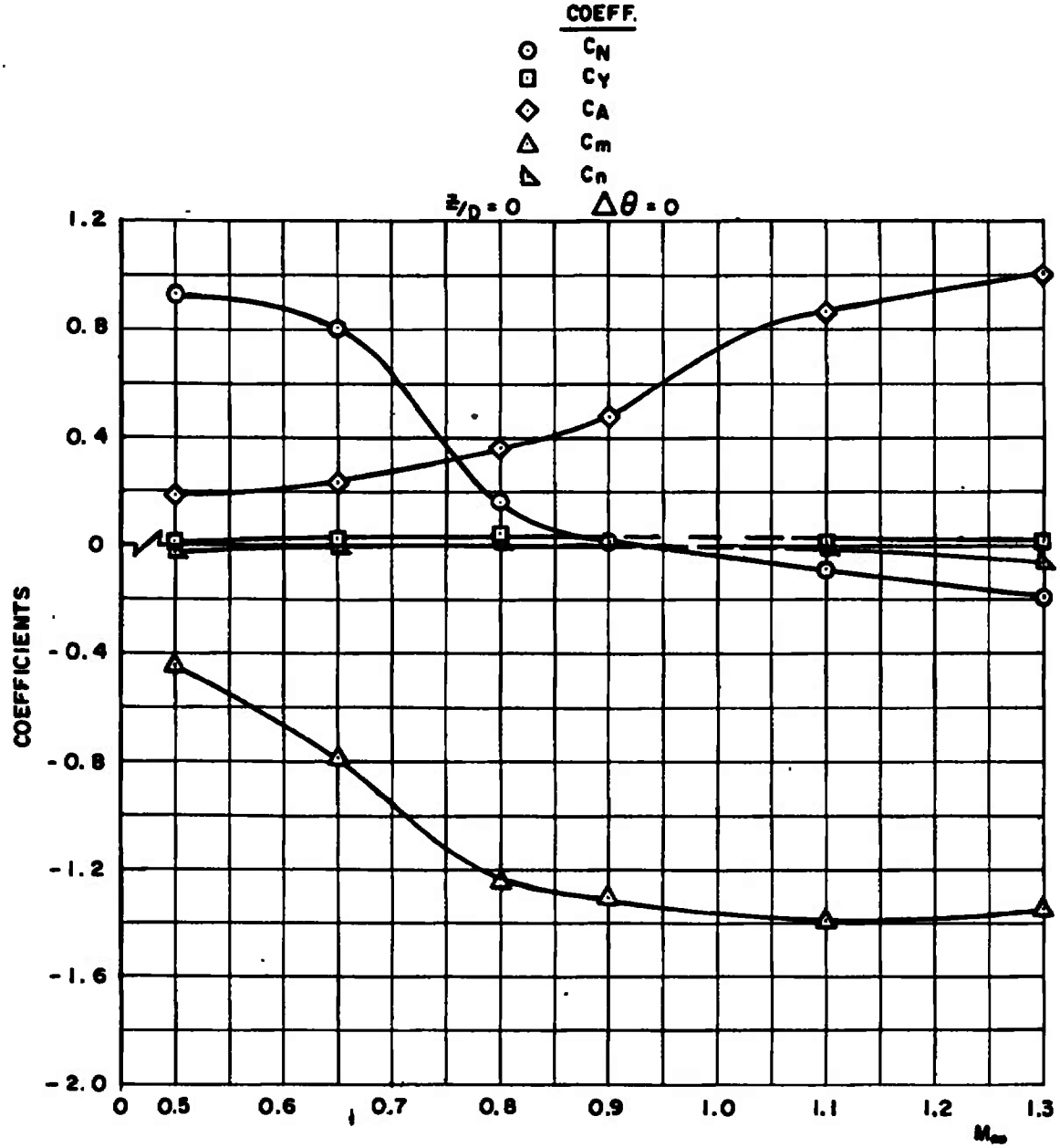

Fig. 22 Effect of Mach Number on the Aerodynamic Forces and Moments Acting on the M-117 in the Carriage Position, Configuration 2; X/D = Y/D = 0, $\Delta\psi = a = 0$

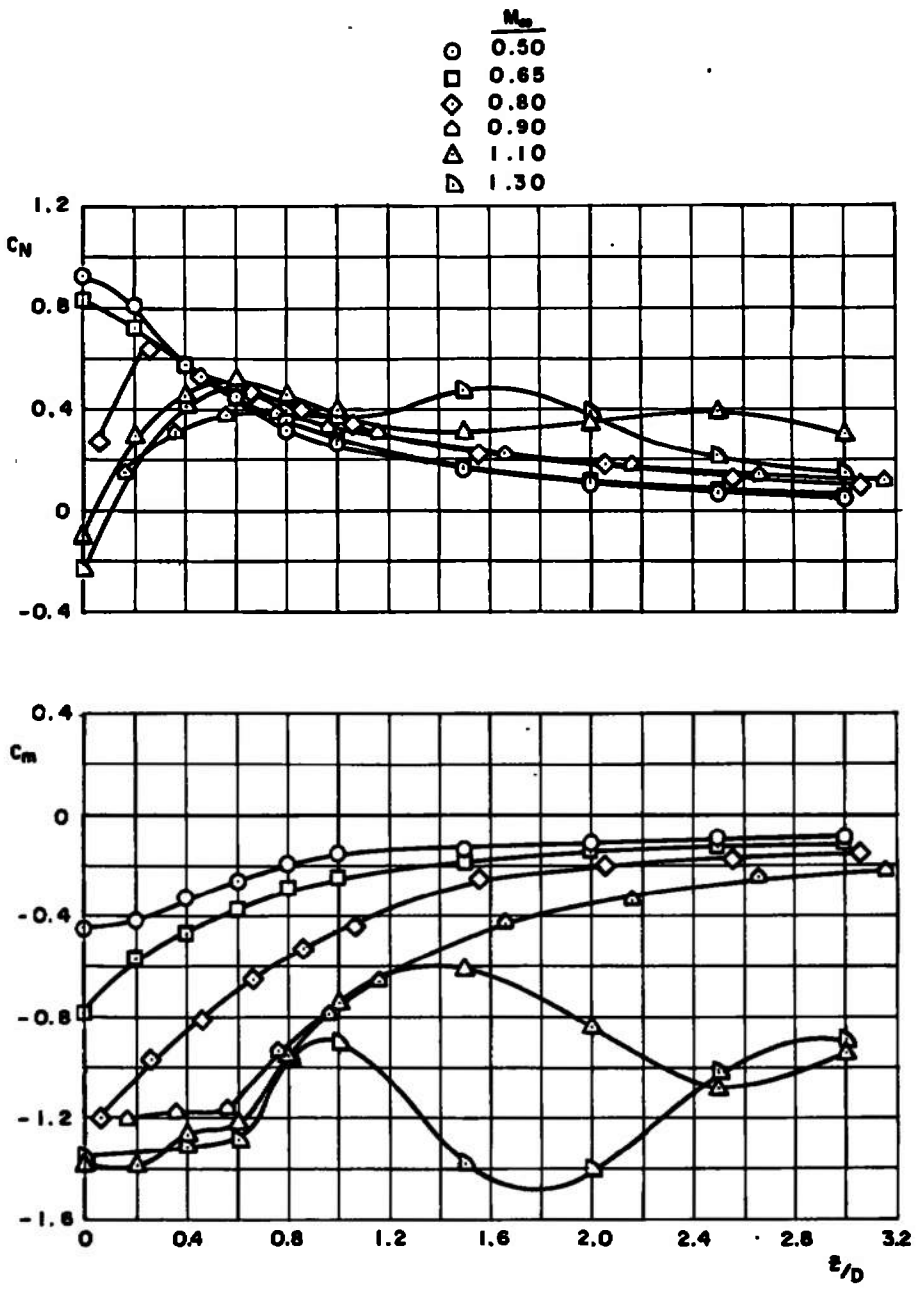

a. α = 0 deg

Fig. 23 Effect of Z/D Location on the Force and Moment Coefficients for the M-117, Configuration 2; X/D = Y/D = 0, $\Delta\psi = \Delta\theta = 0$

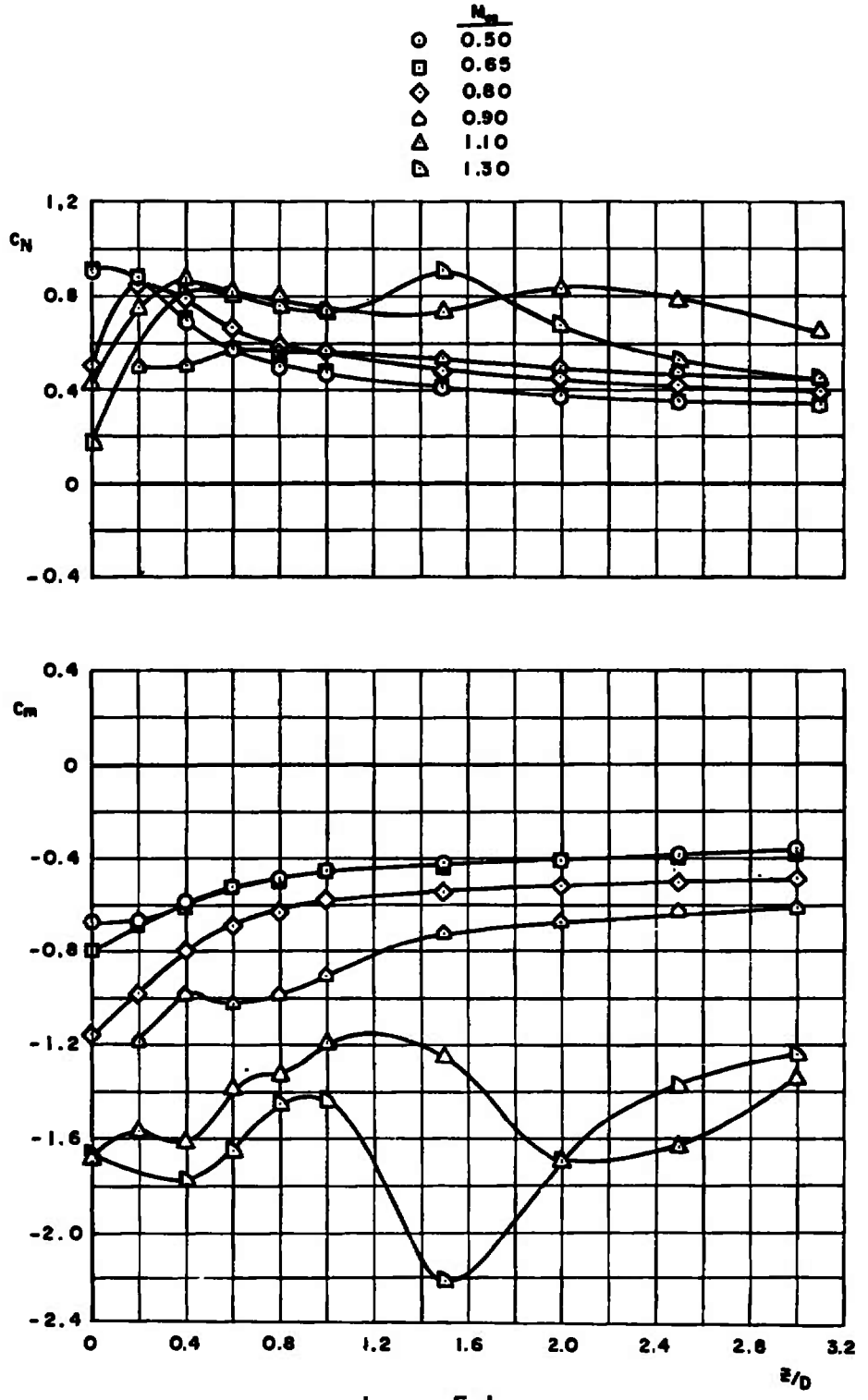

b. α = 5 deg

Fig. 23 Concluded

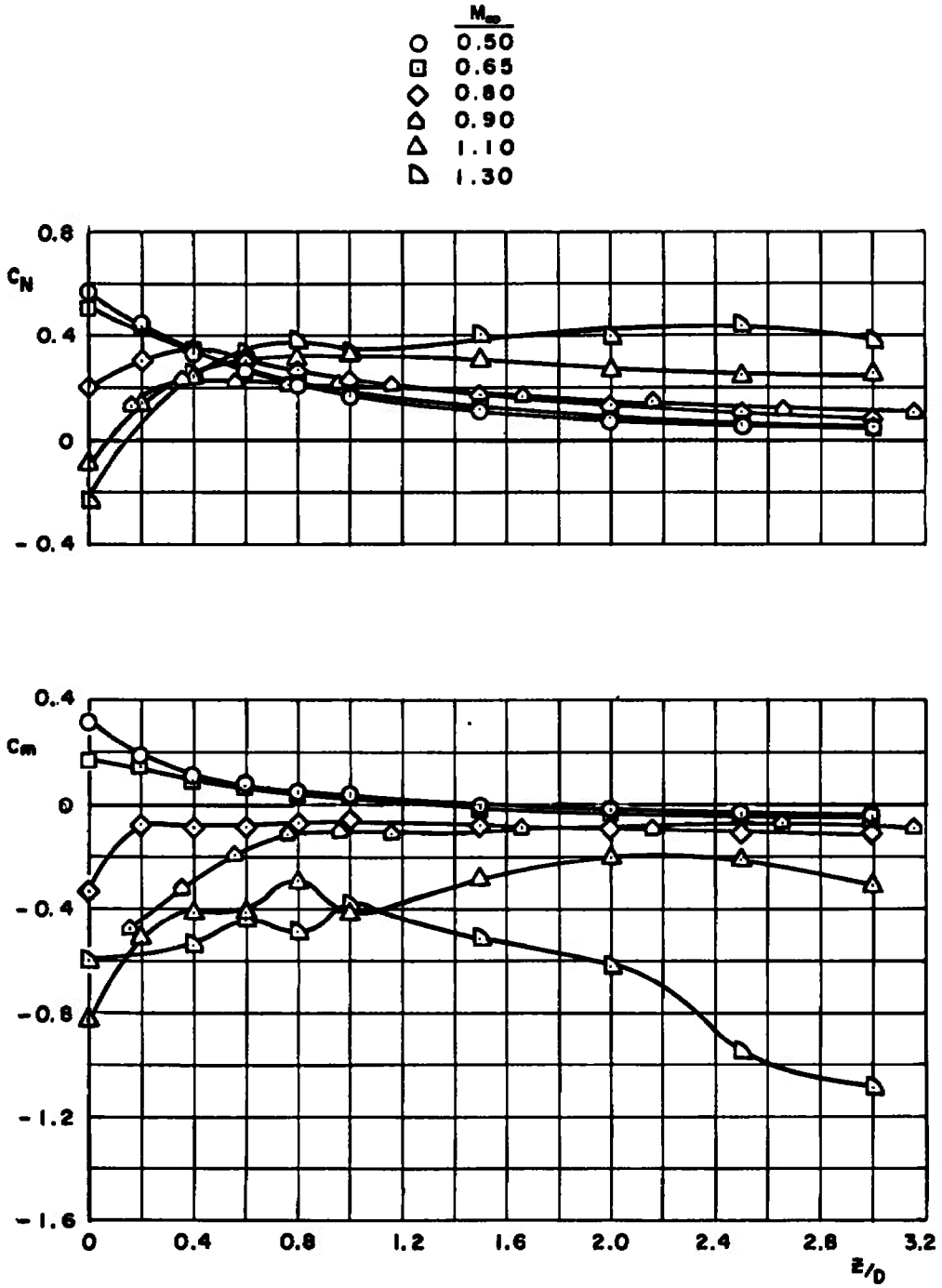

a. α = 0 deg

Fig. 24 Effect of Z/D Location on the Force and Moment Coefficients for the M-117, Configuration 2; X/D = -1.0, Y/D = 0, $\Delta\psi = \Delta\theta = 0$

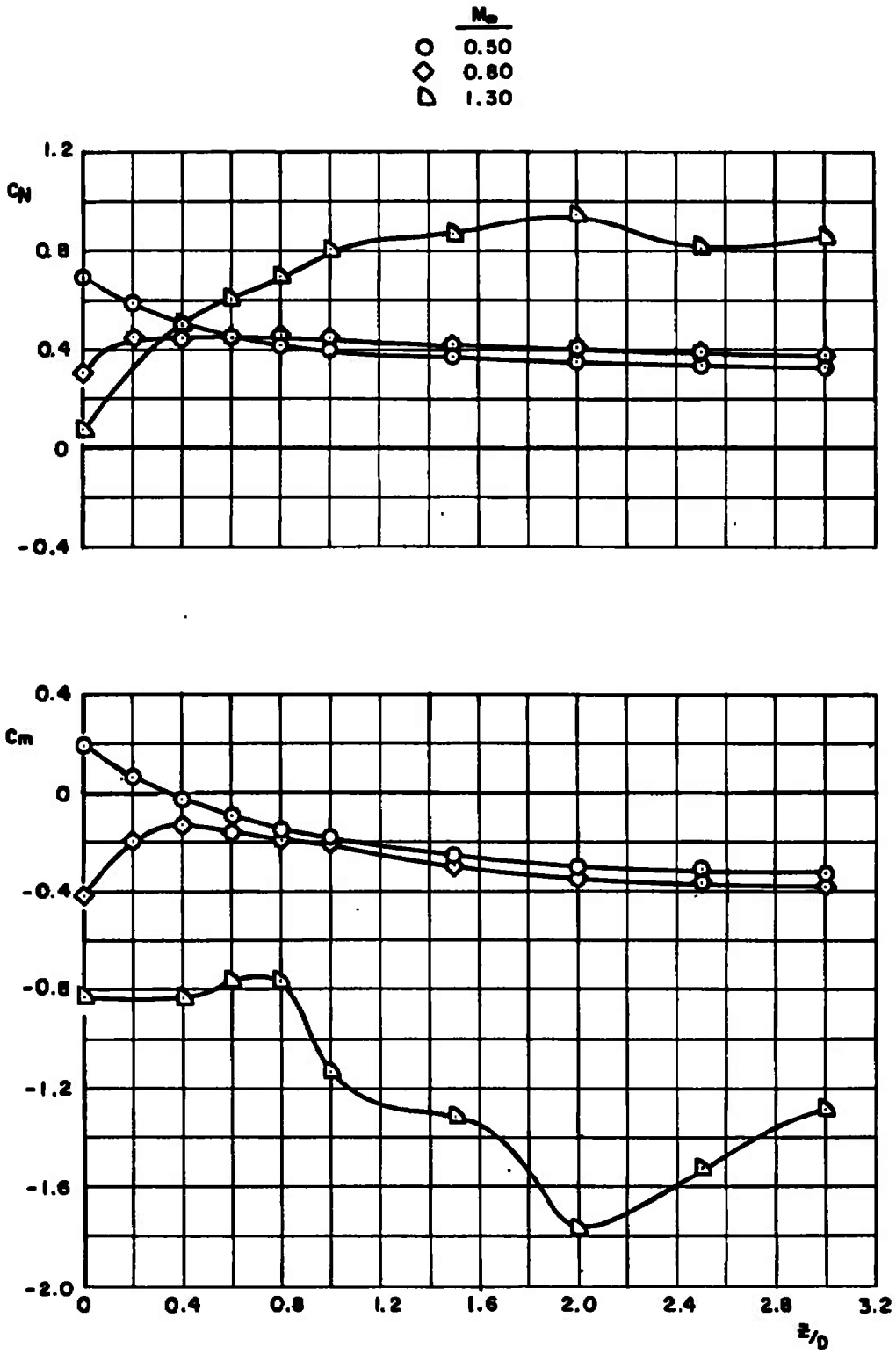

b. α = 5 deg

Fig. 24 Concluded

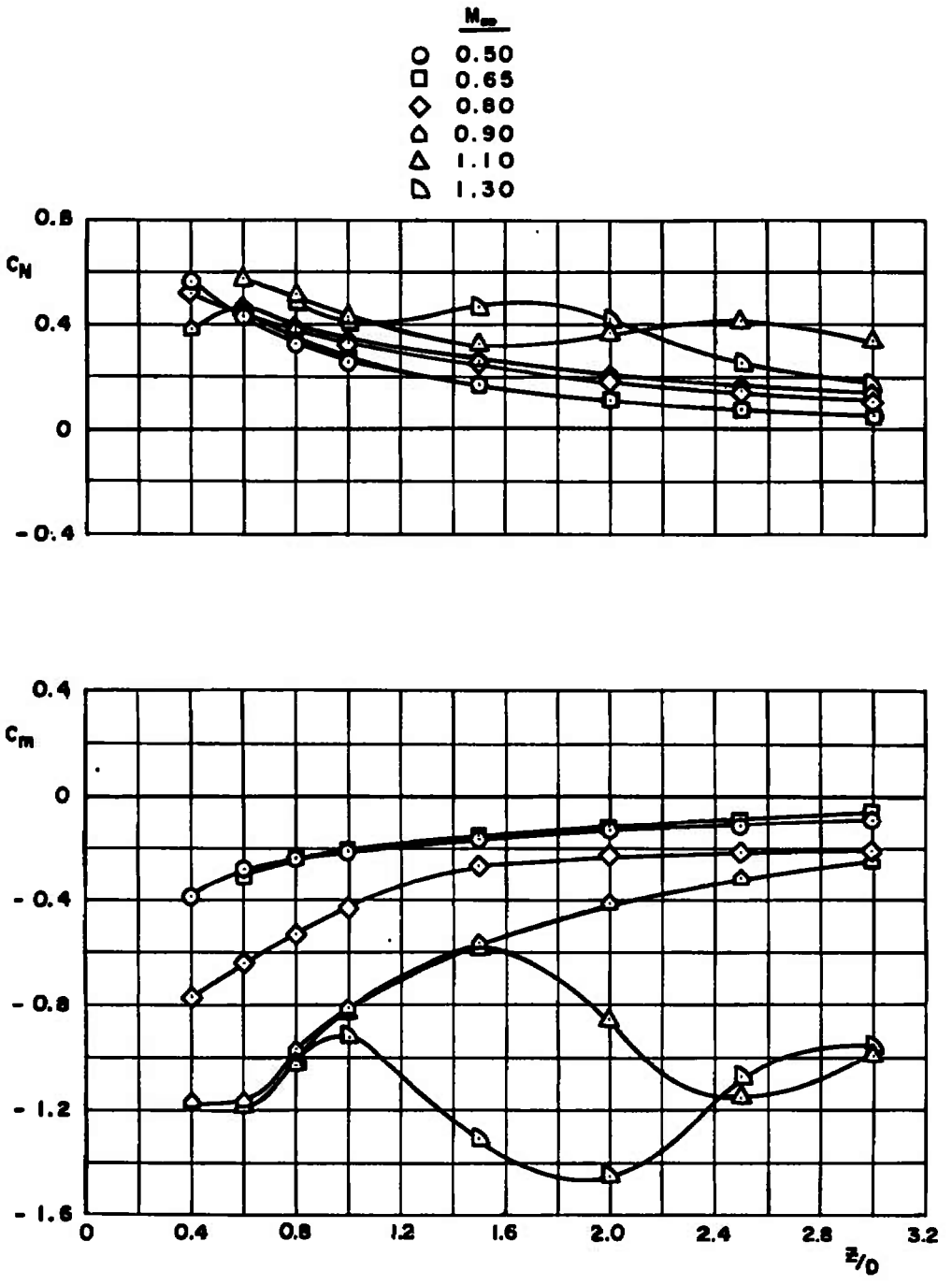

a. α = 0 deg

Fig. 25 Effect of Z/D Location on the Force and Moment Coefficients for the M-117, Configuration 2; Y/D = 0.357, X/D = 0, $\Delta\psi = \Delta\theta = 0$

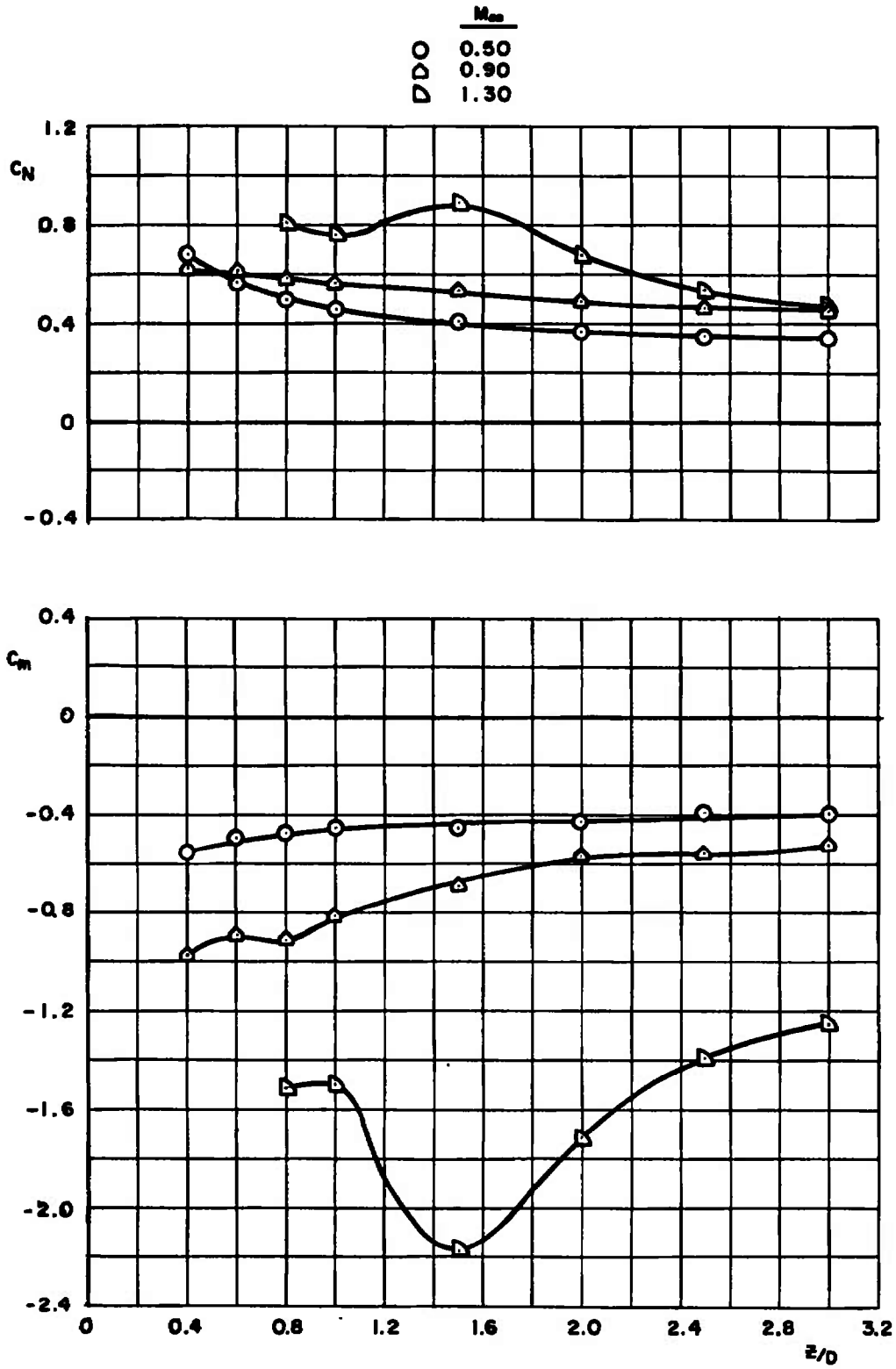

b. α = 5 deg

Fig. 25 Concluded

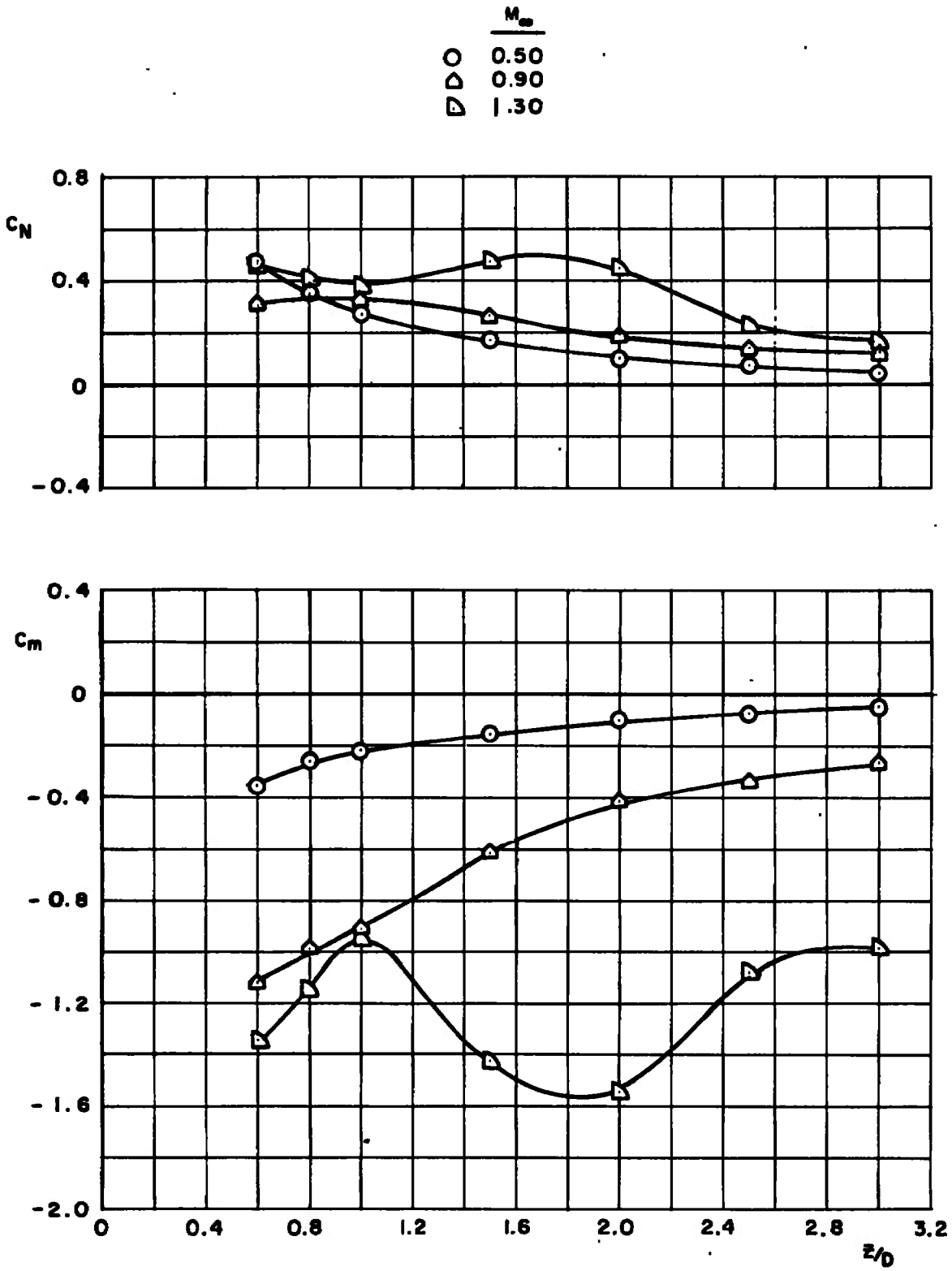

Fig. 26 Effect of Z/D Location on the Force and Moment Coefficients for the M-117, Configuration 2; $\Delta\psi$ = 5 deg, X/D = Y/D = 0, $\Delta\theta = \alpha = 0$

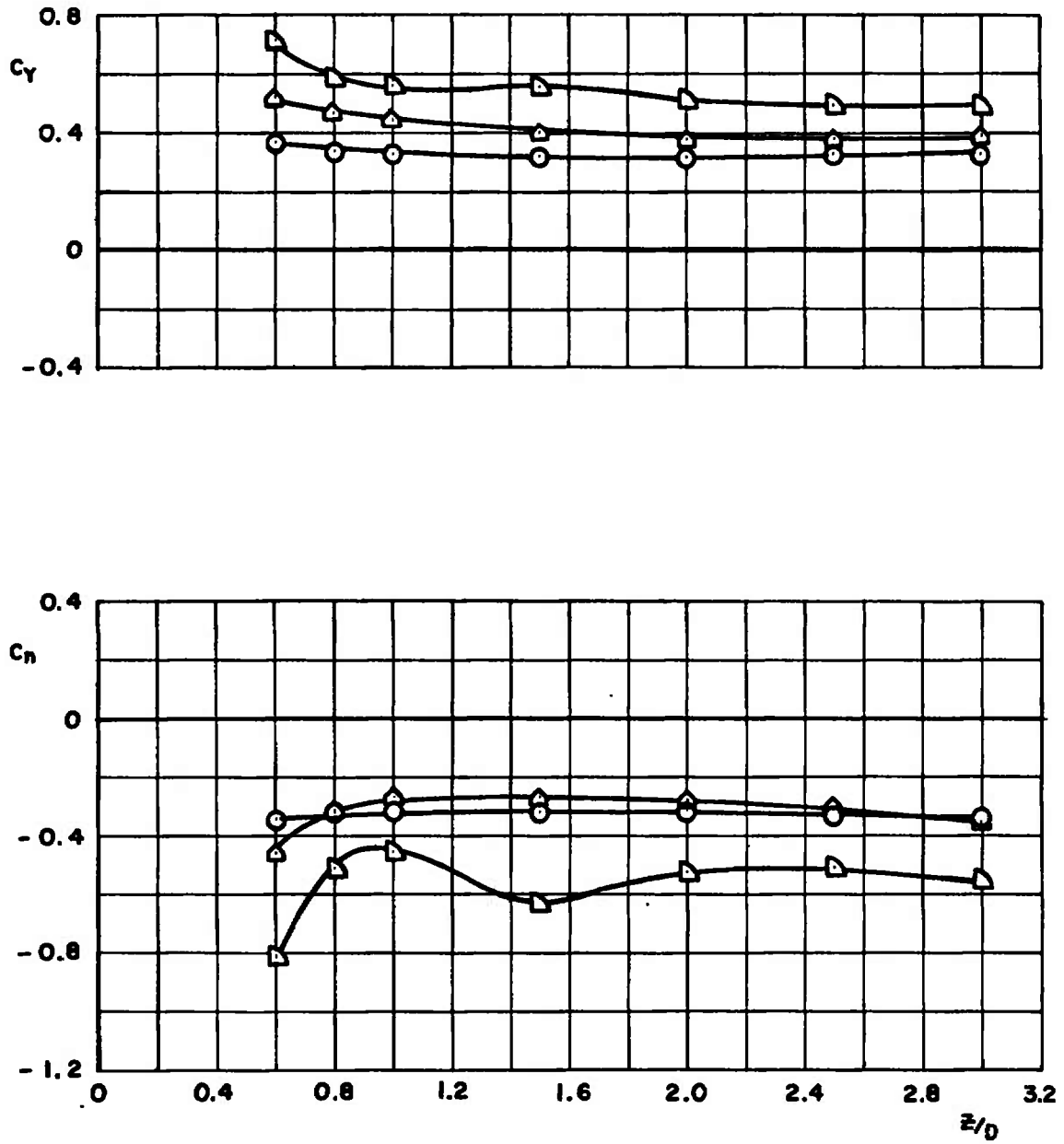

Fig. 26 Concluded

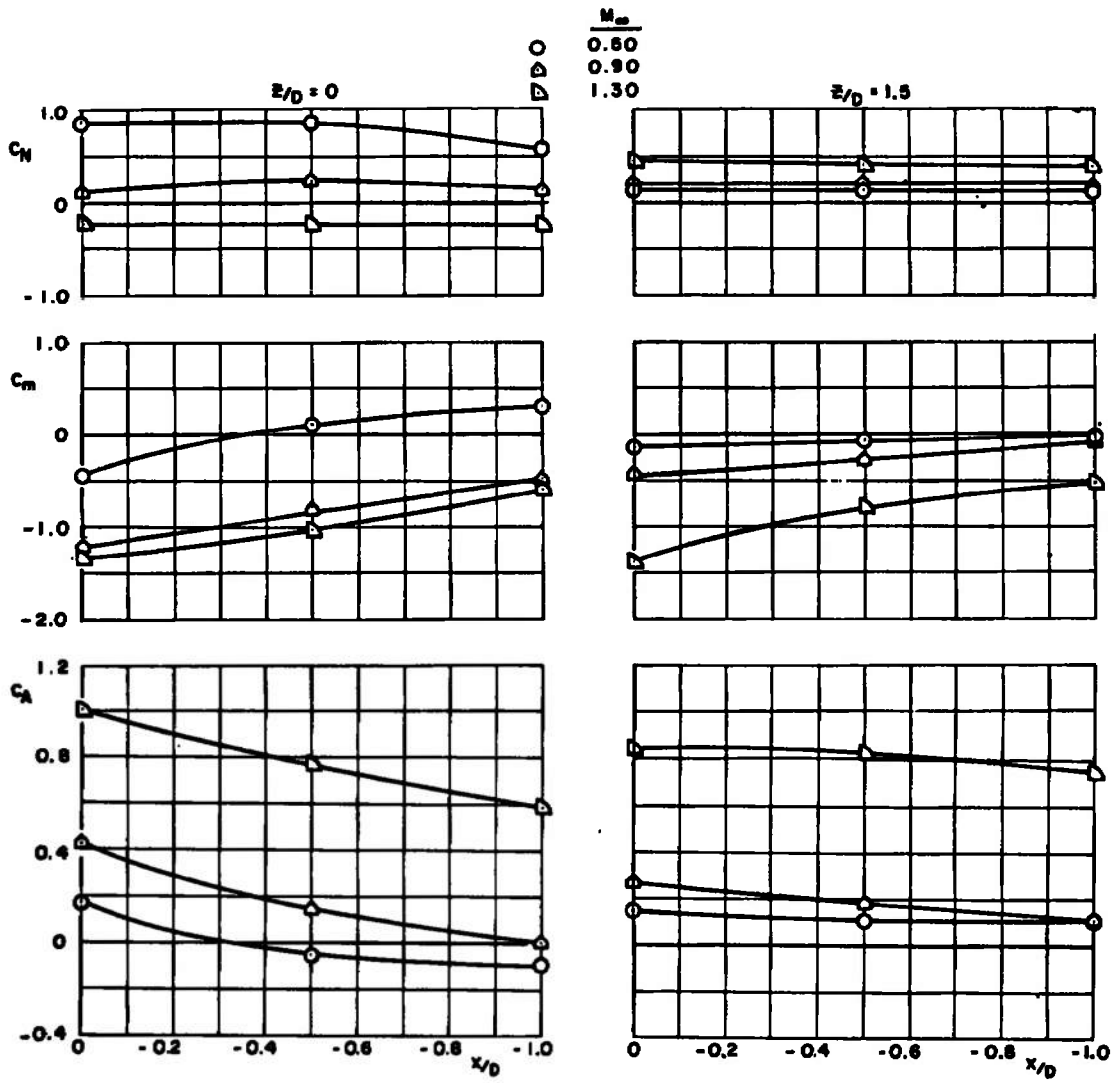

Fig. 27 Effect of Store Axial Position on the Force and Moment Coefficients for the M-117, Configuration 2; Y/D = 0, $\Delta\psi = \Delta\theta = \alpha = 0$

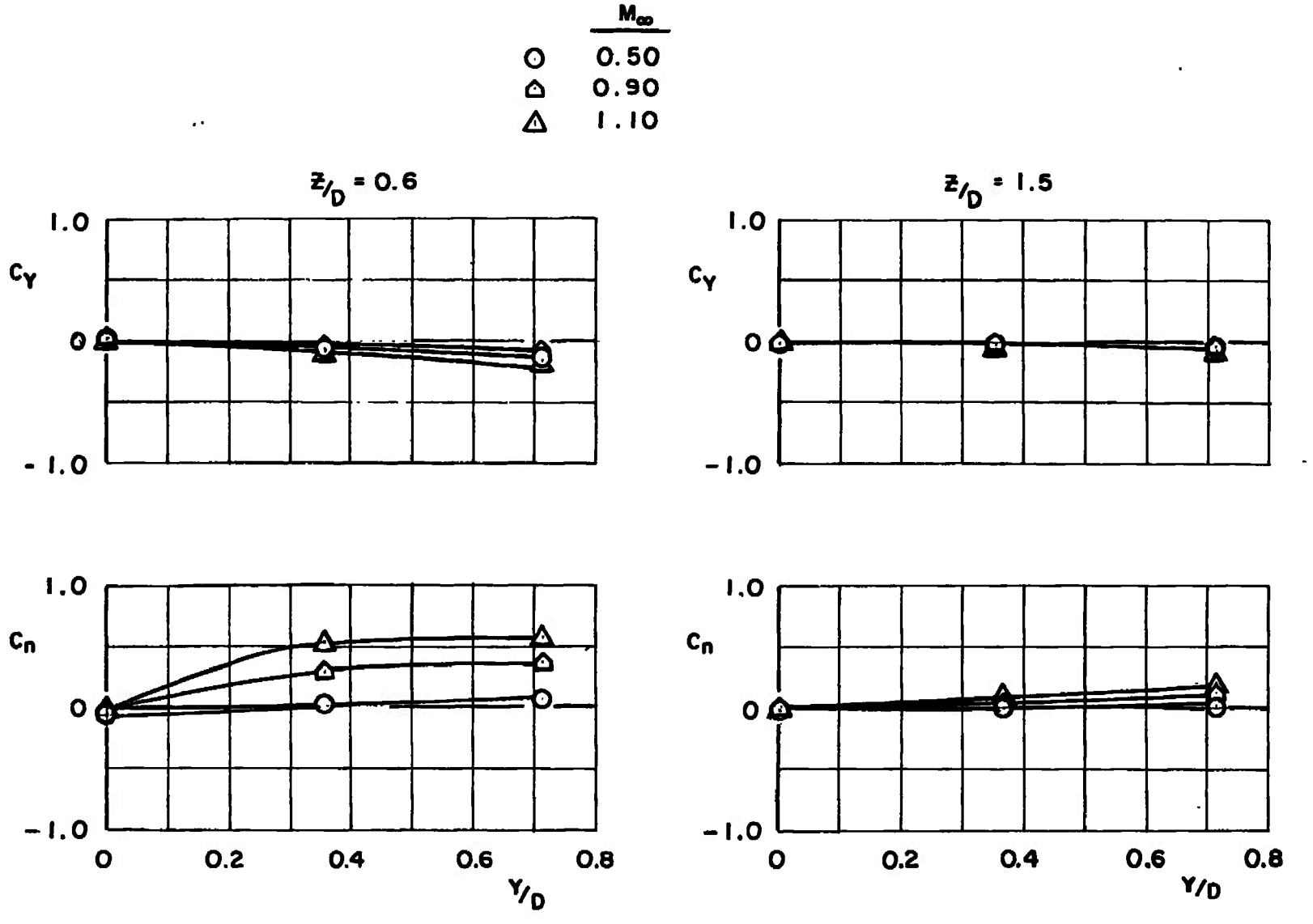

Fig. 28 Effect of Store Lateral Position on Side Force and Yawing Moment for the M-117, Configuration 2; X/D = 0, $\Delta\psi = \Delta\theta = \alpha = 0$

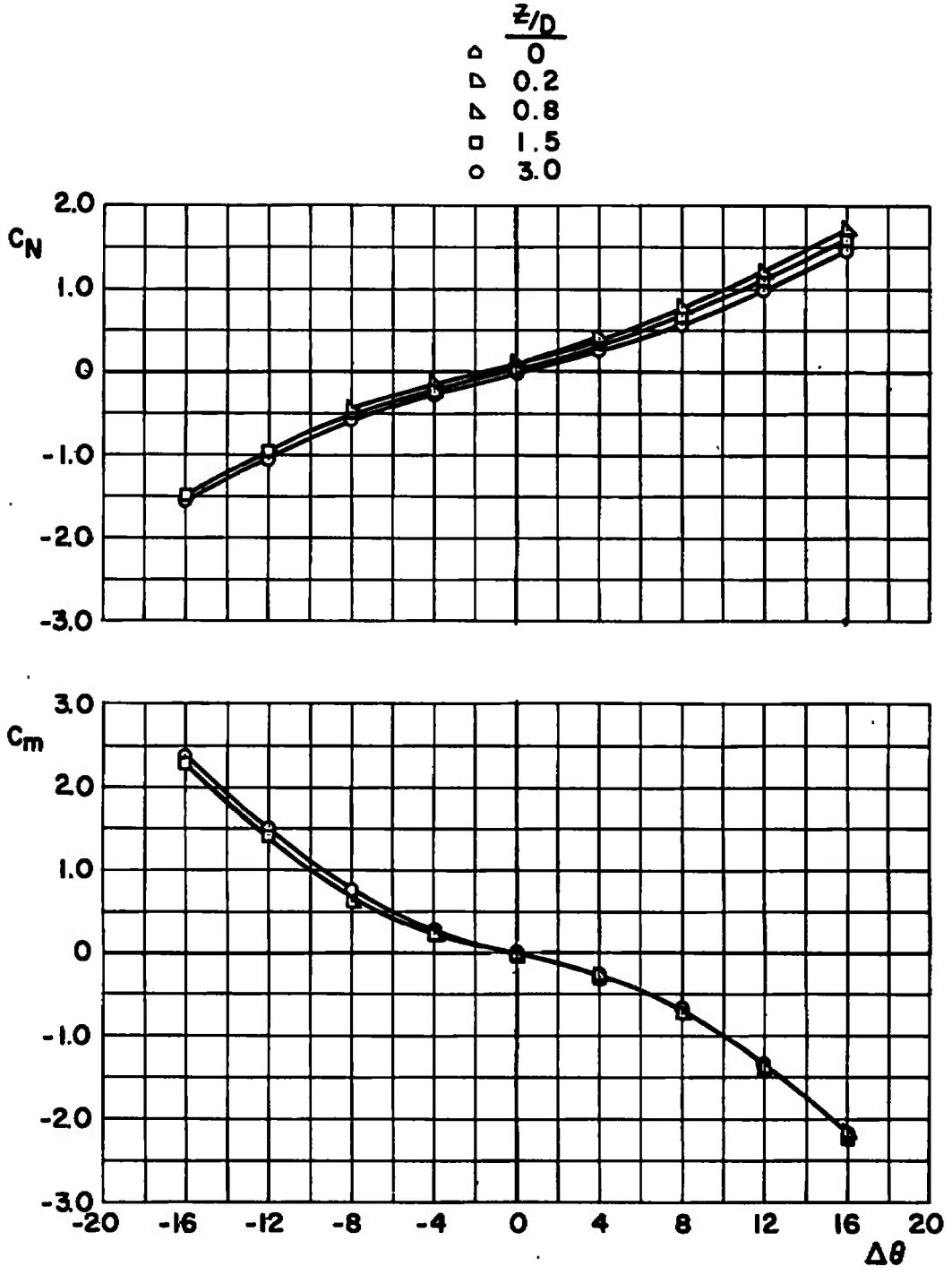

a. $M_\infty = 0.5$

Fig. 29 Force and Moment Data for the M-117 Showing the Effect of Variations in $\Delta\theta$, Configuration 3; X/D = Y/D = 0, $\Delta\psi = \Delta\theta = \alpha = 0$

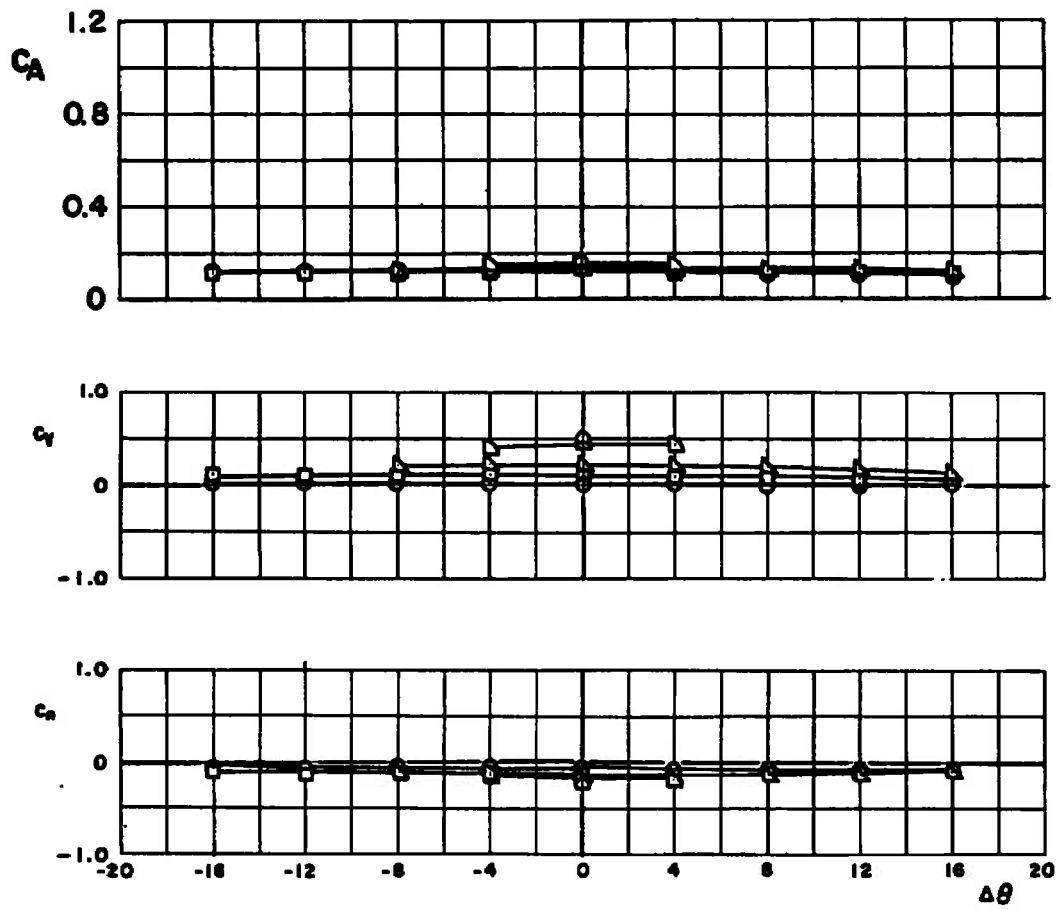

a. Concluded
Fig. 29 Continued

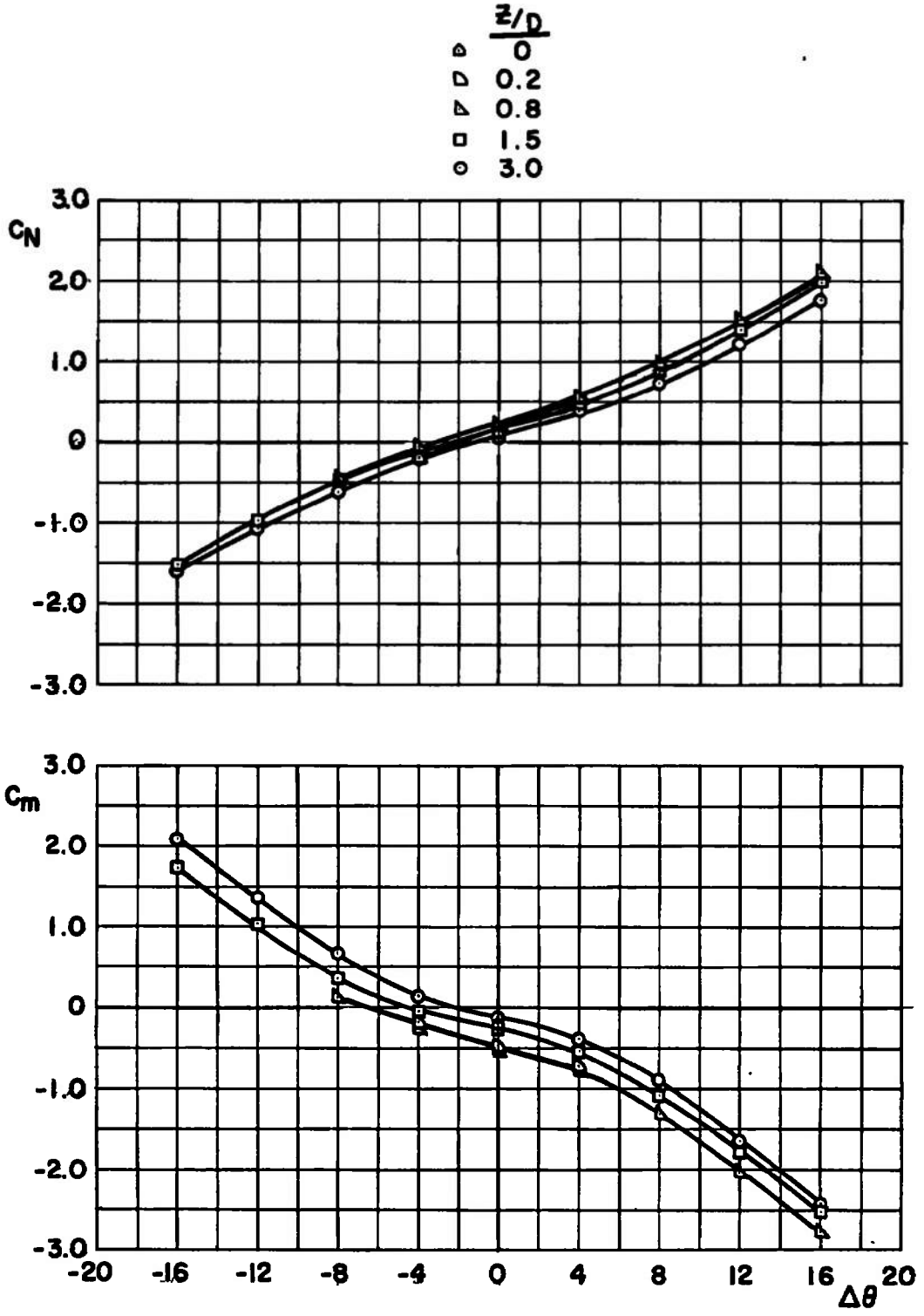

b. $M_\infty = 0.9$

Fig. 29 Continued

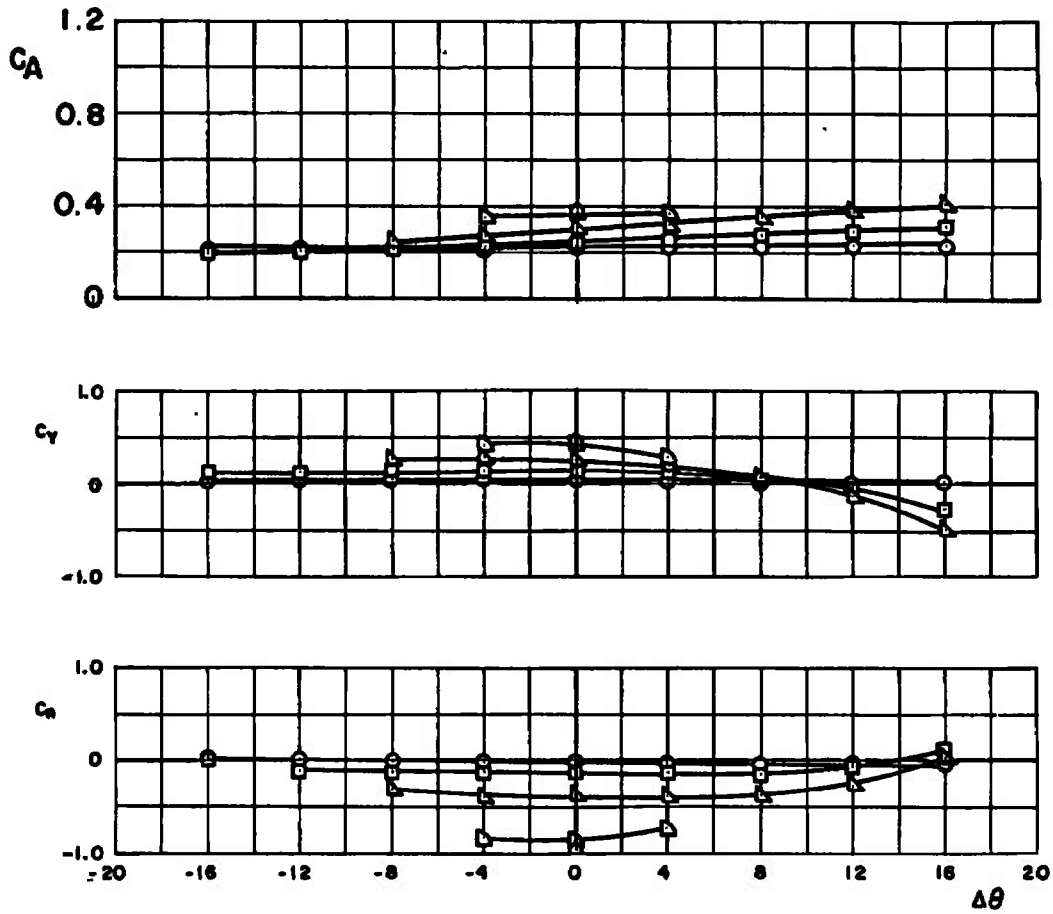

b. Concluded
Fig. 29 Continued

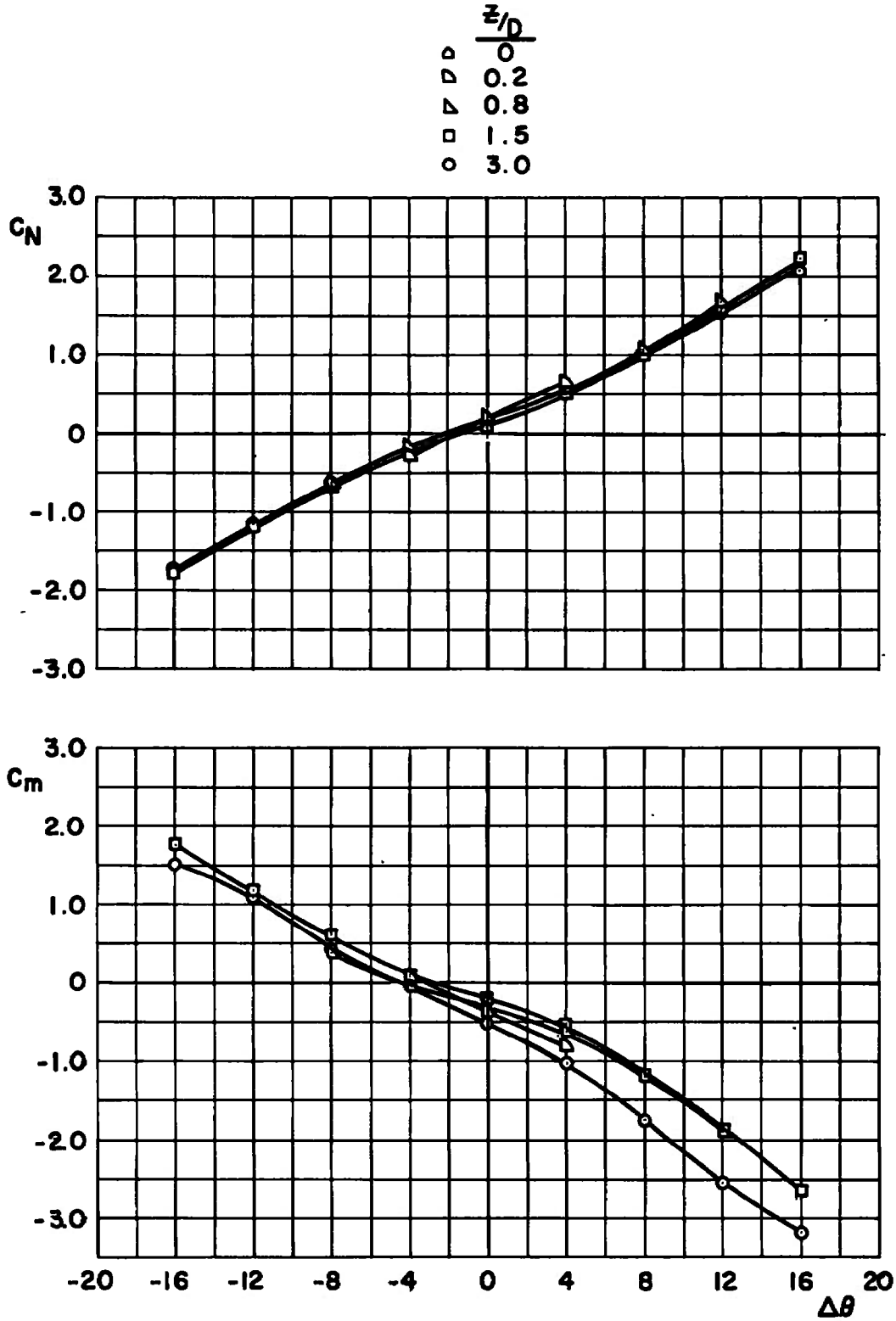

c. $M_\infty = 1.1$
Fig. 29 Continued

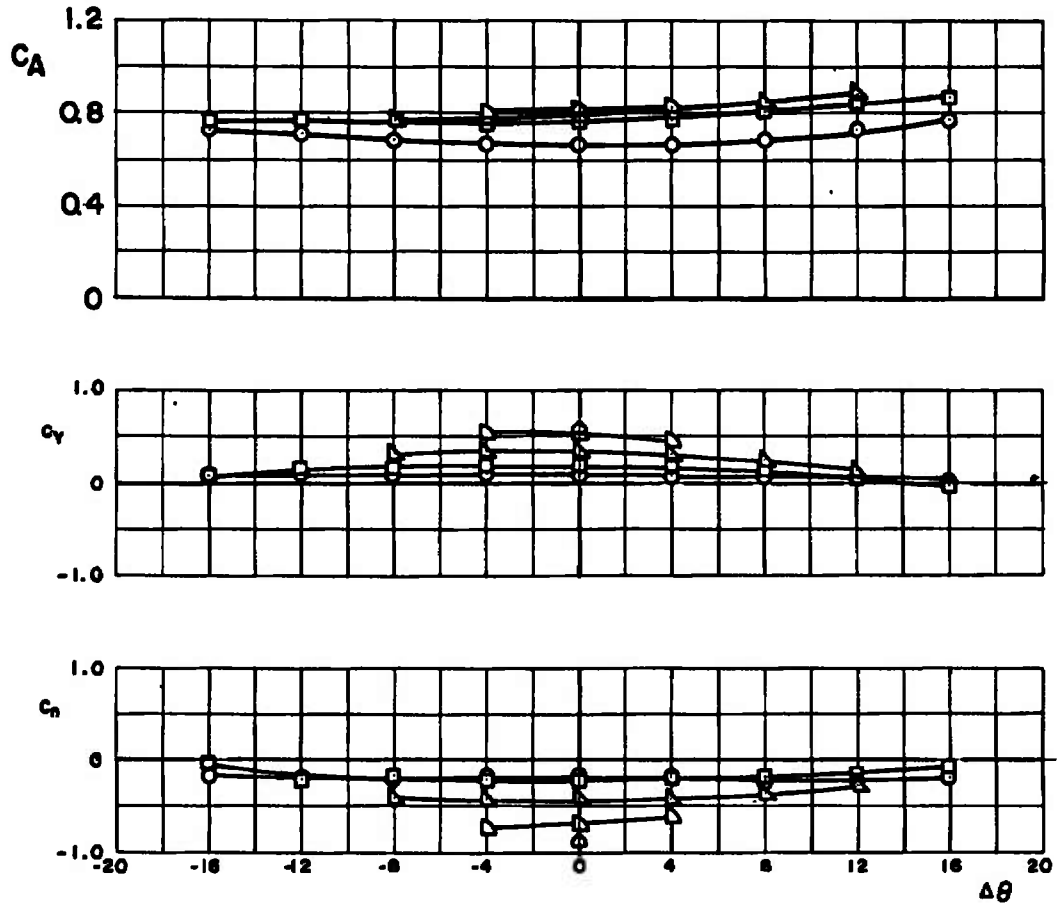

c. Concluded
Fig. 29 Concluded

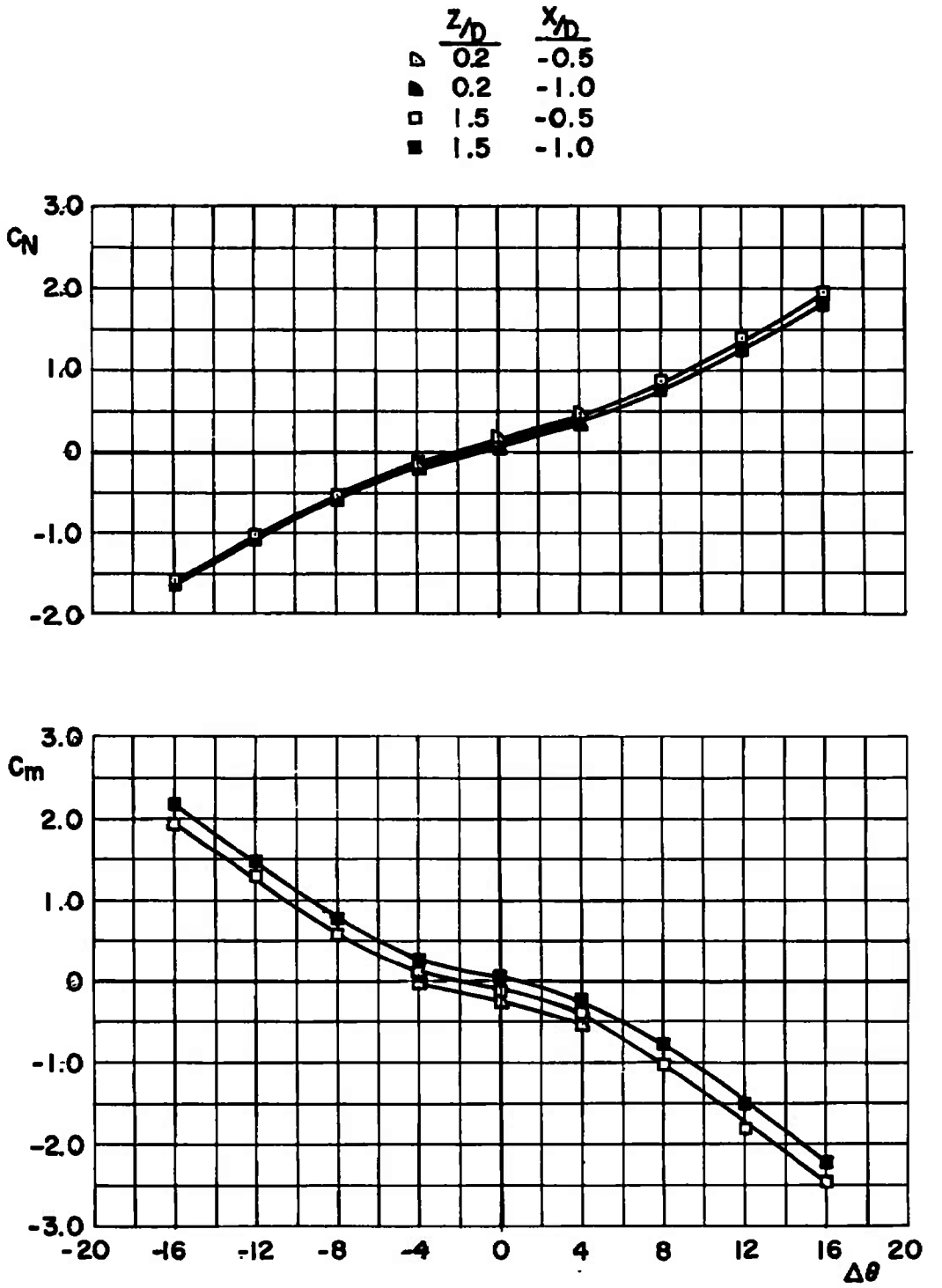

Fig. 30 Force and Moment Data for the M-117 Showing the Effect of Variations in $\Delta\theta$ at $M_\infty = 0.9$, Configuration 3; Y/D = 0, $\Delta\psi = \alpha = 0$

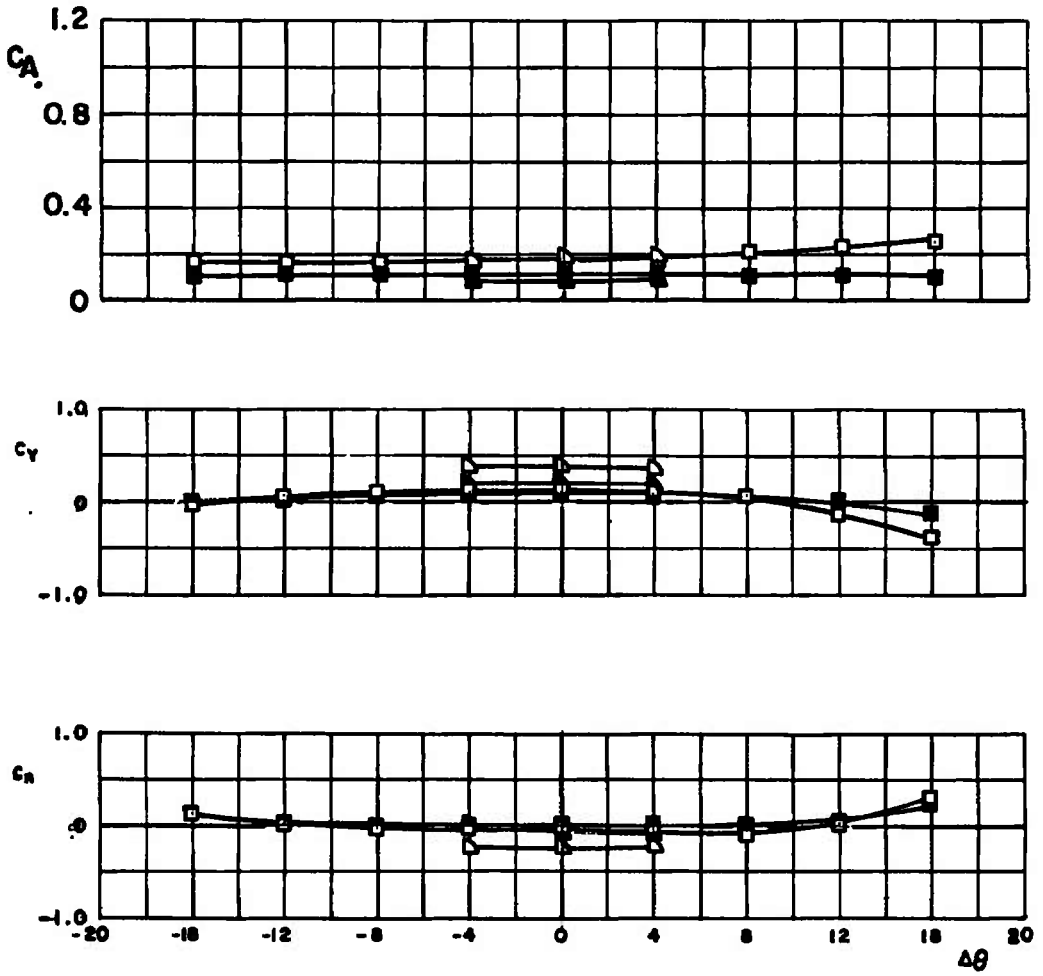

Fig. 30 Concluded

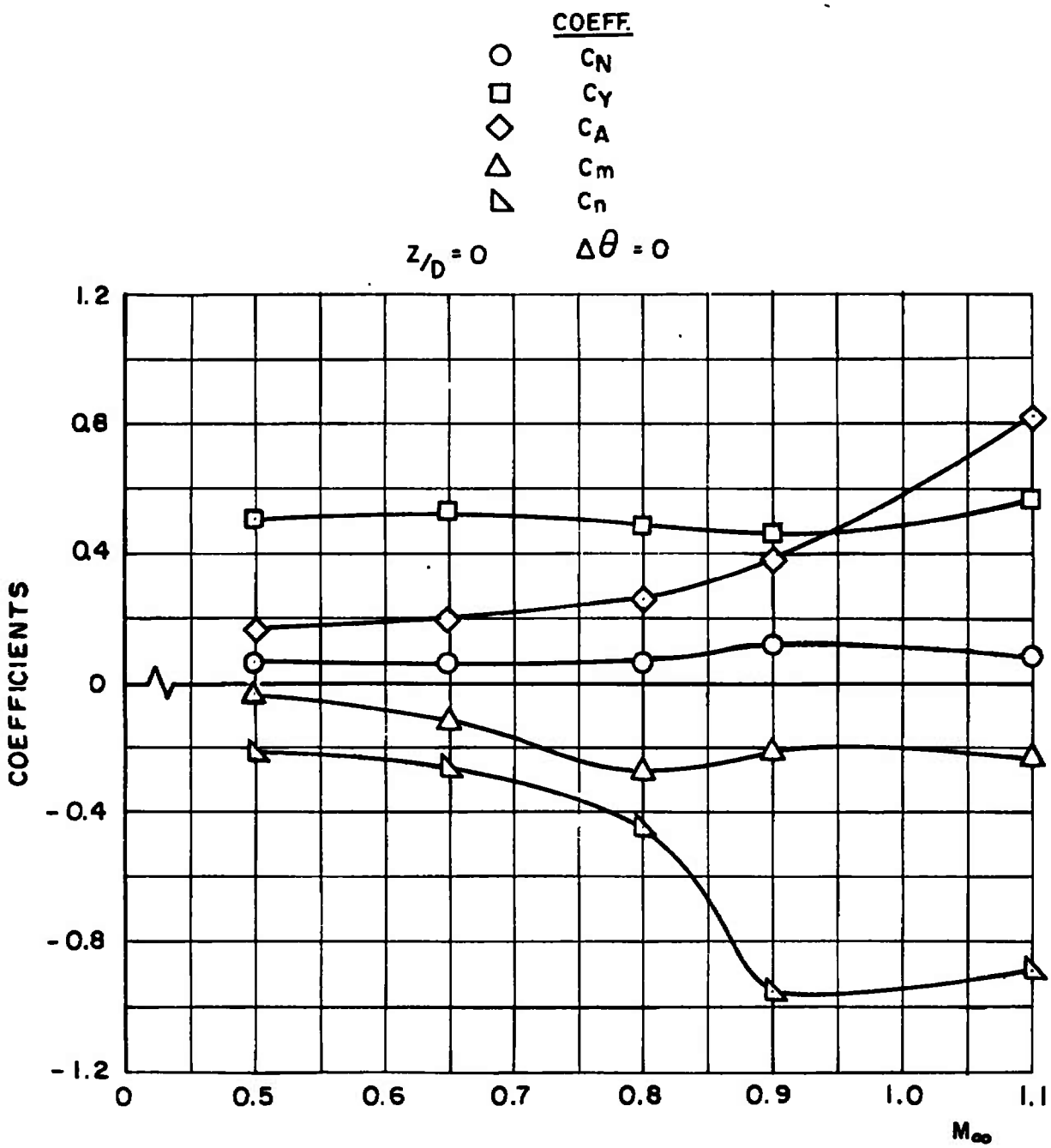

Fig. 31 Effect of Mach Number on the Aerodynamic Forces and Moments Acting on the M-117 in the Carriage Position, Configuration 3; X/D = Y/D = 0, $\Delta\psi = \alpha = 0$

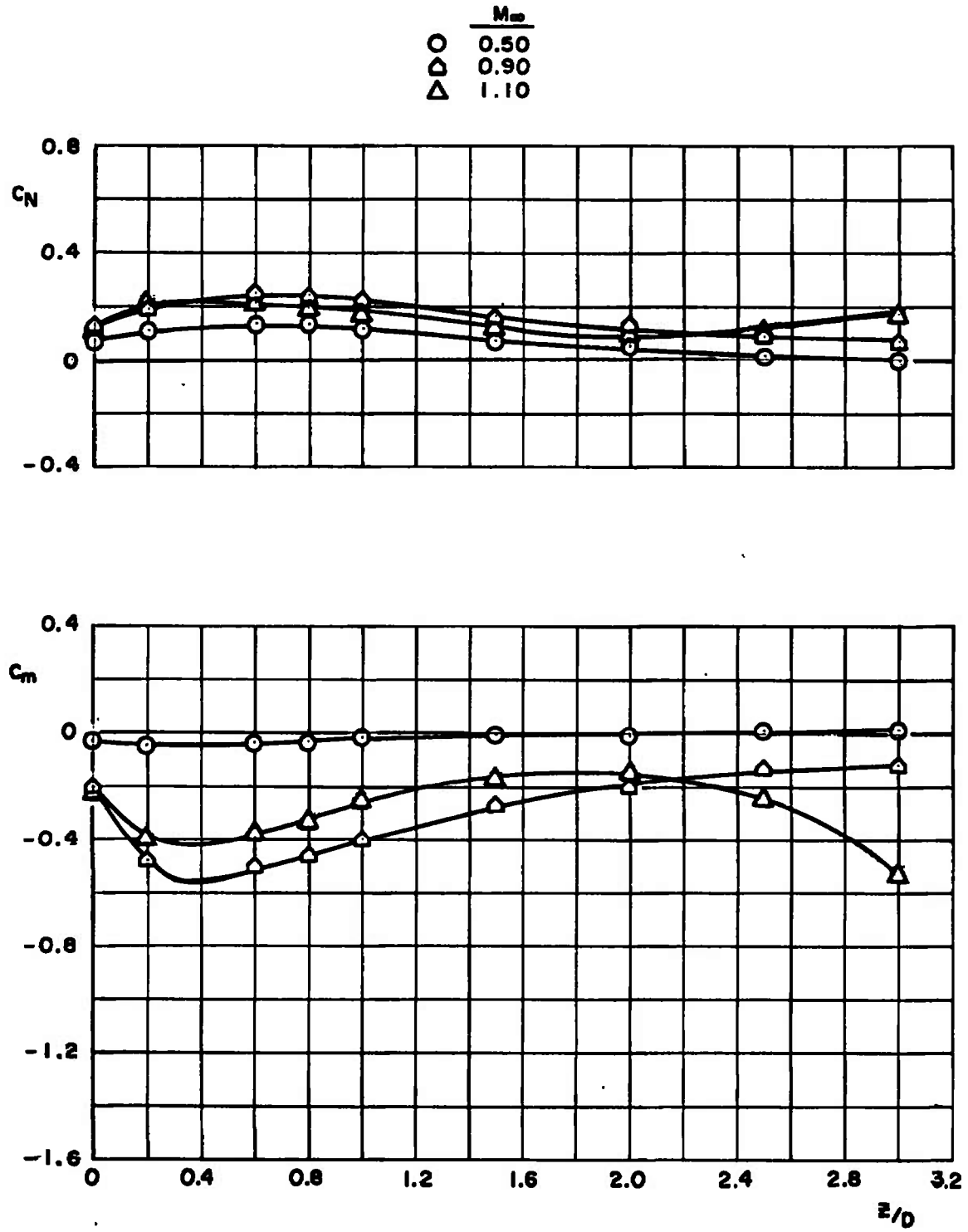

a. α = 0 deg

Fig. 32 Effect of Z/D Location on the Force and Moment Coefficients for the M-117, Configuration 3; X/D = Y/D = 0, $\Delta\psi = \Delta\theta = 0$

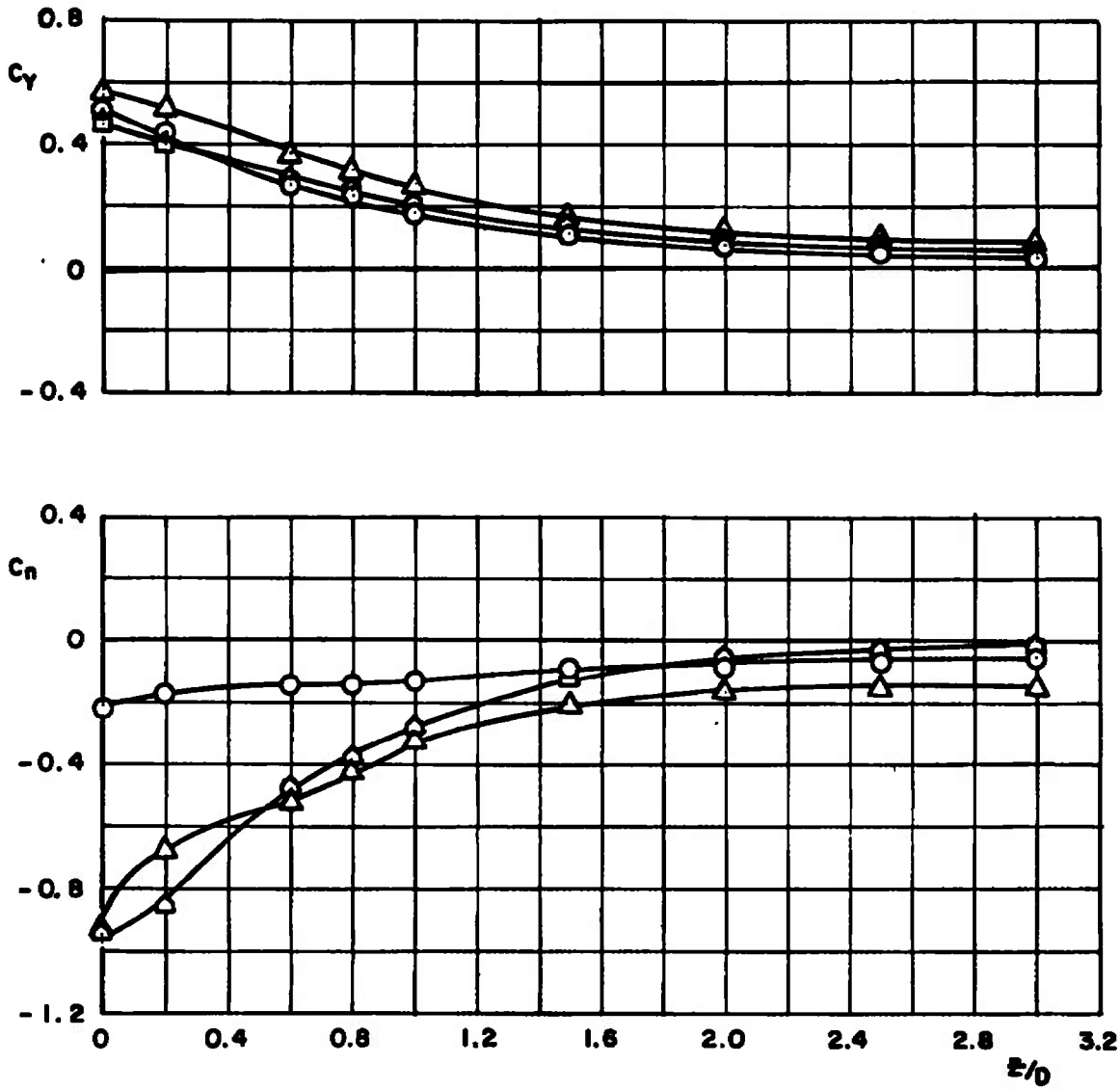

a. Concluded
Fig. 32 Continued

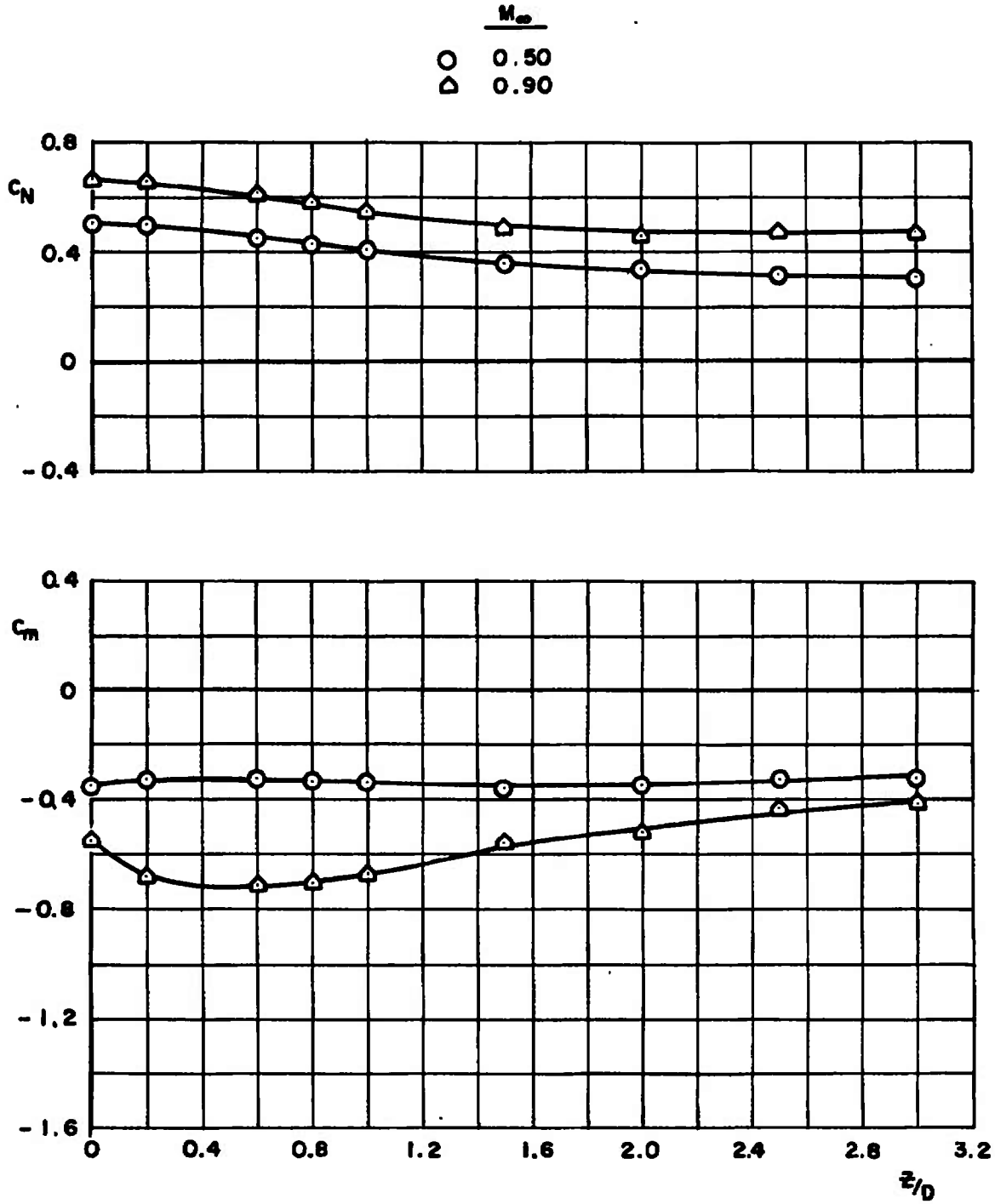

b. α = 5 deg

Fig. 32 Continued

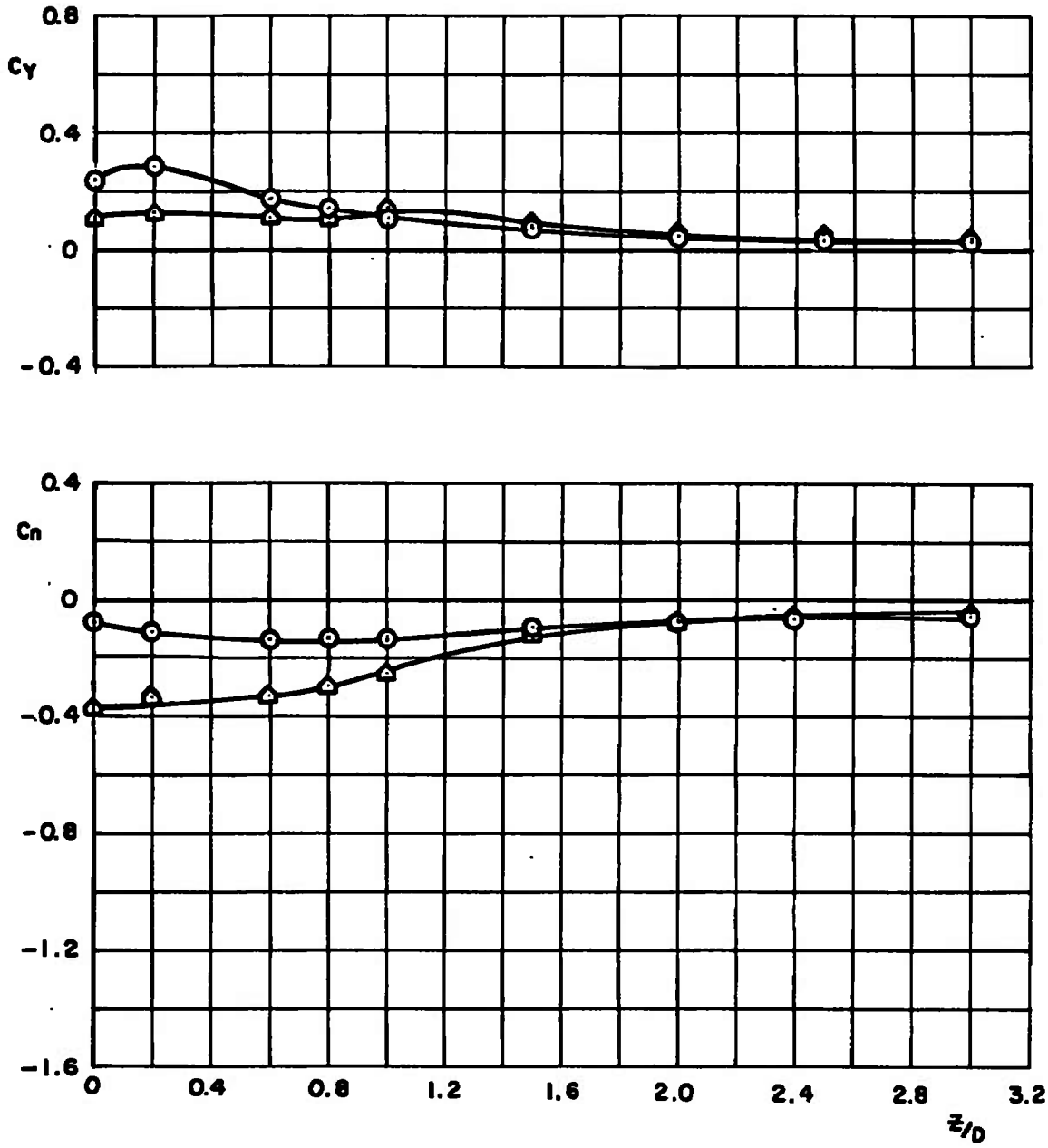

b. Concluded
Fig. 32 Concluded

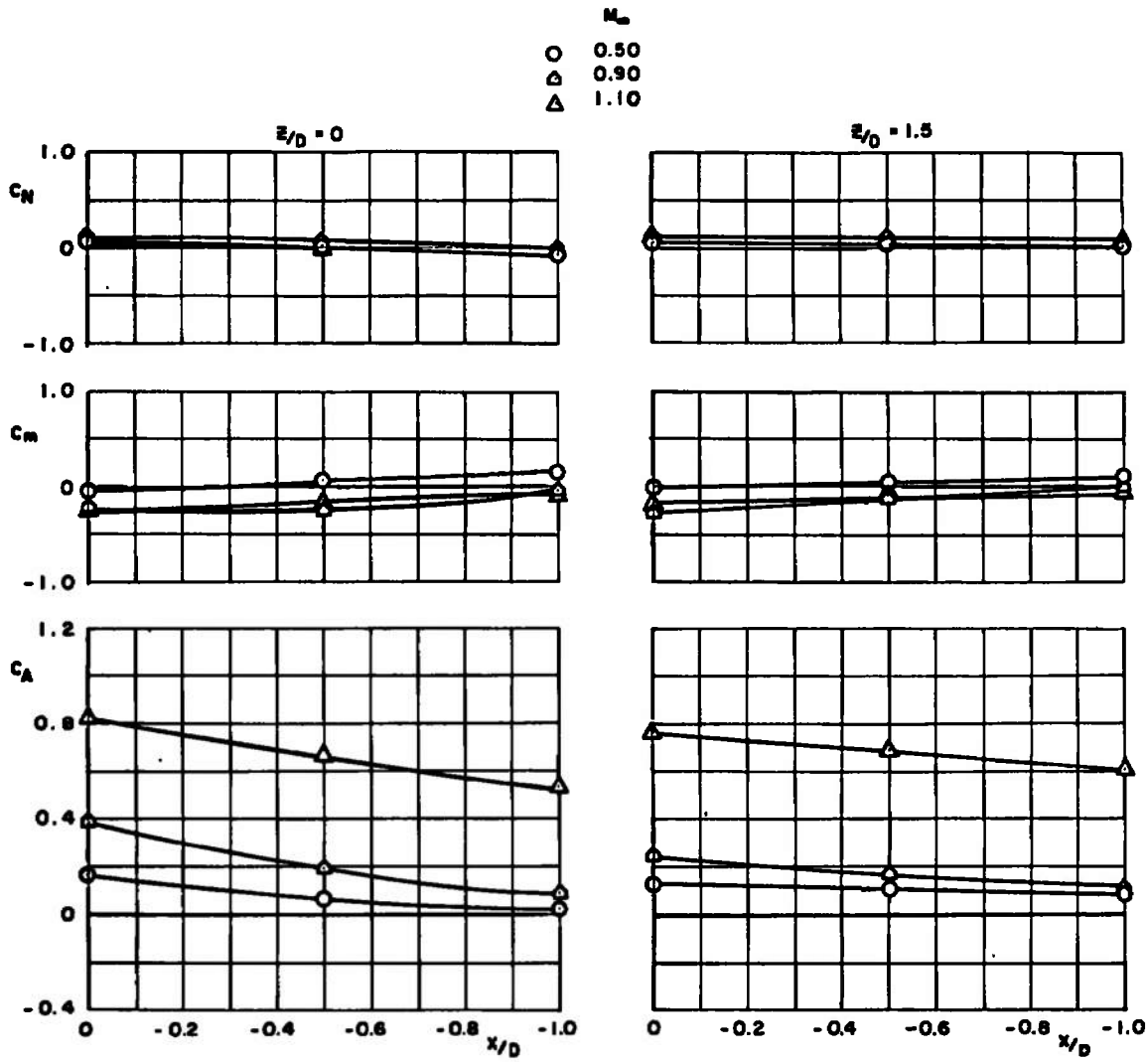

Fig. 33 Effect of Store Axial Position on the Force and Moment Coefficients for the M-117, Configuration 3; Y/D = 0, $\Delta\psi = \Delta\theta = a = 0$

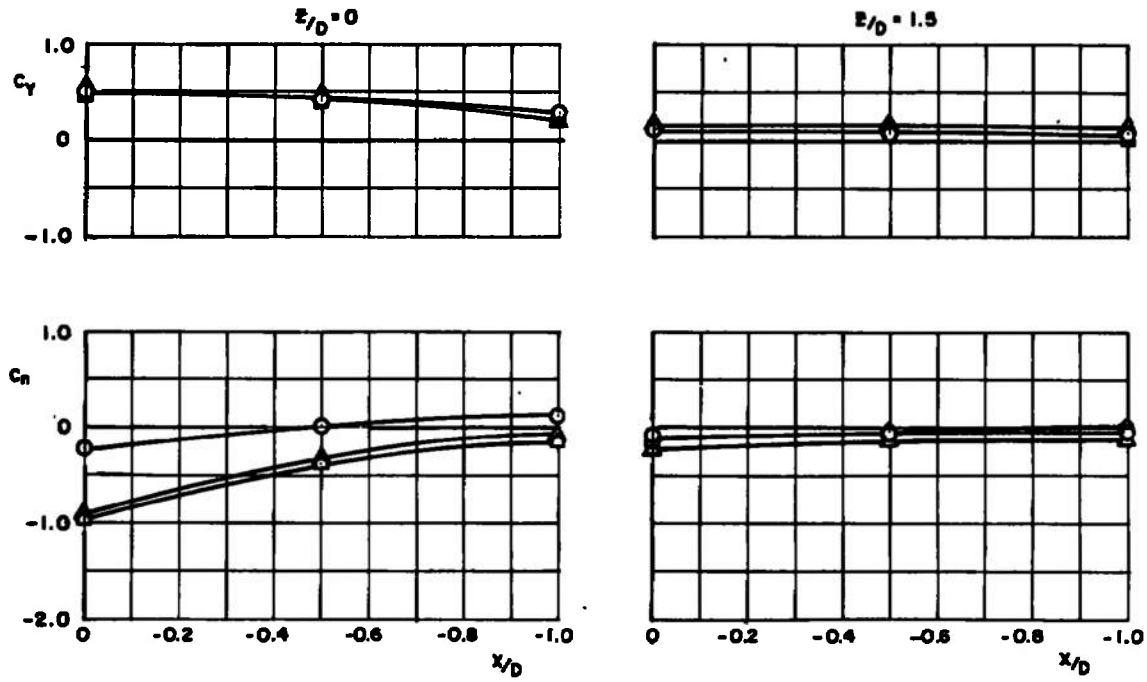

Fig. 33 Concluded

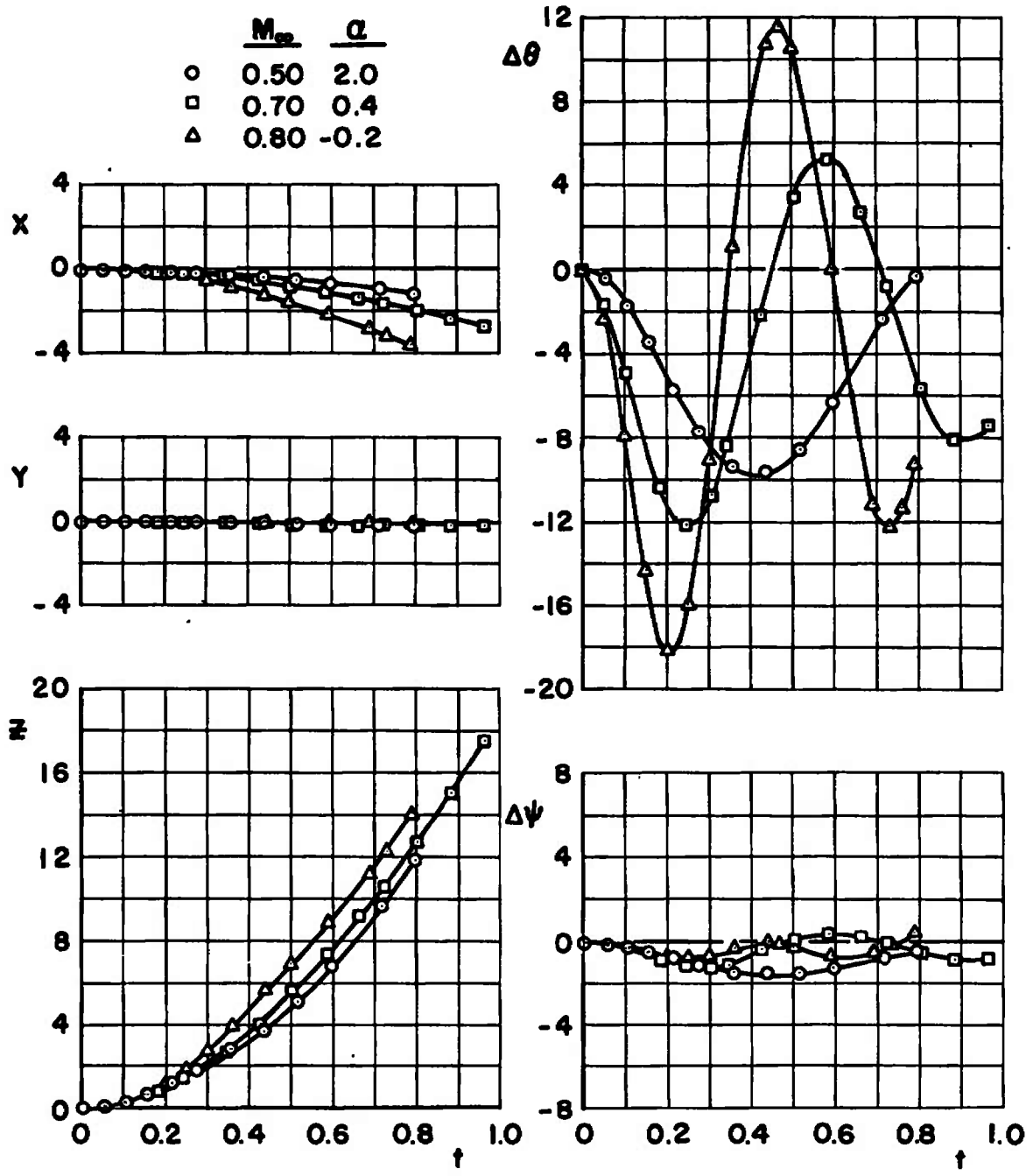

a. Configuration 2

Fig. 34 Separation Trajectory Data for the M-117 for Simulated Level Flight at 5000-ft Altitude

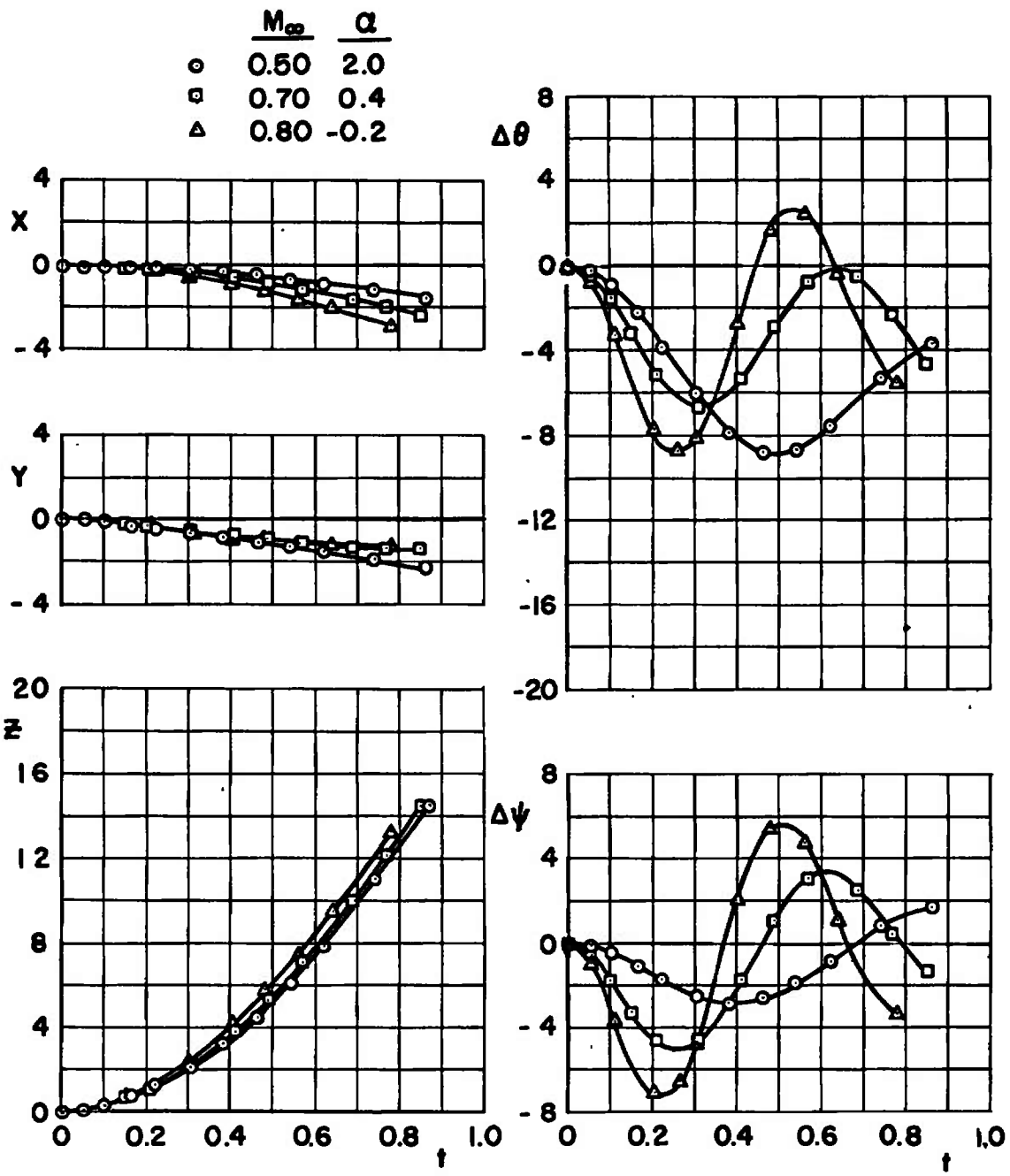

b. Configuration 3
Fig. 34 Concluded

TABLE I
STORE LOCATION AND ORIENTATION FOR FORCE AND MOMENT DATA

$Z_{/D}$	STORE POSITION FOR INITIAL DATA POINT							
	1	2	3	4*	5*	6*	7*	8*
	$X_{/D} = Y_{/D} = 0$ $\Delta\psi = 0$	$X_{/D} = -0.5, Y_{/D} = 0$ $\Delta\psi = 0$	$X_{/D} = -1.0, Y_{/D} = 0$ $\Delta\psi = 0$	$X_{/D} = 0, Y_{/D} = 0.357$ $\Delta\psi = 0$	$X_{/D} = 0, Y_{/D} = 0.714$ $\Delta\psi = 0$	$X_{/D} = Y_{/D} = 0$ $\Delta\psi = 5$	$X_{/D} = -0.5, Y_{/D} = 0$ $\Delta\psi = 5$	$X_{/D} = 0, Y_{/D} = 0.357$ $\Delta\psi = 5$
0	✓	✓	✓	–	–	–	–	–
0.20	✓	✓	✓	–	–	–	–	–
0.27	–	–	–	✓①	–	✓①	✓①	–
0.34	–	–	–	–	✓①	–	–	✓
0.40	✓	✓	✓	✓	✓①	✓①	✓①	✓
0.56	–	–	–	–	–	✓②	✓②	–
0.60	✓	✓	✓	✓	✓	✓	✓	✓
0.80	✓	✓	✓	✓	✓	✓	✓	✓
1.00	✓	✓	✓	✓	✓	✓	✓	✓
1.50	✓	✓	✓	✓	✓	✓	✓	✓
2.00	✓	✓	✓	✓	✓	✓	✓	✓
2.50	✓	✓	✓	✓	✓	✓	✓	✓
3.00	✓	✓	✓	✓	✓	✓	✓	✓

* CONFIGURATIONS 1 AND 2 ONLY

① CONFIGURATION 1 ONLY

② CONFIGURATION 2 ONLY

TABLE II
FULL-SCALE STORE PARAMETERS USED IN
TRAJECTORY CALCULATIONS

PARAMETER	VALUE
$\bar{m}$	23.31
X_{cg}	2.74
I_X	4.0
I_Y	50.0
I_Z	50.0
C_{mq}	-70.0
C_{nr}	-70.0
C_{lp}	0.0
b	1.333
S	1.396
X_L	0.0
$\bar{z}_E$	0.255
F_Z	1200

UNCLASSIFIED

Security Classification

DOCUMENT CONTROL DATA - R & D

(Security classification of title, body of abstract and indexing annotation must be entered when the overall report is classified)

1. ORIGINATING ACTIVITY *(Corporate author)*

Arnold Engineering Development Center
Arnold Air Force Station, Tennessee 37389

2a. REPORT SECURITY CLASSIFICATION

UNCLASSIFIED

2b. GROUP

N/A

3. REPORT TITLE

AERODYNAMIC LOADS DATA ON THE M-117 BOMB IN THE FLOW FIELD OF THE TRIPLE EJECTION RACK AT MACH NUMBERS FROM 0.5 TO 1.3

4. DESCRIPTIVE NOTES *(Type of report and inclusive dates)*

Final Report - January 27 to February 7, 1972

5. AUTHOR(S) *(First name, middle initial, last name)*

Willard E. Summers, ARO, Inc.

This document has been approved for public release its distribution is unlimited. per TAB 16-1916 26 March 1973

6. REPORT DATE	7a. TOTAL NO. OF PAGES	7b. NO. OF REFS
June 1972	91	0

8a. CONTRACT OR GRANT NO.	9a. ORIGINATOR'S REPORT NUMBER(S)
b. PROJECT NO. 2567	AEDC-TR-72-81 AFATL-TR-72-101
c. Program Element 62602F	9b. OTHER REPORT NO(S) *(Any other numbers that may be assigned this report)*
d.	ARO-PWT-TR-72-55

10. DISTRIBUTION STATEMENT Distribution limited to U.S. Government agencies only; this report contains information on test and evaluation of military hardware; June 1972; other requests for this document must be referred to Air Force Armament Laboratory (DLGC), Eglin AFB, FL 32542.

11. SUPPLEMENTARY NOTES	12. SPONSORING MILITARY ACTIVITY
Available in DDC	Air Force Armament Laboratory (DLGC), Eglin AFB, FL 32542

13. ABSTRACT

Experimental data were obtained to check the validity of store forces and moments acquired from theoretical calculations which employed mathematical models to simulate the M-117 bombs and the Triple Ejection Rack (TER). Data were obtained using 0.10-scale models of the physical geometry of the M-117 and TER, and using mathematically simulated geometries representing the M-117 and TER. Store force and moment data were obtained for each store geometry at various locations and orientations relative to the corresponding TER configuration. In addition, free-stream stability data and some separation trajectories were obtained for the M-117 model which represented the physical store geometry. Data were obtained at Mach numbers from 0.5 to 1.3 for the force and moment data, and from 0.5 to 0.8 for the separation trajectory data. During the early part of the test, it was found that the test results for the two models did not correlate well.

Distribution limited to U.S. Government agencies only; this report contains information on test and evaluation of military hardware; June 1972; other requests for this document must be referred to Air Force Armament Laboratory (DLGC), Eglin AFB, FL 32542.

DD FORM 1 NOV 68 1473

UNCLASSIFIED

Security Classification

14. KEY WORDS	LINK A		LINK B		LINK C	
	ROLE	WT	ROLE	WT	ROLE	WT
M-117 bomb						
external stores						
ejection						
interference						
bomb racks						
transonic wind tunnels						